ADAPTIVE CONTROL OF CHEMICAL REACTIONS IN THE ABSENCE OF REACTION KINETICS INFORMATION

Submitted in partial fulfillment of the requirements for
the degree of

DOCTOR OF PHILOSOPHY
in
CHEMICAL ENGINEERING

ZIXI ZHAO
M.S., Chemical Engineering, Carnegie Mellon University
B.E., Polymer Material and Engineering, Jilin University

Carnegie Mellon University
Pittsburgh, Pennsylvania

August 2018

To my family.

ACKNOWLEDGMENTS

My furthest and deepest gratitude goes to my advisor and mentor, Prof. B. Erik Ydstie, for introducing me to the area of process control, offering wise and supportive guidance, and building and keeping my morale through this five-year journey. While I was still a master student doing research with Erik, I always exited our meetings with excitement about next step work and a fuller perspective on the problems. It is still the same feeling that I have today. As a student with a chemistry background and not much computational experience at the beginning, I could always get help and extra time from Erik to catch up with engineering fundamentals, and was always encouraged by Erik to propose my own ideas and learn from its implementation and improvements. He once said that it is never the knowledge that one should learn through a PhD, but the way of thinking precisely and clearly, which is one thing that I will keep practicing and attempt to achieve 'asymptotically' for the rest of my life.

Secondly, I would like to thank my committee members, Dr. John Wassick, Prof. Larry Biegler, Prof. Sinopoli Bruno, and Prof. John Kitchin, for their constructive inputs. Dr. Wassick has involved from the beginning of the project, and has given instructive and practical advice from his industrial experience. Other than receiving critical evaluations on my thesis work from all other committee members, I have also taken courses from them that have provided me with the important tools for my research. The thesis work would not be possible without the funding from and collaboration with DOW. I would like to thank the team at DOW, including Tim Capparella, Dr. Jeff Ferrio, Brandon Wassick and Dr. Pradeep Suresh, for their time and effort. Through the collaboration, many industrial experiments based

the thesis work have been conducted by Tim, and his high standards for careful and comprehensible documentation helps us tremendously in troubleshooting and improving the method. Also, I would like to thank Dana from Ydstie group, for fruitful discussions on our research. It has been exciting to see application of our proposed method in atmospheric problems.

Also, I would like to thank my colleagues and friends from the PSE community and from the department. I remember when I decided to pursue my PhD at the same place where I obtained my Master, it was not only because of the excellent research conducted in the department, but also because of the people that I met here who always amazed and charged me through our interactions. I have been surrounded by this extending group of people since then. In particular, I would like to thank Joyce, Yajun and Jiaying for their friendship, encouragement and continuing support. Moreover, I owe thanks to the department's faculty and staff that have helped me many times in various situations.

Last but not least, I would like to thank my family for their unconditional support, love and warmth, and setting excellent examples for me about what one can achieve through persistence and hard work. I would like to thank my husband, Qi Zhang, for being the source of energy and the perfect company, in good times and in times when everything seems to go against you. I would like to thank my parents, Mr. Wenbin Zhao and Mrs. Xianhong Zhang, who could not have been more supportive and have shaped me into the person I am.

ABSTRACT

In this thesis, we develop a passivity-based adaptive control framework for controlling nonlinear processes with uncertainty. The development of the method is motivated by the question whether we can control reaction systems without the knowledge of reaction kinetics.

The proposed adaptive control framework incorporates the measurements' derivative information in order to estimate the uncertainty involved in output dynamics. The output dynamics is assumed to take a special control-affine structure, and by using the output's derivative information we can avoid using internal state dynamics, which is not usually available. Passivity theory is applied for control and estimation designs and overall closed-loop stability is achieved. By extending the passivity-based control to systems with relative degree higher than one through backstepping, we can obtain cascade feedback schemes with PID controllers that overall control convergence is guaranteed.

The proposed framework allows us to control reaction systems without knowing the reaction kinetics, and estimate unmeasured compositions by utilizing the available partially linear structure of internal dynamics. A reactor temperature control problem that usually has high relative degree is used to illustrate the application of passivity-based backstepping control, and results from industrial trials are presented.

CONTENTS

LIST OF FIGURES

LIST OF TABLES

1. INTRODUCTION

Efficient on-line control of chemical reactions is crucial for the safe and cost-competitive operation of chemical production processes. Advanced model-based control is an effective means of achieving improved process performance. However, due to the complexity and nonlinear behavior of chemical reactions, it is difficult to derive accurate kinetic reactor models needed in many control systems. Moreover, the iterative process of creating high-quality kinetic models through experiments, model construction, and validation is time-consuming.

The main objective of this thesis is to develop a framework for adaptive control of chemical reactors, that does not require accurate reaction kinetics data. In this way, the method developed allows us to circumvent the above-mentioned modeling challenge.

In this work, we address the chemical reactor control problem from a feedback control perspective by deriving estimation and control schemes for two general classes of systems. We show that the proposed passivity-based adaptive control approach can be used for the control of control-affine nonlinear systems with uncertainty; and if the system's internal dynamics can be written in a partially linear form, state estimation is possible. Although our main application is the control of reaction systems, by considering general model formulations, the proposed framework is applicable in more general settings. We present computational results and preliminary results from industrial experiments of chemical reactions controlled with the proposed approach.

The rest of this chapter is structured as follows. Section 1.1 introduces two classes of systems that we consider throughout the thesis, and discusses how they

can be used to represent the reactor control problem and derive control that does not use the knowledge of reaction kinetics. In Section 1.2, we review existing literature on relevant topics related to this work. Section 1.3 gives an overview of the remaining chapters of the thesis.

1.1. Motivation and Thesis Objective

In this thesis, we investigate the usage of outputs measurements and their derivative information for estimating the time-varying uncertainty in nonlinear control systems. Passivity provides the theoretical framework for developing the parameter estimation and output tracking schemes.

We consider nonlinear systems described by the following set of differential equations:

$$\frac{dx}{dt} = f(x) + g(x,u) \tag{1.1a}$$

$$y = h(x) \tag{1.1b}$$

$$y_d = \dot{y} \tag{1.1c}$$

where $x \in \mathbf{X} \subseteq \mathbb{R}^n$ represents the vector of states, $u \in \mathbb{R}^m$ represents the vector of control inputs, and $y \in \mathbb{R}^m$ represents the vector of control outputs. Also, we can measure the time derivative of y, denoted by $y_d \in \mathbb{R}^m$. The vector functions f, g, h are continuously differentiable (C^1) with proper dimensions.

System (1.1a) with output (1.1b) is passive, if there is a nonnegative storage function $W(x)$, s.t.

$$\frac{dW(x)}{dt} \leq u^T y$$

Clearly, passivity is a relationship of a system's inputs and outputs. In our proposed control and estimation methods, we design general passivation transformations on system (1.1), and the resulting passive transformed systems will facilitate the control and estimation designs. The new idea we use is to include measured

output derivatives (1.1c) in the passivity-based estimation scheme.

We assume the measurement vector y, so that the output differential equation takes the following form:

$$\frac{dy}{dt} = L_f h + L_g h = \bar{p}(y) + D\Delta p(x) + \phi(y)u. \tag{1.1d}$$

Here, $\bar{p} \in C^1$ represents the known part of the production rate term, $\Delta p \in C^1$ represents the uncertainty, and $\phi(y)u$ is the supply rate term. D is the known uncertainty involvement matrix. $\bar{p}$ and ϕ can also depend on other known disturbances, parameters other than the measurements vector, and essentially, they can be determined accurately online. Under the circumstance that the production rate $\Delta\hat{p}(x)$ is unknown, we want to determine the control input u that drives the output y to track its setpoint y^*.

Farschman et al. (1998) defines concept of inventory as additive nonnegative extensive variables, such as energy and mass, so that the model used for inventory controller design is inventory balance equations with rates of production and supply (including both addition and depletion). Here, we apply the similar idea to derive the uncertainty structure that we want to address. Here, the output y is not limited to inventories, and can also be other measurable variables, such as concentration or temperature, etc.

A special case of (1.1) is the following system with a partially linear structure:

$$\frac{dx}{dt} = Ax + Bu + D\mu(x,t) \tag{1.2a}$$

$$y = Cx \tag{1.2b}$$

$$y_d = C\dot{x}, \tag{1.2c}$$

where the notation is the same as in the general nonlinear case. Here, $\mu \in \mathbb{R}^q$ represents an unknown function of the unmeasured states x, which is the uncertainty in the model. A, B, C, D are known linear matrices of proper dimensions. We want to design a control law for u to track a time-varying setpoint profile $y^*(t)$, in the

presence of unknown μ. We use the same idea from the previous nonlinear system by assuming with measurement y we can write output differential equations as:

$$\frac{dy}{dt} = \underbrace{CAx + CD\mu}_{\Delta p(x)} + \underbrace{CB}_{\phi} u \tag{1.2d}$$

where the uncertainty is again the unknown production rate term $\Delta p(x)$.

For both systems with similar output dynamics with uncertainty structure, (1.1d) and (1.2d), if the bounds of uncertainty are known, we could use robust control to ensure closed-loop stability (Wang & Ydstie, 2007). A less conservative option is to implement adaptive control that estimates and uses the uncertainty to determine the control input. In this thesis, the latter approach is examined.

The proposed adaptive control framework is developed to address the following problems:

1. For both systems, (1.1) and (1.2), how to estimate the unknown part of production rate $\Delta p(x)$?

2. For the partially linear system (1.2), can we estimate the unmeasured state x and μ in the higher order dynamics?

3. For both systems, how to control y to track y^* with the estimates $\Delta\hat{p}$?

4. How to extend the passivity-based control framework for systems with relative degree greater than one?

To further motivate the formulation and problem statement in the context of reactor control, we give a reactor temperature control example.

Motivating Example The model of a continuous stirred-tank reactor (CSTR) involving n_r reactions and n_c species is:

$$\frac{dC}{dt} = -\frac{F_{in}}{V_r}C + \frac{F_{in}}{V_r}C_{in} + \nu r(C, T_r) \tag{1.3}$$

$$y = T_r(C) \tag{1.4}$$

$$y_d = \dot{T}_r(C) \tag{1.5}$$

where $C \in \mathbb{R}^{n_c}$ are the state variables, i.e. the concentrations of the involved species, and measured output T_r is the reactor temperature, which is a function of the composition. Other known process variables and parameters are, F_{in} representing inlet flow rate, V_r representing reactor volume, C_{in} representing inlet concentrations, and ν being the stoichiometric matrix. Based on energy and mole balance, we can write the temperature differential equation as:

$$\frac{dT_r}{dt} = \frac{F_{in}}{V_r \rho C_p} \left(\rho_{in} C_{p,in} T_{in} - \rho C_p T_r\right) - \frac{Q_j}{V_r \rho C_p} - \frac{\Delta H_r r}{C_p \rho}. \tag{1.6}$$

The control problem we consider is to control reactor temperature, when the concentration vector is not measured, and the reaction kinetics is not known. We can put this temperature dynamics into developed formulation (1.1d) with uncertainty, where

$$\Delta p(C, T_r) = -\frac{\Delta H_r r(C)}{C_p \rho}, \quad \phi^T(T_r) = \begin{bmatrix} \frac{F_{in}}{V_r \rho C_p} \left(\rho_{in} C_{p,in} T_{in} - \rho C_p T_r\right) \\ -\frac{1}{V_r \rho C_p} \end{bmatrix}, \quad u = \begin{bmatrix} 0 \\ Q_j \end{bmatrix} \tag{1.7}$$

The control input is the heat transfer rate between reactor and the jacket, Q_j. The unknown production term Δp is related to the reaction heat generation rate. It is related to the unmeasured concentrations and unknown kinetics, which is essentially the higher order dynamics (1.3). We proposed to compensate for them by using temperature derivative measurements in the proposed estimation scheme.

1.2. Literature Review

In the following, we review existing contributions in the literature on related topics corresponding to the questions being raised in last section.

Section 1.2.1 reviews works that consider the estimation of unknown inputs, referring to the uncertainty in the output dynamics. Section 1.2.2 reviews the re-

construction methods of measurement derivatives, and its usage in uncertainty estimation. The literature reviewed in these two sections provide background of our estimation scheme to answer Question 1.

Section 1.2.3 provides the background of our approach in response to Question 2, state estimation for the partially linear system (1.2). We review the unknown input observer (UIO) and a special case thereof, the asymptotic observer (AS) tailored for estimating unmeasured reaction compositions. Section 1.2.4 provides a review of the concepts and applications of reaction variants and invariants, which are the transformed states used for constructing asymptotic observers.

To provide background on techniques answering the rest two control related questions, Section 1.2.5 reviews the topic of passivity-based adaptive control, and our adaptive control is presented in Chapter 5; Section 1.2.6 reviews the topic of control systems with high relative degree, and our passivity-based solution is given in Chapter 6.

1.2.1. Estimation of Unknown Inputs

A process model usually comes with uncertainties, which can be collectively modeled as an unknown vector in the model, and determined through estimation algorithms using measured outputs. The unknown vector is referred as unknown inputs in the literature, which includes unknown nonlinearities, parameters, faults and external disturbances (Mhamdi & Marquardt, 2004). Unknown inputs reconstruction methods are usually used to improve tracking control and monitoring for systems with uncertainty. The problem is relevant when we estimate some unknown part of the inputs. Examples include the estimation of exerted force in machine tool applications (Corless & Tu, 1998), the magnitude of unknown maneuvers in tracking problems (Lee & Tahk, 1999), fault detection (Chen et al., 1996), and reaction heat estimation (Schuler & Schmidt, 1992). For reactor modeling, mechanisms of reactions, heat and mass transfers are hard to model accurately or sometimes remain unknown, the relevant rates without good quality model can be considered as unknown inputs.

Existing methods to design the estimation schemes fall into three categories. The first type is state observer based method, where the unknown inputs are proposed with a certain dynamic model, and estimates are obtained through using state observer techniques derived from Luenberger or Kalman filter. Schuler & Schmidt (1992) applied Kalman filter technique to estimate the reaction heat and other observable heat flows based on a reactor calorimetric model. Aguilar-López (2003) and Aguilar et al. (2002) used the high gain observer and the interval observer respectively to estimate the reaction heat. The second type of method solves an on-line optimization problem to minimize the residual errors of the measurements, to which the moving horizon estimator belongs. The third type are dynamics inversion based methods, of which underlying idea is analogy to synthesize a model-based controller. The estimates are calculated using a process model inverse to force the estimated outputs converge to the measured values with a certain stability (Tatiraju & Soroush, 1998). Tatiraju & Soroush (1998) designed an inversion based estimator for reaction heat generation rate and heat transfer coefficient and show that the proposed method can out perform state observer based method when model mismatch and measurement noise exist through simulations. Mhamdi & Marquardt (2004) and Zhao et al. (2016) used nonlinear system inversion method and conditions to estimates reaction rates.

In Chapter 3, we propose the passivity-based input estimator that falls into the third category. It is later applied for reaction rates and reaction rates using conservation balances, and the approach avoids the difficulty of modeling reaction kinetics.

1.2.2. Approximated Measurement Derivatives for Parameter Estimation

Derivatives of process measurements provide useful information for process monitoring and control (Preisig, 1988; Preisig & Rippin, 1993). Fundamentally, when the analytical expression of the signal is not known, perfect estimation is not possible (Levant, 1998). Various of numerical differentiator are proposed to reconstruct derivatives from noisy data.

Levant (1998) developed the sliding mode differentiator using knowledge of Lipschitz constant and maximum noise magnitude. Mboup et al. (2007) proposed the algebraic time-derivative estimation method that calculates the derivative estimates as linear combinations of finite time-integrations of the signal. Reger & Jouffroy (2009) derived the same result from the standard linear system reconstructibility theory. The Savitzky-Golay filter (Baedecker, 1985) for time derivative estimation assumes that the signal can be expressed as a polynomial. The derivatives of the regressed polynomial are estimated derivatives. Co & Ydstie (1990) applied modulating function and fast Fourier transformation method to estimate derivatives. A well approximated derivatives will reduce transmitted noise to the estimation without losing much on capturing the output true dynamics.

Including measurement derivatives in control and estimation algorithms is controversial due to the existence of derivative reconstruction errors and exaggeration of noise. However, as many numerical differentiator techniques have been developed, we propose to use derivative information in our method for both control and estimation purpose.

1.2.3. Unknown Input Observer and Asymptotic Observer

Measuring the states of reactions, including compositions, temperature, pressure etc., in a on-line fashion facilitates making timely control decisions and preventing process disruptions, process shutdowns and even failures (Ali et al., 2015). However, since on-line measurement devises especially for measuring compositions are expensive, the development of soft sensors and state observers for estimating unmeasured variables has been of major interest in the process industry. The classic Luenberger observer (Luenberger, 1971) and Kalman filter (Welch & Bishop, 1995) lay the conceptual and theoretical foundation for the later development of a variety of state observers (Ali et al., 2015).

When the process model has uncertain or unknown dynamics, the extended Kalman filter and Luenberger observer cannot be directly applied to estimate unmeasured states. To address this type of state estimation problem, the unknown

input observers (UIO) were proposed (Wang et al., 1975; Hou & Muller, 1992; Park & Stein, 1988a; Darouach et al., 1994).

The problem becomes relevant in the context of chemical reactor, when the reaction kinetics for modeling reaction rates is an absent knowledge. For this situation, Bastin & Dochain (1990) and Dochain et al. (1992, 2009) proposed the asymptotic observer (OA) for unmeasured composition estimation, with the reaction rates considered as the unknown inputs. The developments of OA and UIO both involve transforming the states of the system into two components, the invariants and variants. The invariants evolution is not affected by the unknown inputs, and the effects of the unknown inputs is only constrained in the variants subspace. Then, a Luenburger observer is applied to invariants unknown-input-free dynamics, and finally estimated invariants together with output measurements are used to compute state estimates.

Though the most UIO considers only state estimation, unknown input reconstruction are performed simultaneously in some UIO designs. Park & Stein (1988b) inverted the state dynamics and use derivatives of output measurements to reconstruct the unknown input vector. Corless & Tu (1998) put constraints on how fast the varying inputs change to avoid using derivatives of output measurements.

1.2.4. Reaction Variants and Invariants

The first step in constructing a UIO or an AO is to express the reaction model with transformed states, the variants and invariants. In the reaction context, concepts of reaction variants and invariants were introduced by Asbjørnsen and co-workers in the early 1970s (Asbjørnsen, 1972; Asbjørnsen & Fjeld, 1970; Fjeld et al., 1974), and nonunique transformation is found through reaction stoichiometry. The reaction variants define state variables that are affected by the reactions, and the reaction invariants define state variables that are not influenced by the advancement of the reactions. It was shown that the dynamics of a reaction system with n_r independent reactions and n_c species can be decomposed into n_r variants and $n_c - n_r$ invariants.

The theory was proposed for the purpose of model reduction to ease the anal-

ysis of nonlinear reaction system dynamics. Systematic studies on formulating linear and nonlinear mappings to obtain reaction variant and invariant form models have been performed by Srinivasan et al. (1998) and Rodrigues et al. (2015).

The concept of reaction variants has been applied to control reaction systems. It was shown that the unstable dynamics of the reaction system can be controlled by controlling the dynamics of reaction variants (Hoang et al., 2014). Feedback linearizability of the reduced reaction variants model was discussed in Srinivasan et al. (1998), and the corresponding feedback linearization control approach was proposed by Rodrigues et al. (2015) for reactor temperature control. Passivity-based inventory control was applied by Hoang et al. (2014) for reduced reaction variants control. However, previous control strategies are based on the assumption that complete composition information is available through on-line measurements.

There are also works regarding the control of reaction systems with the integration of the estimates given by the AO. In Hoang et al. (2012) and Hoang et al. (2013), the usage of observer estimates for feedback control is illustrated through the passivity-based inventory control and nonlinear control, respectively; however, unlike the observer, the proposed control schemes in these papers require the knowledge of reaction kinetics. In this thesis, we propose to integrate the AO in control development that does not require the knowledge of reaction kinetics.

1.2.5. Passivity-based Adaptive Control

Passivity is an input-output property of process systems, and very useful in stability analysis for interconnected systems (Bao & Lee, 2007). Farschman et al. (1998) used macroscopic balance of inventories (for example total mass and energy) to construct the passive input-output pairs, and proposed inventory control based on the idea that passive system can be stabilized through a input strict passive controller. To handle system uncertainties, sliding mode based robust inventory control Wang & Ydstie (2007) was developed where high gain feedback was used to achieved global stability. Li et al. (2010) proposed the adaptive inventory control that was able to estimate constant uncertainty and achieved control stability at the

same time. In this thesis, we propose the passivity-based adaptive control scheme where time-varying uncertainty can be estimated as well.

1.2.6. Passivity-based Control of Systems with Relative Degree Higher Than One

Passivity-based control techniques are well developed for systems with relative degree one. In practice, many control problems have high-relative degree, and it is also worthwhile to generalize the theory to cover those types of systems.

The notion of relative degree will be given in Chapter 2, and here we give a real example in chemical reactor control and current control practice. In most reactor temperature control configurations, the actual manipulated variable, such as cooling water flow rate or steam flow rate, usually does not directly act on the reactor temperature. Its effect is transferred through intermediate cooling/heating mechanisms. Proportional-integral-derivative (PID) controllers arranged in a cascade fashion are usually adopted to control this type of systems, where the relative degree is higher than one. The cascade control includes more state measurements and captures disturbance upsets in the process more effectively (Seborg et al., 2010). However, this traditional control method based on a linear control theory has no guarantee of stability when nonlinear dynamics is involved and the process is not operated at a steady state, as in the case of semi-batch or batch reactions.

The backstepping method is widely used to control nonlinear systems with relative degree higher than one (Krstic et al., 1995). Application of backstepping results in a control logic similar to a cascade structure, and it can be easily implemented in standard process control systems, such as the Emerson DeltaV system used in the industrial trials presented in the thesis. The method has been studied by researchers in the chemical process control area to control continuous chemical reactors. Gopaluni et al. (2003) applied the backstepping method to control the composition of a CSTR. Nonlinear nonadaptive and adaptive backstepping controllers were designed for cases with and without parameter uncertainty, respectively. A robust adaptive backstepping controller was designed using Lyapunov stability theory in this work. Similarly, Biswas & Samanta (2013) designed an adaptive back-

stepping controller to control the monomer concentration and the temperature of a polymerization CSTR. Both works show that the adaptive backstepping method guarantees setpoint tracking in the presence of parameter uncertainty. Salehi & Shahrokhi (2009) introduced the fuzzy estimator into the backstepping method and used this approach for temperature control in a CSTR. Hua et al. (2009) discussed the development of backstepping for systems with time delay, and applied the design to a two-stage reactor system.

The connection between passivity and backstepping control was first shown in Kokotović et al. (1992), where the backstepping was used to remove the limitation of passivity for systems of relative degree higher than one. In the thesis, we propose a model-based cascade control scheme through backstepping method, and used passivity-based control incorporating PID for control error feedback to design control law at individual level.

1.3. Thesis Outline

The remainder of the thesis is organized as follows,and in according to the questions we posed in the in beginning of this chapter:

- In Chapter 2, we review stability, passivity and passivity-based control to introduce the theoretical foundations for this work.

- In Chapter 3, we present our answer to Question 1. We address the estimation of the uncertainty $\mu(x,t)$ in both the partially linear system case and the unknown production term $p(x)$ in the nonlinear system case, (1.1). In the given reactor control problem, we estimate reaction rates and transport rates if multi-phase reaction is involved and heat transfer is considered.

- In Chapter 4, we present our answer to Question 2. We address the estimation of unmeasured states x without knowing $\mu(x,t)$ for the partially linear system (1.2). In the given reactor system, the compositions are the unmeasured states. We present the derivations of the UIO and AO, the existence condi-

tions, discuss their connections and issues regarding estimation convergence, and apply the AO to both homogeneous and heterogeneous reactions.

- In Chapter 5, we present our answer to Question 3. We integrate the observers and use estimates with feedback control to adaptively control y, for the systems of interest, and to derive conditions under which zero dynamics are stable. In the given reactor control problem, we use proposed adaptive control to stabilize a semi-batch reactor.

- In Chapter 6, we present our answer to Question 4. We extend the passivity-based control to control nonlinear systems with relative degree higher than one. The proposed approach is applied to the on-line temperature control for a jacked polymerization reactor, and industrial trial result is presented.

- In Chapter 7, we provide a summary of the thesis and recommendations for future work.

2. Stability, Passivity and Zero Dynamics

In this chapter, we review the fundamental concepts of stability and passivity, and show how we can infer overall stability of interconnected systems from passivity of individual systems. This idea is useful in controller design since a feedback control loop can be viewed as a connected system of a process and a controller.

2.1. Stability

A well-controlled process should be stable in a sense that it can withstand small perturbations and converge to the desired operating point. Achieving good stability should also be kept in mind when we design and integrate estimation schemes with controllers to design adaptive controllers.

In the following, we present the definitions of uniform stability, uniformly asymptotic stability, and uniformly exponential stability.

Definition 2.1. Consider the following system:

$$\frac{dx}{dt} = f(x), \tag{2.1}$$

with its equilibrium point at the origin, i.e. $f(0) = 0$. The origin is said to be

- uniformly stable, if for any $\varepsilon > 0$, there is a $\delta(\varepsilon) > 0$ such that $\|x(0)\| < \delta(\varepsilon)$ implies $\|x(t)\| < \varepsilon, \forall t \geq 0$.
- uniformly asymptotically stable, if there is a positive constant δ, such that $\|x(0)\| < \delta$ implies $\|x(t)\| \to 0$ as $t \to \infty$.

- uniformly exponentially stable, if there are positive constants δ, k, λ, such that $\|x(t)\| \leq k\|x(0)\|e^{-\lambda(t)}, \forall \|x(0)\| < \delta$.

Such stabilities hold globally if the corresponding inequalities are satisfied for any initial condition $x(0) \in \mathbb{X}$.

The most obvious way to determine stability is from the analytical solution of (2.1). However, it can can be a difficult task if the model is of high order, and can even be impossible if there is uncertainty in the differential equations. Lyapunov stability theory provides a tool to determine the stability without obtaining an analytical solution.

A Lyapunov function $V(x)$ is a continuously differentiable, positive definite scalar function of the state vector x. One can think of it as a generalized energy function, for which the energy is greater than zero anywhere in the $\mathbb{X}$ domain other than at the equilibrium point, where the energy is zero. The stability, asymptotic stability, and exponential stability conditions of the equilibrium point can be derived based on $V(x)$ and its time derivative, $\dot{V}(x)$, using the following Lyapunov theorem.

Theorem 2.2. Consider system (2.1), and let $V(x) : \mathbb{X} \to \mathbb{R}^+$ be a continuously differentiable, positive definite function.

- if $\dot{V}(x)$ is negative semidefinite, the origin is stable.
- if $\dot{V}(x)$ is negative definite, the origin is asymptotically stable..
- if $\dot{V}(x) \leq -kV(x), k > 0$, the origin is exponentially stable.

To put stability in to the context of control, we consider the system:

$$\frac{dx}{dt} = f(x) + g(x)u \tag{2.2a}$$

$$y = h(x) \tag{2.2b}$$

where $x \in \mathbb{X} \subseteq \mathbb{R}^n$ is the state vector; $u \in \mathbb{U} \subseteq \mathbb{R}^m$ is the control input vector; $y \in \mathbb{R}^m$ is the output vector; and f and h are C^1 vector functions.

The objective of process control is to control and stabilize the process at a desired operating state. This desired operating state can be denoted as the set point of the output y^*. We design control input so that y^* is a asymptotically or even exponentially stable equilibrium for the closed-loop system. For example, if we can measure the state and design an appropriate state feedback control law to calculate the control input $u = \alpha(x)$, then the closed-loop system:

$$\frac{dx}{dt} = f(x) + g(x)\alpha(x) \tag{2.3}$$

$$y = h(x), \tag{2.4}$$

should be asymptotically stable at y^*. With a change of coordinates, y^* being a stable equilibrium point indicates that the control error $e = y^* - y$ is stable at the origin, $e = 0$.

2.2. Passivity and Passivity-based Control

Definition 2.3. A system is passive if there exists a continuously differentiable, positive semi-definite function, $W(x)$ (called storage function), such that

$$\frac{dW(x)}{dt} \leq u(t)^T y(t), \forall t \geq 0. \tag{2.5}$$

Moreover, the system is said to be input strictly passive if

$$\frac{dW(x)}{dt} \leq u(t)^T y(t) - u^T \phi(u), \quad u^T \phi(u) > 0, \ \forall u \neq 0, \tag{2.6}$$

where ϕ is a function of u, that ensures $u^T \phi(u)$ positive definite.

Passivity is a little different from Lyapunov stability, since it is an input-output property. Passive systems are very useful when we study the overall stability of interconnected systems. In this work, we are interested in using passivity of systems to help us approach closed-loop stability either from a parameter estimation or a control point of view.

A control loop is essentially a negative feedback connection of a controller and

a process or a transformation of the process if some model-based inversion is involved. Passivity arises if we choose a right pair of input and output. Passivity thereof depends on the choice of the input and output, and a system may be passive for some combinations of inputs and outputs and not passive for the other choices.

For control purposes, in the following theorem, we define a pair of synthetic inputs and outputs that can be generally applied to system (2.2), and transform the system into a passive one.

Theorem 2.4. Consider system (2.2) with output equation:

$$y = h(x), \tag{2.7}$$

and a control setpoint y^*. We define a pair of synthetic inputs u_c and outputs e:

$$u_c = \frac{dy^*}{dt} - L_f h(x) - L_g h(x) u, \quad e = y^* - y, \tag{2.8}$$

where rank$(L_g h(x)) = m$, indicating that the system (2.2) has relative degree one.$L_f h(x)$ and $L_g h(x)$ are Lie derivatives, defined as:

$$L_f h(x) = \frac{\partial h}{\partial x} f(x), \quad L_g h(x) = \frac{\partial h}{\partial x} g(x) \tag{2.9}$$

Then, transformed system,

$$\frac{de}{dt} = u_c, \tag{2.10}$$

is passive with the storage function $W = \frac{1}{2} e^T e$.

Proof. The passivity is shown by taking the time derivative of W. We find

$$\frac{dW}{dt} = e^T u_c, \tag{2.11}$$

and the passivity result follows according to Definition 2.3. □

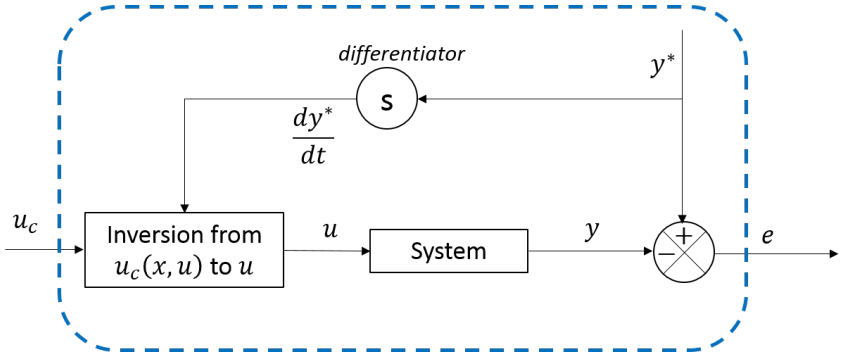

Figure 2.1: Schematic of passive transformation

Figure 2.1 shows the passive transformation graphically. In order to utilize the passivation transformation in Theorem 2.4 for controlling y to y^*, we need to be able to determine u uniquely from u_c, which can be ensured by the rank condition $\text{rank}(L_g h(x)) = m$. It also means the original system with input u and output y has relative degree one. The definition of relative degree is shown in the following.

Definition 2.5. (Relative degree) The relative degree r of a SISO system output y to the manipulated input u is the smallest integer for which:

$$L_g L_f^{r-1} h(x) \neq 0. \tag{2.12}$$

Therefore, the transformation in Theorem 2.4 is for controlling relative-degree-one systems. The transformation and consequent passivity-based control for high-relative-degree SISO systems will be addressed in Chapter 6 using backstepping which is a generalization of cascade control.

With the transformation presented above, we can take a look at how we can control a passive system.

Theorem 2.6. The passive system (2.10) can be asymptotically stabilized at origin $e = 0$ with negative proportional feedback control action:

$$u_c = -K_c e, \quad K_c > 0. \tag{2.13}$$

Proof. Consider the Lyapunov function $V = W = \frac{1}{2} e^T e$. For $u_c = -K_c e$, the time

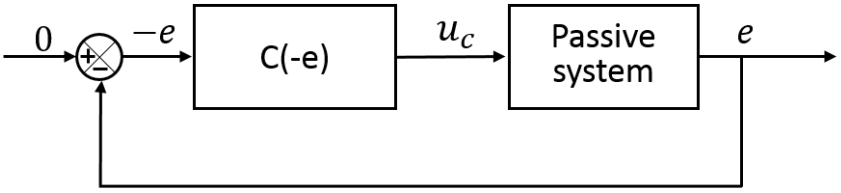

Figure 2.2: Feedback connection of the passive system and a controller

derivative of the Lyapunov function is:

$$\frac{dV}{dt} = -K_c e^T e. \tag{2.14}$$

The Lyapunov function strictly decreases, until the control error reaches the origin, and $\dot{V} = 0$. Therefore, the origin $e = 0$ is asymptotically stable. □

Theorem 2.7. Consider the negative feedback connection of the passive system and a controller $C(\cdot)$ shown in Figure 2.2.

- If the controller is input strictly passive, then the closed-loop is L_2 stable;
- If the storage functions of the passive and the input strictly passive controller are positive definite functions of error vector e, then the closed-loop is asymptotically stable.

Proof. First, we prove the first statement. Define W_1 and W_2 as the storage functions of the input strictly passive controller and the passive system, respectively. The time derivatives of the two subsystems' storage functions satisfy:

$$\dot{W}_1 \leq -e^T u_c - \gamma e^T e, \quad \dot{W}_2 \leq u_c^T e, \tag{2.15}$$

where $\gamma > 0$. Then, the sum of two time derivatives is:

$$\dot{W}_1 + \dot{W}_2 \leq -\gamma e^T e. \tag{2.16}$$

Define

$$W = W_1 + W_2, \tag{2.17}$$

and we can write,

$$\int_{t_0}^{t} e^T e d\tau \leq \frac{1}{\gamma}\left(W(t_0) - W(t)\right) \leq \frac{1}{\gamma} W(t_0). \tag{2.18}$$

Hence, $e \in L_2$, and the feedback connection is stable.

In the second statement, since W becomes positive definite function of e, and

$$\dot{W(e)} \leq -\gamma e^T e < 0, \quad \text{when } e \neq 0, \text{ and } \dot{W}(0) = 0, \tag{2.19}$$

the closed-loop is asymptotically stable. □

Theorem 2.8. The PID control

$$u = k_c\left[e(t) + \frac{1}{\tau_I}\int_0^t e(\tau)d\tau + \tau_D \frac{de(t)}{dt}\right], \tag{2.20}$$

where $k_c > 0, \tau_I > 0$ and $\tau_D \geq 0$, is input strictly passive with input $e \in R$ and output $u \in R$. The dissipation rate is given by $\beta_C = k_c$.

Proof. Define the variable s as : $s = \int_0^t e(\tau)d\tau$, and the storage function $W_{PID} = \frac{k_c}{2\tau_I}s^2 + \frac{k_c\tau_D}{2}e^2$. Differentiate the storage function W_{PID} to obtain:

$$\begin{aligned}
\dot{W}_{PID} &= \frac{k_c}{\tau_I} s\dot{s} + k_c\tau_D e\dot{e} \\
&= \frac{k_c}{\tau_I} se + k_c\tau_D e\dot{e} \\
&= e\left[k_c e + \frac{k_c}{\tau_I}s + k_c\tau_D\dot{e}\right] - k_c e^2 \\
&= eu - k_c e^2
\end{aligned} \tag{2.21}$$

Since $-k_c e^2$ is negative definite, the PID controller is input strictly passive as depicted in Definition 2.3. □

In Chapter 3, similar transformations will be performed to derive a passivity-based input observer to estimate unknown inputs to the system. From the parameter estimation perspective, we consider the difference between the estimated state and the true state, or the estimated output and the measured output, as the synthetic output. The estimated state or estimated output is obtained from integrating system dynamics using the estimated parameter. The synthetic input is the derivative of this synthetic output.

2.3. Zero Dynamics Stability with Passivity-based Control

Passivity-based control addresses the control problem from an input and output perspective. It can ensure the stabilization and tracking of the output, but not necessary of the internal states. We illustrate this point through comparing the control of a single-input and single-output (SISO) linear system with a classic state-feedback pole placement method and the passivity-based control method.

Consider the linear system example motivated (Hou & Muller, 1992):

$$\dot{x} = \underbrace{\begin{bmatrix} -1 & 1 & 0 \\ -1 & 0 & 0 \\ 0 & -1 & -1 \end{bmatrix}}_{A} x + \underbrace{\begin{bmatrix} 1 \\ 0 \\ 0 \end{bmatrix}}_{B} u \tag{2.22}$$

$$y = Cx. \tag{2.23}$$

The pair (A, B) is controllable, indicating that the control input vector u can control the system from any initial state to any final state. We are interested in controlling the output y at a reference value y^*. We will analyze three control cases with three different output C matrices. By changing the output matrix, we have different zero dynamics. We show that

- the zero dynamics stability cannot be ensured by the passivity-based control if the system has nonnegative zeros; but with classic state-feedback control, the zero dynamics can be guaranteed to be stable as long as the system is

controllable;

- tracking a non-constant reference cannot be ensured by the classic state-feedback control if the system has zeros at the origin; but tracking can be achieved with passivity-based control, as long as $\mathrm{rank}(CB) = \dim(y) = \dim(u)$.

For all three cases, with state-feedback control we place the state dynamics closed-loop poles at [-1 -2 -0.5], and with passivity-based control the eigenvalue of control error dynamics is placed at -1, with scalar gain $K_c = 1$.

- Case 1. The output is:

$$y = \begin{bmatrix} 1 & 1 & 1 \end{bmatrix} x. \tag{2.24}$$

The open-loop transfer function is:

$$G(s) = \frac{s^2}{s^3 + 2s^2 + 2s + 1}. \tag{2.25}$$

The system is controllable and observable, but the zero dynamics has eigenvalues at the origin, reflected by the zeros of the system's transfer function at the origin.

The zero at origin leads to the failure of tracking non-zero reference using state-feedback control. Standard state-feedback with pole placement gives the control law: $u = py^* - kx$, where $k \in \mathbb{R}^3$ is the feedback gain vector chosen to place the closed-loop poles at [-1 -2 -0.5]; p is the feedforward gain to adjust output steady state at the reference. But in this case, since there are two zeros at the origin, the output steady state is fixed at zero. As shown in Figure 2.3a, the output is stabilized at zero instead of the set point $y^* = 2$.

With passivity-based proportional control, the set point $y^* = 2$ is tracked, as shown in Figure 2.3b. But the internal states grow unboundedly, and if we were to simulate it longer, they will not stabilize at any values.

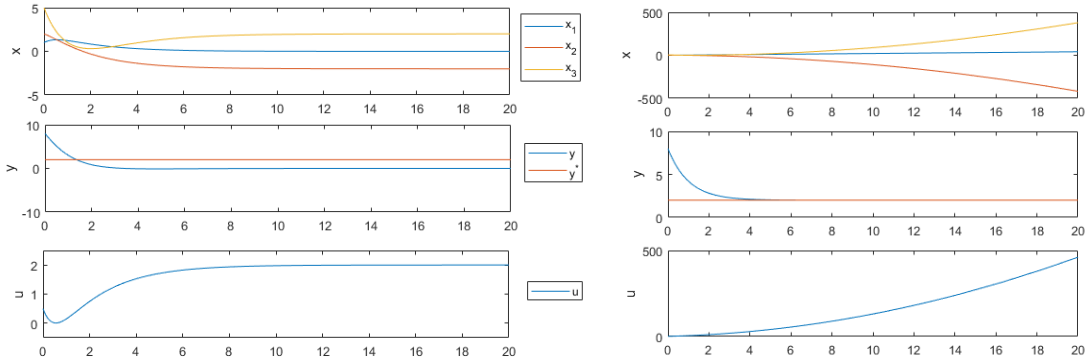

(a) State-feedback Control **(b)** Passivity-based Control

Figure 2.3: Case 1 control results

- Case 2. The output is

$$y = \begin{bmatrix} 1 & 1 & 0 \end{bmatrix} x \tag{2.26}$$

The open-loop transfer function is:

$$G(s) = \frac{s^2 - 1}{s^3 + 2s^2 + 2s + 1}. \tag{2.27}$$

The system is unobservable, due to common zero and pole at -1. Also, the system has one unstable zero at 1.

The state-feedback control can ensure the stability of the zero dynamics and the tracking as shown in Figure 2.4a, while the passivity-based control can only ensure the tracking, and the zero dynamics again are not stabilized.

- Case 3. The output is

$$y = \begin{bmatrix} 1 & 0.5 & 2 \end{bmatrix} x. \tag{2.28}$$

The open-loop transfer function is:

$$G(s) = \frac{s^2 + 0.5s + 1.5}{s^3 + 2s^2 + 2s + 1}. \tag{2.29}$$

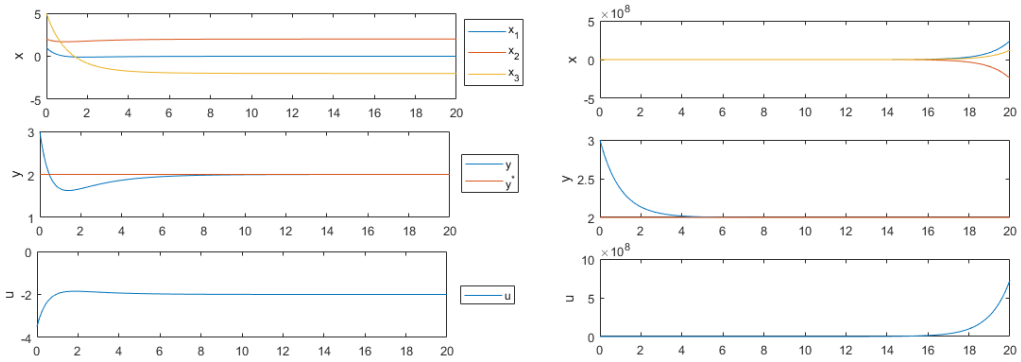

(a) State-feedback Control **(b)** Passivity-based Control

Figure 2.4: Case 2 control results

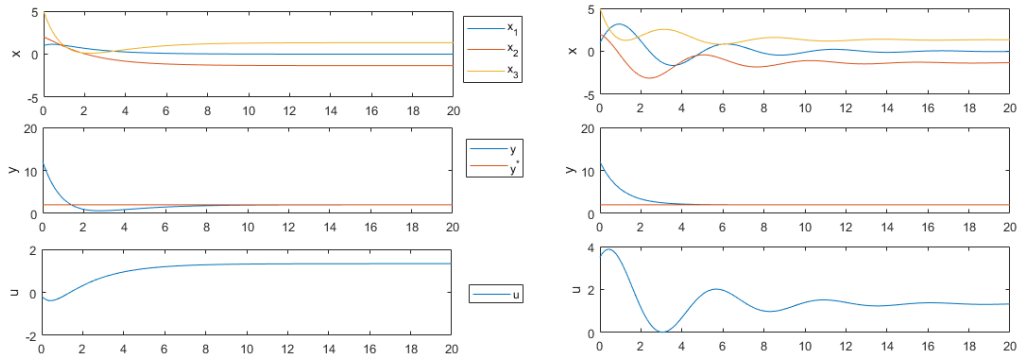

(a) State-feedback Control **(b)** Passivity-based Control

Figure 2.5: Case 3 control result

With this output, the system is observable and has stable zeros.

The state-feedback control and passivity-based control results are shown in the Figures 2.5a and 2.5b, respectively. Both tracking and zero dynamics stabilization are achieved for this case.

The zero dynamics stability analysis shows that passivity-based control focuses on output stabilization and tracking instead of internal states' stability. In the context of controlling a reaction process, we will show later in Chapter 4 that if the number of outputs is at least as large as the number of reactions, the zero dynamics are stable.

2.4. Summary

The fundamental tools of stability and passivity are reviewed. We have given a flavor of passivity-based control through presenting a general transformation that makes a system passive, and then arrived at closed-loop stability by stabilizing it with a proportional and PID control action. We also show that passivity-based control can ensure output tracking but not necessarily zero dynamics stability, depending on whether the system has negative zeros. This idea will be used later in designing the passivity-based input estimator and the adaptive control scheme in Chapters 3 and 5, respectively. It will be further extended and combined with backstepping to control systems with high relative degree in Chapter 6.

3. PASSIVITY-BASED INPUT ESTIMATOR

In this chapter, we propose the passivity-based input estimator (PBIE) that uses output measurements and time derivatives to estimate the uncertainty in the process model. In Section 3.1, we introduce the problem in chemical reaction control that motivates the development of the method and the utilization of the time derivatives of measurements. In Section 3.2, we develop the theory of the proposed PBIE for partially linear systems, and show simulation results of numerical examples; the extension of the estimation method to a class of nonlinear systems is shown in Section 3.3, followed by an application to on-line estimation of the reaction heat generation rate and heat transfer rate in a jacketed chemical reactor. Section 3.5 completes the chapter with a summary and concluding remarks.

3.1. Problem Statement and Motivation

As been proposed in the beginning of the thesis, we generally consider the system with chosen output y could be described as:

$$\frac{dx}{dt} = f(x) + g(x,u) \tag{3.1a}$$

$$y = h(x) \tag{3.1b}$$

$$y_d = \dot{y} \tag{3.1c}$$

$$\frac{dy}{dt} = L_f h + L_g h = \bar{p}(y) + D\Delta p(x) + \phi(y)u. \tag{3.1d}$$

where $y \in \mathbb{R}^m$ refers to measured states and $x \in \mathbb{R}^n$ refers to unmeasured states. We are interested in estimating $\Delta p(x) : \mathbb{R}^{m+n} \to \mathbb{R}^p$, which is a vector of C^1 functions.

In a chemical reaction system context, $\phi(y)u$ represents the supply function, assumed to be known or measured and does not have recursive dependency on the higher order dynamics represented by (3.1a). $p(y,x)$ represents the production function that couples the dynamics of the measured states z with unmeasured x. The knowledge of this time-varying term $p(y,x)$ is useful to compensate in feedback control, indicate of reaction stage, and provide history of reaction evolution. This term could be composed of a known part $\bar{p}(y)$ and an unknown part $D\times\Delta p(x)$ that needs to be estimated on-line. To further explain the problem, we use the following chemical semi-batch reaction example.

Semi-batch reactor example Assume that we have a semi-batch reaction system with only one reaction $A + B \rightarrow C$. The dynamics of the reaction can be modeled as:

$$\frac{dC_A}{dt} = \frac{F_{in}}{V}C_{A,in} - r, \tag{3.2}$$

$$\frac{dC_B}{dt} = \frac{F_{in}}{V}C_{B,in} - r, \tag{3.3}$$

$$\frac{dC_C}{dt} = r, \tag{3.4}$$

$$r = k_0 e^{\frac{-E_a}{RT_r}} C_A C_B, \tag{3.5}$$

$$\frac{dT_r}{dt} = \frac{F_{in}}{V\rho C_p}\left(\rho_{in}C_{p,in}T_{in} - \rho C_p T_r\right) - \frac{\Delta H_r r}{C_p\rho} - \frac{UA(T_r - T_j)}{V\rho C_p}, \tag{3.6}$$

$$\frac{dV}{dt} = F_{in} - F_{out}. \tag{3.7}$$

We can measure the concentration of A, C_A, i.e.

$$y = C_A, \tag{3.8}$$

and want to estimate the reaction rate r. Follow similar notation as for reaction model in Section 1.1.

The conventional way of estimation solves the algebraic-differential equations, (3.2) - (3.7), and uses a regression method, for example a Kalman filter, to match the

model to the measurements. Another way is to just use the differential equation of measured C_A, (3.2). By comparing (3.2) and (3.1d), we assume to know the inlet flow information $\phi = \frac{F_{in}}{V} C_{A,in}$. The task is to estimate the reaction production term $\Delta p(C_A, C_B, T_r, V) = r$.

Obviously, following the conventional approach increases the number of states or requires more measurements. Thus, we ask the question: can we just use (3.2) and measured C_A to achieve the estimation of $r(t)$? If this were possible, we would benefit in two respects:

1. it saves the work of modeling the rest of the system;
2. it frees the estimation task from knowing the reaction kinetics.

The solution seems obvious at the first glance. One might think that we could compute or measure $\frac{dC_A}{dt}$, and then calculate reaction rate r algebraically from (3.2). The obstacles preventing us from doing so are the following:

1. without having the analytical expression of C_A, exact differentiation to obtain $\frac{dC_A}{dt}$ is not possible;
2. if the measurement of C_A is corrupted with noise, differentiation will further exaggerate the noise in the derivatives.

The two obstacles lead us to ask for a better solution that can dampen the noise translated into the estimates of $r(t)$.

Above all, considering only (3.2), and assuming $F_{in}C_{A,in}$ is known, we can measure:

$$y = C_A, \tag{3.9}$$

$$y_d = \frac{dC_A}{dt}, \tag{3.10}$$

but the derivative measurement could be corrupted with some noise. Therefore, the objective is to design an estimator for the time-varying production term $p(x) = r(t)$ with attenuation of noise in the derivative measurements.

3.2. Passivity-based Input Estimator for Partially Linear Systems

3.2.1. Ideal Case

We start with a scalar first order nonlinear system:

$$\dot{z}(t) = az(t) + b\mu(z,t), \quad a < 0, \tag{3.11a}$$

$$y_1(t) = z(t), \tag{3.11b}$$

$$y_2(t) = \dot{z}(t). \tag{3.11c}$$

The system has two outputs. i.e. the measured output and its time derivative. The task is to estimate the time-varying parameter $\mu(z,t)$. Motivated by solving the estimation problem as a control problem, we manipulate the estimated input $\mu(z,t)$ so that the estimation error of the state from the estimator model (3.12) asymptotically declines to zero. Using Lyapunov function, $V(\tilde{z}) = \frac{1}{2}(z-\hat{z})^2$, we use passivity transformation and Theorem 2.6 from Chapter 2 to derive the following passivity-based input estimator to solve the problem:

$$\dot{\hat{z}}(t) = a\hat{z}(t) + b\hat{\mu}(t), \tag{3.12}$$

$$\hat{\mu}(t) = \frac{1}{b}\left(k\left(y_1(t) - \hat{z}(t)\right) + y_2(t) - a\hat{z}(t)\right), \; k > 0, \tag{3.13}$$

where k is the proportional gain. From here, we drop the dependence of time in the notations for convenience.

Theorem 3.1. Given system (3.11a), with unknown time-varying parameter $\mu(t)$, state and time derivative measurements (3.11b), (3.11c), the passivity-based estimator, (3.12) and (3.13), provides asymptotic estimates of unknown parameter.

Proof. Express the true value of the parameter as:

$$\mu = \frac{\dot{z} - az}{b}, \tag{3.14}$$

and substract it from (3.13) to obatin:

$$\mu - \hat{\mu} = -\frac{a+k}{b}(z - \hat{z}). \tag{3.15}$$

The application of Lyapunov function $V(\tilde{z}) = \frac{1}{2}(z - \hat{z})^2 = \tilde{z}^2$ guarantees $z - \hat{z}$ converges to zero since the closed-loop dyanmics of $\tilde{z}$ is:

$$\frac{d\tilde{z}}{dt} = -k\tilde{z}. \tag{3.16}$$

It is then obvious that $\mu - \hat{\mu}$ converges to zero, too.

□

3.2.2. *Nonideal Case*

In practice, it may not be possible to obtain accurate measurements of the derivatives. To study the effect of error in differentiation, we rewrite the model in the following manner:

$$\dot{z}(t) = az + b\mu(z,t), \quad a < 0, \tag{3.17a}$$

$$y_1 = z(t), \tag{3.17b}$$

$$y_2 = \dot{z}(t) + \delta(t). \tag{3.17c}$$

In this case, we do not measure the exact derivative, thus the second output y_2 is composed of the true time derivative of the state plus a noise term, $\delta(t)$. The noise term could result from the use of a numerical differentiator, such as the deadbeat method of Reger & Jouffroy (2009). The following result derives the frequency response of the estimated error with respect to the noise term.

Theorem 3.2. Given system (3.17a), with time-varying parameter $\mu(t)$, we assume that the state is perfectly measured, (3.17b), but derivative measurement is corrupted with noise, (3.17c). Assume that we can model the noise as $\delta(t) = \delta_0 + A_\delta \sin(\omega_\delta t + \phi_\delta)$. The estimator (3.12) - (3.13) provides parameter estimates with

bounded error $\tilde{\mu}(t)$ as $t \to +\infty$:

$$\begin{aligned}&\tilde{\mu}(t \to +\infty)\\ &= \frac{a}{bk}\delta_0 + \frac{(\sqrt{(a^2+\omega_\delta^2)k^2 + a^2\omega_\delta^2 + \omega_\delta^4}\sin(\omega_\delta t + \phi'_\delta)}{b(k^2+\omega_\delta^2)}A_\delta.\end{aligned} \tag{3.18}$$

Proof. First we differentiate $\tilde{\mu}$ and $\tilde{z}$, combining the results with equations (3.12) and (3.13), then we can obtain following relationships:

$$\dot{\tilde{z}} = -k\tilde{z} - \delta, \tag{3.19a}$$

$$\dot{\tilde{\mu}} = \frac{(a+k)k}{b}\tilde{z} + \frac{a+k}{b}\delta - \frac{1}{b}\dot{\delta}, \tag{3.19b}$$

$$\tilde{\mu} = -\frac{a+k}{b}\tilde{z} - \frac{1}{b}\delta. \tag{3.19c}$$

The solution to (3.19a) and (3.19b) are:

$$\tilde{z}(t) = e^{-kt}\tilde{z}_0 - e^{-kt}\int_0^t e^{k\tau}\delta(\tau)d\tau, \tag{3.20}$$

$$\tilde{\mu}(t) = -\frac{a+k}{b}e^{-kt}\tilde{z}_0 + \frac{a+k}{b}e^{-kt}\int_0^t e^{k\tau}\delta(t)d\tau - \frac{1}{b}\delta(t). \tag{3.21}$$

The noise $\delta(t)$ in the derivative is modeled as:

$$\delta(t) = \delta_0 + A_\delta \sin(\omega_\delta t + \phi_\delta), \tag{3.22}$$

which can be plugged in the solutions, and for $\tilde{z}(t)$ we have:

$$\begin{aligned}\tilde{z}(t) &= e^{-kt}\tilde{z}_0 - e^{-kt}\int_0^t e^{k\tau}\delta(\tau)d\tau\\ &= e^{-kt}\left(\tilde{z}_0 + \frac{\omega_\delta\cos(\phi_\delta) - k\sin(\phi_\delta)}{k^2+\omega^2} - \frac{1}{k}\right)\\ &+ \frac{A_\delta\left(k\sin(\omega_\delta t+\phi_\delta) - \omega_\delta\cos(\omega_\delta t+\phi_\delta)\right)}{k^2+\omega_\delta^2} + \frac{\delta_0}{k}\\ &= e^{-kt}\left(\tilde{z}_0 + \frac{\omega_\delta\cos(\phi_\delta) - k\sin(\phi_\delta)}{k^2+\omega^2} - \frac{1}{k}\right)\end{aligned}$$

$$+ A_\delta \frac{\sqrt{k^2+\omega_\delta^2}\sin(\omega_\delta t + \phi_\delta'')}{k^2+\omega_\delta^2} + \frac{\delta_0}{k}, \tag{3.23}$$

where

$$\phi_\delta'' = \phi_\delta + \arctan(-\frac{\omega_\delta}{k}). \tag{3.24}$$

In (3.23), except for the exponential decaying term, the magnitude of the periodic signal amplitude and modeled average are both dampened by the estimator gain k. For $\tilde{\mu}$, we have:

$$\begin{aligned}
\tilde{\mu}(t) &= \frac{a+k}{b}e^{-kt}\left(-\tilde{z}_0 + \frac{\omega_\delta\cos(\phi_\delta) - k\sin(\phi_\delta)}{k^2+\omega_\delta^2} - \frac{1}{k}\right) \\
&+ \frac{a+k}{bk}\delta_0 - \frac{1}{b}\left(\delta_0 + A_\delta\sin(\omega_\delta t + \phi_\delta)\right) \\
&+ \frac{a+k}{b}\frac{A_\delta\left(k\sin(\omega_\delta t+\phi_\delta) - \omega_\delta\cos(\omega_\delta t+\phi_\delta)\right)}{k^2+\omega_\delta^2} \\
&= \frac{a+k}{b}e^{-kt}\left(-\tilde{z}_0 + \frac{\omega_\delta\cos(\phi_\delta) - k\sin(\phi_\delta)}{k^2+\omega_\delta^2} - \frac{1}{k}\right) + \\
&\frac{a}{bk}\delta_0 + \frac{\sqrt{(a^2+\omega_\delta^2)k^2 + a^2\omega_\delta^2 + \omega^4}\sin(\omega_\delta t + \phi_\delta')}{b(k^2+\omega_\delta^2)}A_\delta,
\end{aligned} \tag{3.25}$$

where

$$\phi_\delta' = \phi_\delta + \arctan\left(\frac{-(a+k)\omega_\delta}{ak - \omega_\delta^2}\right). \tag{3.26}$$

Similar situation with (3.25), the not exponential decaying terms can be dampened by large estimator gain. □

Discussion Above derivation results show the tendency of magnitude $|\tilde{\mu}_\infty|$ to change along the noise parameter, and it is summarized as follows:

$$|\tilde{\mu}_\infty| = |\frac{a}{bk}\delta_0|, \text{ as } A_\delta = 0 \text{ or } \omega_\delta = 0;$$
$$|\tilde{\mu}_\infty| \to |\frac{A_\delta}{b}|, \text{ as } \omega_\delta \to \infty.$$

The dampening effect of estimator in the estimates of the derivative noise can be shown in a Bode diagram. We first derive the transfer function relations between $\tilde{z}(t)$ vs. $\delta(t)$ and $\tilde{\mu}(t)$ vs. $\delta(t)$. From (3.19a) and (3.19b), the transfer functions of these two pairs of outputs and inputs are:

$$G_1(s) = \frac{\tilde{z}(s)}{\delta(s)} = -\frac{1}{s+k} \tag{3.27}$$

$$G_2(s) = \frac{\tilde{\mu}(s)}{\delta(s)} = -\frac{s(s-a)}{bs(s+k)} \tag{3.28}$$

Assume $a = -1, b = 1$. The Bode diagrams of $G_1(s)$ and $G_2(s)$ are shown in Figures 3.1 and 3.2, respectively. Responses of high gain estimator, $k = 10$, and low gain estimator , $k = 2$, are compared. The error bound can be reduced by increasing the estimator gain k while the noise frequency is small. As shown in both magnitude diagrams of $G_1(s)$ and $G_2(s)$, the noise δ is much more dampened in $\tilde{z}$ and $\tilde{\mu}$ by the high gain estimator than low gain estimator while the noise frequency is small. As the frequency increases, the differences between using high gain and low gain grows smaller. However, from Figure 3.2, we can see the estimator is not able to dampen the noise in $\tilde{\mu}$ when noise frequency is very high.

3.2.3. Simulation Results

A simple scalar linear system with one varying parameter is used to test the developed passivity-based estimator:

$$\dot{z}(t) = -z(t) + \mu(t), \tag{3.29a}$$

$$\mu(t) = 0.1\sin(0.5t), \tag{3.29b}$$

$$y_1(t) = z(t), \tag{3.29c}$$

$$y_2(t) = \dot{z}_d(t), \tag{3.29d}$$

where $\dot{z}_d$ is an estimate of the derivative of z.

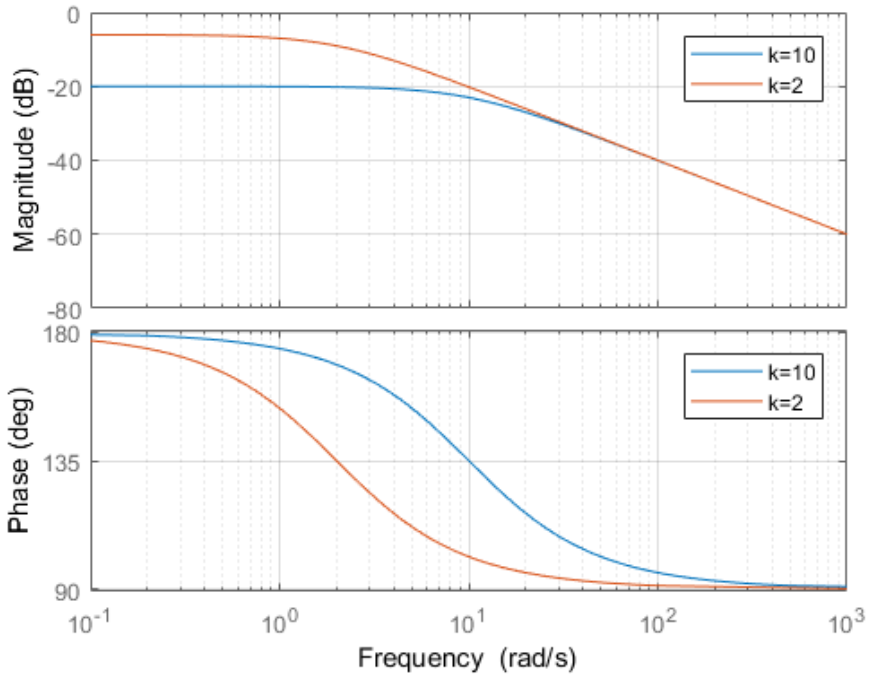

Figure 3.1: Bode diagram of $G_1(s) = \frac{\tilde{z}(s)}{\delta(s)}$

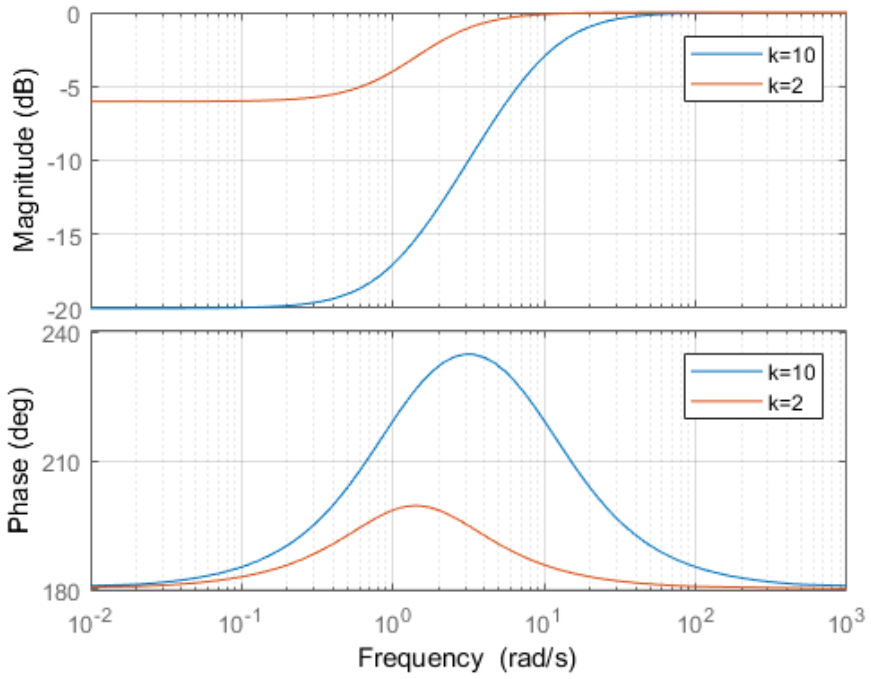

Figure 3.2: Bode diagram of $G_2(s) = \frac{\tilde{u}(s)}{\delta(s)}$

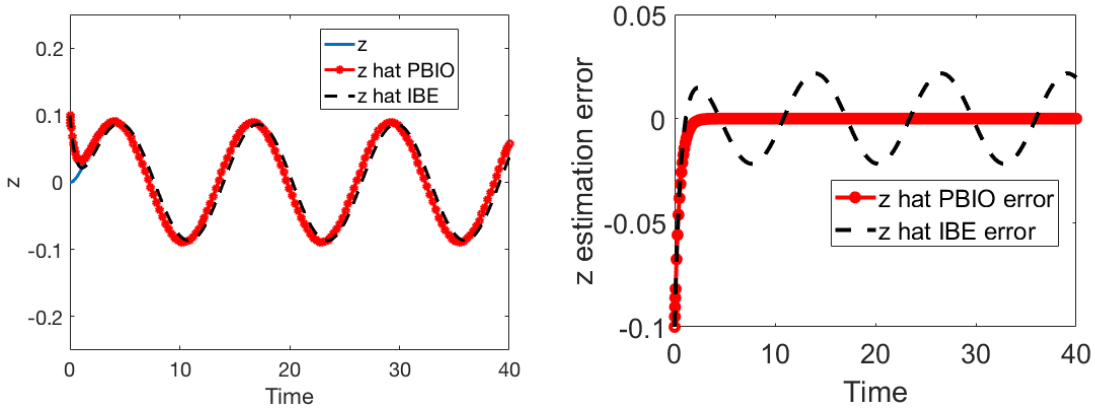

(a) Profiles of z and $\hat{z}$ ($k = 2$)

(b) Profiles of $\tilde{z}$ ($k = 2$)

Figure 3.3: Estimator performance in ideal case (z and $\tilde{z}$)

Ideal case ($\dot{z}_d = \dot{z}$) Both the state and derivative are measured continuously and accurately, more specifically $\dot{z}_d = \dot{z}$. (3.12) and (3.13) are used to estimate the parameter $\mu(t)$. The results of the estimation are shown in Figures 3.3 and 3.4. We also compare the passivity-based input estimator (PBIE) result with inversion-based estimator (IBE) (Tatiraju & Soroush, 1998) result. The IBE also treats the time-varying parameter estimation problem, but does not use information of derivative of measurement in the estimation equation (3.13). Figure (3.3a) shows that the estimator starts with the same wrong initial condition, which also results in the deviation of the estimated parameter, $\hat{\mu}$ from the true value, Figure (3.4a). Because of the asymptotic stability of PBIE , the estimation errors converge asymptotically to zero in Figures (3.3b) and (3.4b). In comparison, the IBE is shown to be marginal stable, due to fail to capture the dynamic change of the measurement.

Nonideal case ($\dot{z}_d = \dot{z} + \delta$): using a deadbeat differentiator together with passivity-based estimator Again, we consider the example system: (3.29a) - (3.29d). The difference from the ideal case is that the second output $y_2(t)$ is calculated by using deadbeat differentiator,

$$\dot{z}_d(t) = \dot{z}(t) + \delta(t), \tag{3.30}$$

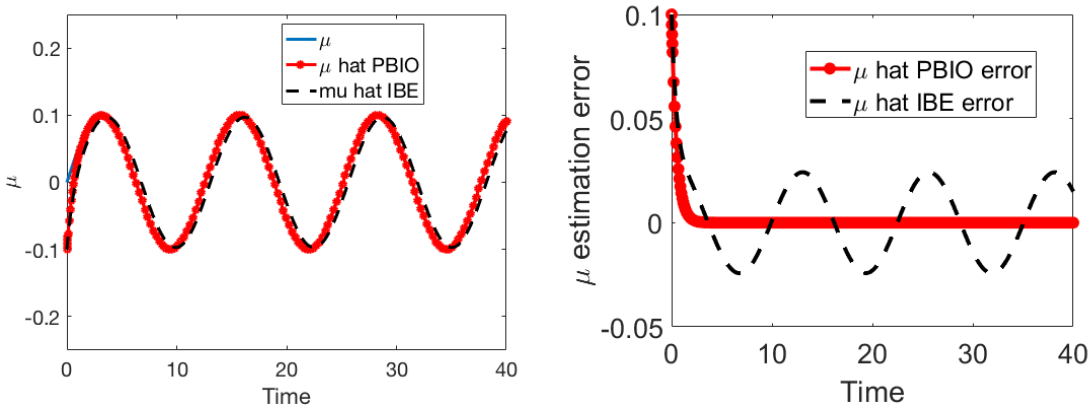

(a) Profiles of μ and $\hat{\mu}$ ($k = 2$)

(b) Profiles of $\tilde{\mu}$ ($k = 2$)

Figure 3.4: Estimator performance in ideal case(μ and $\tilde{\mu}$)

where $\delta(t)$ is the differentiation error.

Any type of differentiator would produce error in the reconstructed derivatives. Here, we choose the deadbeat differentiation technique proposed by Reger & Jouffroy (2009) as an example. The work re-derives the derivative estimation scheme in Mboup et al. (2007) based on the reconstructibility Gramian. Deadbeat differentiation treats the signal as a polynomial signal of time within the differentiation moving horizon T. Here we use $T = 0.1$, and assume that the signal $z(t)$ is a degree-one polynomial. First order derivative can be reconstructed using the following formula from the paper:

$$\dot{z}_d(t) = \frac{6}{T^2}\int_{t-T}^{t} z(\tau)d\tau + \frac{12}{T^3}\int_{t-T}^{t}(\tau - t)z(\tau)d\tau, \tag{3.31}$$

The assumption of a degree of 1 polynomial signal is required to derive the weighting factors of the integration terms. Other types of numerical differentiators are reviewed in Appendix E.

The proposed passivity-based estimator (3.12) - (3.13) with proportional gain $k = 10$ is used. The simulation results are shown in Figure 3.6. The estimator starts with a wrong initial condition with an error of 0.1 as shown in Figure (3.5a), then converge close to the true profile. The same performance can be found for

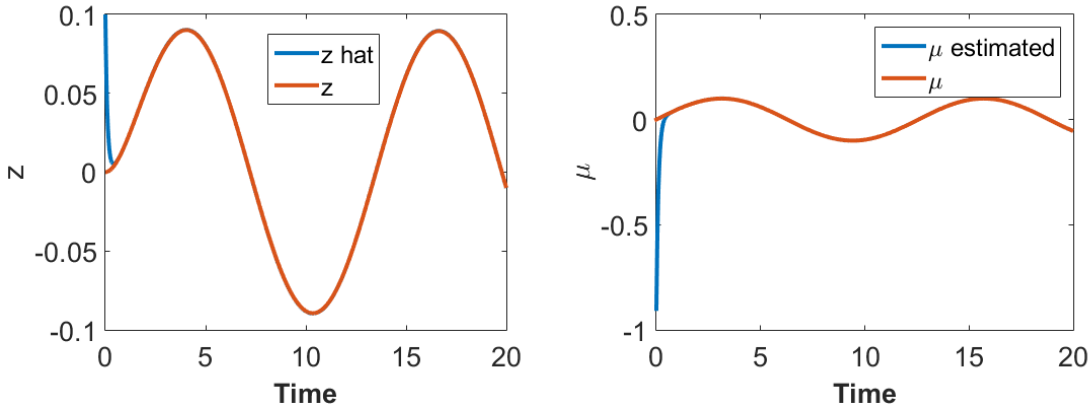

(a) Profiles of z and $\hat{z}$ (k = 10)

(b) Profiles of μ and $\hat{\mu}$ (k = 10)

Figure 3.5: Estimator performance in nonideal case (z and μ)

the parameter estimate in Figure (3.5b). The estimation error of μ is very small, but still exists in Figure (3.6b). However, we can see that the magnitude of the μ error is very much dampened by the estimator, compared with the magnitude of the differentiator estimated derivative error. Also, in this figure, we can observe the magnitudes of noise reduction with different k. As shown in the theory, with higher k, the bounds of estimation error are smaller.

3.3. Passivity-based Input Estimator for Nonlinear Systems

The estimator can be used for th following class of nonlinear system:

$$\frac{dz}{dt} = \bar{p}(z, \gamma_1) + D\Delta p(x, \gamma) + \phi(z, u, \gamma_1), \tag{3.32a}$$

$$\frac{dx}{dt} = f(z, x) + g(x, u), \tag{3.32b}$$

$$y_1 = z, \tag{3.32c}$$

$$y_2 = \dot{z}, \tag{3.32d}$$

when $z \in \mathbf{R}^p$, are measured outputs or states, of which the dynamics can be written as a sum of the unknown parts $\Delta p(x, \gamma)$ and the known parts: $\bar{p}(z, \gamma_1) + \phi(z, u, \gamma_1)$. The derivatives of z are also accurately measured. $x \in \mathbf{R}^m$ are unmeasured internal

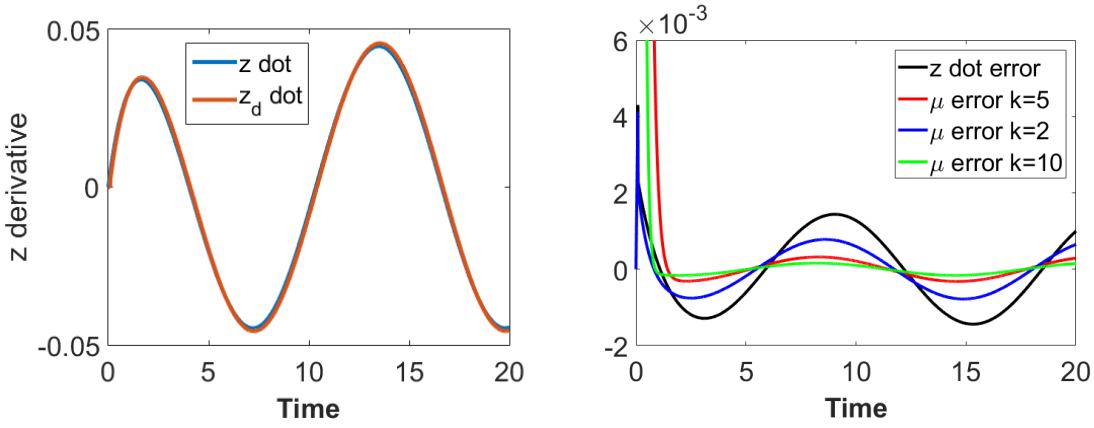

(a) Profiles of $\dot{z}$ and $\dot{z}_d$ ($k = 10$)

(b) Profiles of δ and $\tilde{\mu}$

Figure 3.6: Estimator performance in nonideal case ($\dot{z}$ and $\tilde{\mu}$)

states. All the nonlinear functions involved are vectors of C^1 functions with appropriate dimensions. γ represents the vector of parameters, and γ_1 is the sub-vector that includes all the known parameters. In this case, the passivity-based estimator is:

$$\frac{d\hat{z}}{dt} = \bar{p}(\hat{z}, \gamma_1) + D\Delta\hat{p}(t) + \phi(\hat{z}, u), \tag{3.33a}$$

$$\Delta\hat{p}(t) = D^{-1}\left(y_2 + K(y_1 - \hat{z}) - \phi(\hat{z}, u) - \bar{p}(\hat{z}, \gamma_1)\right). \tag{3.33b}$$

$\mathbf{K} \in diag(k_1, k_2, k_3, ..., k_p)$ is positive definite.

Theorem 3.3. Consider the class of nonlinear system (3.32), where we can both measure outputs and their derivatives. The passivity-based input estimator shown in (3.33) provides asymptotic estimates $\Delta\hat{p} \to \Delta p$.

Proof. Express Δp through inverting (3.32a), and then subtract it by the estimation law (3.33b). After re-organizing, we can write the input estimation error as:

$$\Delta p - \Delta\hat{p} = D^{-1}(\bar{p}(\hat{z}) - \bar{p}(z) + \phi(\hat{z}, u) - \phi(z, u) - K_E(z - \hat{z})). \tag{3.34}$$

Same as in the linear case where $z - \hat{z}$ converges to zero asymptotically, therefore $\Delta p - \Delta\hat{p}$ converges to zero asymptotically as well. □

3.4. Application to Estimation of Reaction Calorimetric Variables

The main application of the proposed passivity-based input estimator is the estimation of reaction calorimetric variables, which are reaction heat generation rate and reactor-jacket heat transfer rate. Only credible energy balance and easily available measurements, such as temperature, reaction weight, flows, are used, and kinetic information is not needed. On-line knowledge of these two thermal variables can be utilized to monitor the evolution of production, residual level of reactants, and control reactor temperature. Successful applications of calorimetric variable estimation schemes for process control (Tatiraju & Soroush, 1998) and composition monitoring and reaction runaway prevention (Schuler & Schmidt, 1992) have been reported in the literature. In DOW Chemical, a dynamics-inversion based scheme is implemented for estimating standing monomer level and temperature control purposes, and in test trails, the composition evolution calculated based on calorimetric estimation agrees with Raman spectrometer measurement. The derivatives are calculated using Euler method based on filtered temperature measurements.

In this section, we show the application result of passivity-based input estimator based on energy balances and temperature measurements; we also compare the result with other similar estimation schemes that only use present data for estimation.

The estimator is constructed based on the temperature differential equations of the reactor and jacket:

$$\frac{dT_r}{dt} = \frac{F_{in}}{V\rho C_p}\left(\rho_{in}C_{p,in}T_{in} - \rho C_p T_r\right) - \frac{\Delta H_r r}{C_p\rho} - \frac{UA(T_r - T_j)}{V\rho C_p}, \tag{3.35}$$

$$\frac{dT_j}{dt} = \frac{F_j}{V_j}\left(T_{j,in} - T_j\right) + \frac{UA(T_r - T_j)}{V_j\rho_w C_{p,w}}, \tag{3.36}$$

where $Q_r = -\Delta H_r r$ and $Q_j = UA(T_r - T_j)$ are unknown inputs to be estimated. The reactor temperature T_r and jacket temperature T_j are measured, and their deriva-

tives are reconstructed. Define

$$\Delta p = \begin{bmatrix} Q_r \\ Q_j \end{bmatrix}, \quad D = \begin{bmatrix} \frac{1}{C_p \rho} & -\frac{1}{V \rho C_p} \\ 0 & \frac{1}{V_j \rho_w C_{p,w}} \end{bmatrix}, \quad \phi = \begin{bmatrix} \frac{F_{in}}{V_r \rho C_p} \left(\rho_{in} C_{p,in} T_{in} - \rho C_p T_r \right) \\ \frac{F_j}{V_j} \left(T_{j,in} - T_j \right) \end{bmatrix}, \tag{3.37}$$

we can put the model in the form of (3.32), and follow (3.33) to obtain the corresponding PBIE.

A jacketed exothermic reaction $2A \rightarrow B \rightarrow C$ is modeled in Matlab. The temperatures and numerical derivatives provided by the ODE solver are given to the passivity-based estimator to obtain estimates, $\hat{Q}_r$ and $\hat{Q}_j$. We also compare the results from PBIE and IBE, as the latter estimator does not use the derivatives. We use the same, correct initialization for the estimator states $\hat{T}_r$ and $\hat{T}_j$, and the same gains $K_E = \text{diag}([0.5,\ 0.5])$. Errors of temperatures estimates and $\hat{Q}_r$ and $\hat{Q}_j$ are zeros form beginning as shown in Figures 3.7 and 3.8, and it is because that correct initial values of the estimator states, $\hat{T}_r$ and $\hat{T}_j$, are given. In comparison, the IBE estimates error exists while temperatures are not at steady states, and gradually converge towards zero while the the temperature profiles approach steady states.

3.5. Conclusions

In this chapter, we developed a passivity-based input estimator for estimating time-varying uncertainties in partially linear system and nonlinear systems. The estimator is derived from a Lyapunov stability perspective, and requires the use of a measured or estimated output derivative. In the ideal case, the derivative is perfectly measured, and the estimator estimates have asymptotic convergence to the true values. In the nonideal case, the derivative is not perfectly measured. Instead it is obtained through a differentiation technique, such as a deadbeat differentiator. We showed that the proposed estimator could dampen the magnitude of the derivative error in the parameter estimates by using large estimator gains. Illustrative examples are simulated to show the proposed estimator performance for

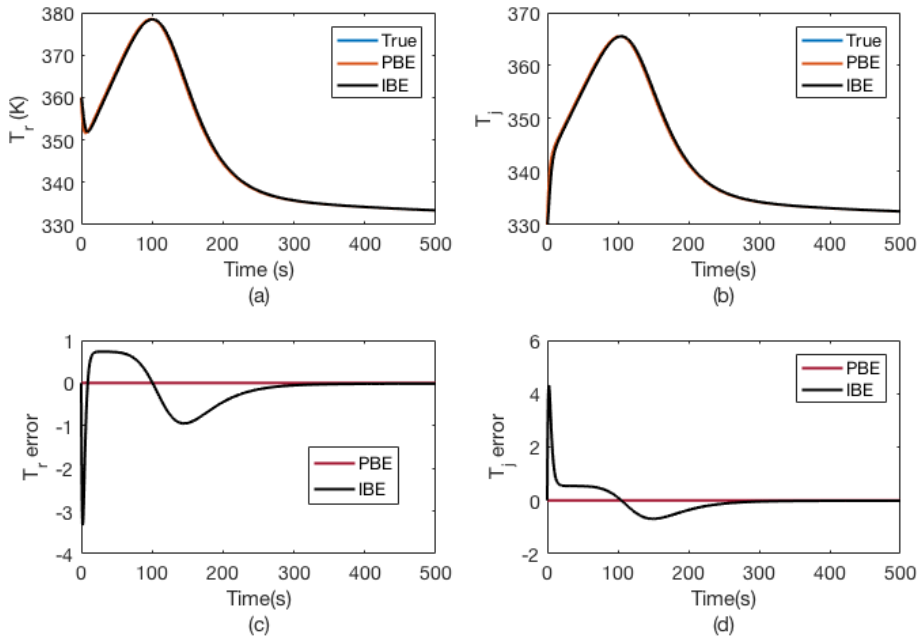

Figure 3.7: Estimated temperatures and errors from PBIE and IBE

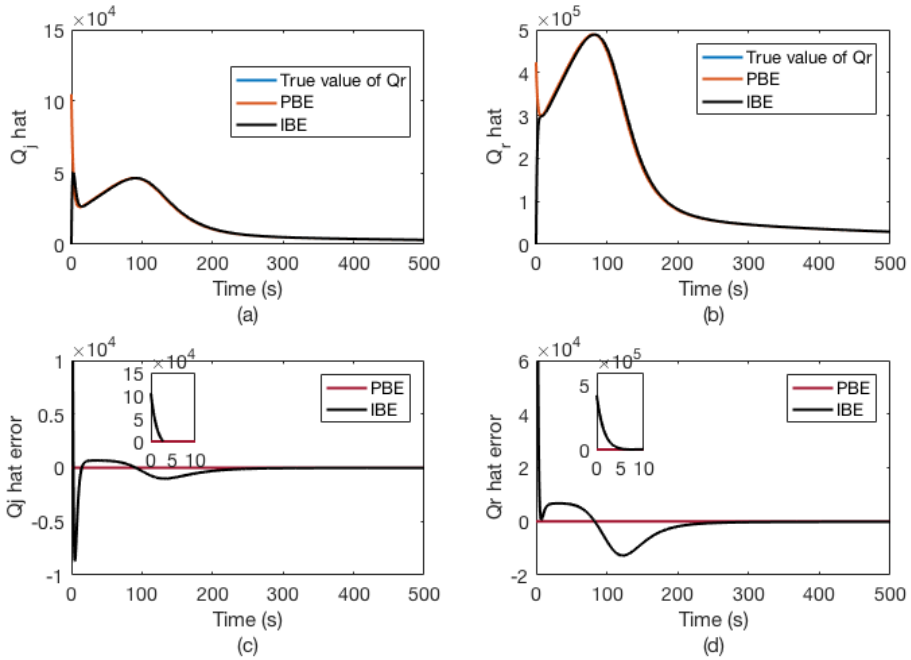

Figure 3.8: Estimates and errors of Q_r and Q_j from PBE and IBE

ideal and nonideal cases. Potential applications include production estimation in chemical reaction systems for process control and monitor, as shown in the reaction calorimetric variables estimation example. Inclusion of the proposed estimator in a model-based control scheme can reduce control model size and save modeling cost.

4. State Estimation with Process Uncertainty

In this chapter, we consider the state estimation of a special class of nonlinear systems with partially linear structures with respect to the states and uncertainty parameters. We first show how to construct the unknown input observer (UIO) in Section 4.1. Section 4.2 presents the concepts of reaction variants and invariants in reaction systems. In Section 4.3, we use them to construct the asymptotic observer (AO) for estimating unmeasured compositions without the knowledge of reaction kinetics. Section 4.4 compares the UIO and AO, and discusses some of the observers' convergence issues. We apply the proposed observers to numerical examples and two reaction examples for which the results are shown in Section 4.4. Finally, we close this chapter with some concluding remarks in Section 4.6.

4.1. Unknown Input State Observer (UIO)

We consider a partially linear system of the following form:

$$\frac{dx}{dt} = Ax + Bu + D\mu(x,t) \tag{4.1a}$$

$$y = Cx, \tag{4.1b}$$

where $x \in \mathbb{R}^n$, $u \in \mathbb{R}^p$, $\mu \in \mathbb{R}^q$, and $y \in \mathbb{R}^m$. Here, μ is a unknown function vector, referred to as unknown inputs. In this system, all the nonlinearity and uncertainty are incorporated in the vector μ. We are interested in estimating the states from the measurements y and the deterministic linear information, matrices A, B, C, D, and

known inputs u. We also assume that $\mathrm{rank}(CD) = q$, which indicates that we have at least the same number of output measurements as the unknown inputs, $m \geq q$. The first step of constructing the state observer aims to decouple the unknown inputs μ from part of the system dynamics.

First, find the nonsingular transformation matrix $T \in \mathbb{R}^{n\times n}$,

$$T = \begin{bmatrix} N & D \end{bmatrix}, \quad \text{with } N \in \mathrm{null}(D). \tag{4.2}$$

Therefore,

$$T^{-1} = \begin{pmatrix} D^{\perp} \\ D^{+} \end{pmatrix}, \tag{4.3}$$

where

$$D^{\perp}D = 0_{q\times n}, \text{ and } D^{+}D = I_{(n-q)\times n}. \tag{4.4}$$

Pre-multiply (4.1a) by T^{-1}, and define $z = T^{-1}x$, then we obtain:

$$\frac{dz}{dt} = T^{-1}Ax + T^{-1}Bu + \begin{bmatrix} 0 \\ I \end{bmatrix}\mu. \tag{4.5}$$

Above equation is equivalent to

$$\frac{dz}{dt} = \bar{A}z + \bar{B}u + \begin{bmatrix} 0 \\ I \end{bmatrix}\mu, \tag{4.6}$$

where $\bar{A} = T^{-1}AT$, $\bar{B} = T^{-1}B$.

Then we can partition the new state vector z as

$$z = \begin{bmatrix} z_I \\ z_V \end{bmatrix}, \tag{4.7}$$

where $z_I \in \mathbb{R}^{n-q}$ and $z_V \in \mathbb{R}^{q}$. z_I is called the invariants, as it does not explicitly de-

pend on the unknown input vector μ. z_V is called the variants, since each element of z_V varies only with one unknown input in the vector, μ.

The matrices $\bar{A}$ and $\bar{B}$ are partitioned correspondingly:

$$\bar{A} = \begin{pmatrix} \bar{A}_{11} & \bar{A}_{12} \\ \bar{A}_{21} & \bar{A}_{22} \end{pmatrix}, \quad \bar{B} = \begin{bmatrix} \bar{B}_1 \\ \bar{B}_2 \end{bmatrix}. \tag{4.8}$$

The dynamics of invariants and variants are now given by:

$$\frac{dz_I}{dt} = \bar{A}_{11} z_I + \bar{A}_{12} z_V + \bar{B}_1 u, \tag{4.9}$$

$$\frac{dz_V}{dt} = \bar{A}_{21} z_I + \bar{A}_{22} z_V + \bar{B}_2 u + \mu. \tag{4.10}$$

To decouple z_I from z_V, we utilize the output equation (4.1b). With the state transformation, the output equation is written as:

$$y = CTz. \tag{4.11}$$

We now find a nonsingular matrix ,

$$U = \begin{bmatrix} CD & Q \end{bmatrix}, \quad \text{with } Q \in \text{null}(CD) \subseteq \mathbb{R}^{m \times (m-q)}, \quad U \in \mathbb{R}^{m \times m}. \tag{4.12}$$

The inverse can be partitioned as,

$$U^{-1} = \begin{pmatrix} U_1 \\ U_2 \end{pmatrix}, \quad \text{where } U_1 \in \mathbb{R}^{q \times m} \text{ and } U_2 \in \mathbb{R}^{(m-q) \times m}, \tag{4.13}$$

and the submatrices satisfy the following conditions:

$$U_1 CD = I_{q \times q}, \quad U_2 CD = 0_{(m-q) \times q}. \tag{4.14}$$

Pre-multiply the output equation with the matrix U to obtain:

$$U_1 y = U_1 CN z_I + z_V, \tag{4.15a}$$

$$U_2 y = U_2 C N z_I. \tag{4.15b}$$

Based on (4.15a), we can express z_V in terms of measured outputs y and invariants z_I in (4.9) and obtain:

$$\frac{dz_I}{dt} = \tilde{A}_1 z_I + \bar{B}_1 u + E_1 y, \tag{4.16a}$$

$$y_I = \tilde{C}_1 z_I, \tag{4.16b}$$

where

$$\tilde{A}_1 = \bar{A}_{11} - \bar{A}_{12} U_1 C N,\ E_1 = \bar{A}_{12} U_1,\ y_I = U_2 y,\ \tilde{C}_1 = U_2 C N. \tag{4.17}$$

Then, an exponential state observer like Luenburger observer can be designed for (4.16a)-(4.16b) if the pair $(\tilde{A}_1, \tilde{C}_1)$ is observable. The observer equation, referred as the closed-loop UIO is:

$$\frac{d\hat{z}_I}{dt} = (\tilde{A}_1 - L\tilde{C}_1)\hat{z}_I + \bar{B}_1 u + (LU_2 + E_1) y, \tag{4.18a}$$

$$\hat{z}_V = U_1 y - U_1 C N \hat{z}_I \tag{4.18b}$$

$$\hat{x} = T \begin{pmatrix} \hat{z}_I \\ \hat{z}_V \end{pmatrix} \tag{4.18c}$$

where L is the observer gain matrix.

However, when the number of measurements equals the number of unknown inputs, we lose the extra degree of freedom to assign the observer estimation convergence rate through output y_I feedback. When $m = q$, $y_I \in R^{m-q}$ is an empty vector. Under this situation, we can still construct an open-loop UIO if eigenvalues of $\tilde{A}_1$ only have negative real parts. We can formulate the open-loop unknown input state observer as:

$$\frac{d\hat{z}_I}{dt} = \tilde{A}_1 \hat{z}_I + \bar{B}_1 u + E_1 y, \quad \text{Re}(\text{eig}(\tilde{A}_1)) < 0 \tag{4.19a}$$

$$\hat{z}_V = U_1 y - U_1 C N \hat{z}_I \tag{4.19b}$$

$$\hat{x} = T \begin{pmatrix} \hat{z}_I \\ \hat{z}_V \end{pmatrix} \tag{4.19c}$$

The open-loop UIO is asymptotically stable, and the existence of asymptotic stability entirely depends on the original system (4.1) matrices and cannot be imposed or improved through output feedback.

The open-loop UIO applied to reaction systems with uncertain kinetics becomes the so-called asymptotic observer. The stability of the asymptotic observer depends on the hydrodynamics of the reactor, and exists in semi-batch reactors or CSTRs, where persistent excitation conditions are fulfilled (Moreno & Dochain, 2008).

4.2. Reaction Variants, Invariants

We start from the dynamic model of a well-mixed homogeneous liquid phase CSTR, with n_r independent reactions and n_c species. The state of the reactor can be described using the state vector, $x = (C_1, C_2, ..., C_{n_c}, U_r, V_r)$. The dynamic model of the CSTR can be written as follows:

$$\frac{dC}{dt} = \frac{F_{in}}{V_r}(C_{in} - C) + \nu r, \tag{4.20}$$

$$\frac{dV_r}{dt} = F_{in} - F_{rout} + \phi, \tag{4.21}$$

$$\frac{dU_r}{dt} = H_{in} - \frac{F_{rout}}{V_r} H_r + Q_j + W_s - P_r \frac{dV_r}{dt}. \tag{4.22}$$

We make the following assumptions, which are realistic for homogeneous liquid phase reactors (Dochain et al., 2009): (1) the liquid mixture is ideal and incompressible; (2) the CSTR is operated at constant pressure; (3) the volume change due to mixing and reaction is negligible. As a result, the energy balance and volume balance can be written as follows:

$$\frac{dH_r}{dt} = H_{in} - \frac{F_{rout}}{V_r} H_r + Q_j + W_s, \tag{4.23}$$

$$\frac{dV_r}{dt} = F_{in} - F_{rout}. \tag{4.24}$$

Asbjørnsen (1972) shows that there exists non-unique nonsingular linear transformation matrices $T^{-1} \in \mathbb{R}^{n_c \times n_c}$ to transform the composition states C into reaction variants $z_V \in \mathbb{R}^{n_r}$ and reaction invariants $z_I \in \mathbb{R}^{n_c - n_r}$:

$$T^{-1}C = \begin{pmatrix} z_I \\ z_V \end{pmatrix}. \tag{4.25}$$

The matrix T^{-1} can be found as:

$$T^{-1} = \begin{pmatrix} \nu^{\perp}_{(n_c-n_r)\times n_c} \\ \nu^{+}_{n_r \times n_c} \end{pmatrix}_{n_c \times n_c}, \tag{4.26}$$

$$\text{s.t. } \nu^{+}\nu = I_{n_r \times n_r},\ \nu^{\perp}\nu = 0_{(n_c-n_r)\times n_r}. \tag{4.27}$$

Note that T^{-1} is not unique, so that the choice of invariants and variants may vary with measurement availability and control strategies. Through the transformation, the mole balance part of the reaction dynamics (4.20) is expressed in terms of z_I and z_V:

$$\frac{dz_I}{dt} = \frac{F_{in}}{V_r}(z_{I,in} - z_I), \tag{4.28}$$

$$\frac{dz_V}{dt} = \frac{F_{in}}{V_r}(z_{V,in} - z_V) + r. \tag{4.29}$$

One can make the following observations: (1) the effects of n_r reactions are decoupled such that one reaction variant $z_{V,i}$, $i = 1, 2, ...n_r$, is only influenced by the corresponding ith reaction; (2) the reaction invariants z_I are not affected by the reaction rates. The asymptotic stability of the reaction invariants follows from the solution of (4.28) given by:

$$z_I(t) = (z_I(t_0) - z_{I,in})e^{-\frac{F_{in}}{V_r}t} + z_{I,in}, \tag{4.30}$$

where $z_I(t_0)$ is the initial condition vector of the reaction invariants. The reaction

invariants will converge to $z_{I,in}$ as long as $\frac{F_{in}}{V_r} > 0$, which is fulfilled in CSTRs and semi-batch reactors, but not in batch reactors. It can also be noticed that the implicit reaction-dependent states, internal energy U_r and enthalpy H_r, can also be utilized similarly as the invariants later in estimation.

Illustrative example Consider a CSTR reaction system characterized by the following reaction network with $n_r = 2$ reactions and $n_c = 3$ species: $2A \rightarrow B \rightarrow C$. The stoichiometric matrix $\boldsymbol{\nu}$, the linear transformation T, and two variants, i.e. $z_{V,1}, z_{V,2}$, and one invariant z_I, are as follows:

$$\nu = \begin{bmatrix} -2 & 0 \\ 1 & -1 \\ 0 & 1 \end{bmatrix}, \quad T^{-1} = \begin{pmatrix} \nu^{\dagger}_{2\times 3} \\ \nu^{\perp}_{1\times 3} \end{pmatrix} = \begin{pmatrix} \begin{bmatrix} -\frac{1}{2} & 0 & 0 \\ 0 & 0 & 1 \end{bmatrix} \\ \begin{bmatrix} \frac{1}{2} & 1 & 1 \end{bmatrix} \end{pmatrix},$$

$$\text{s.t.} \begin{bmatrix} z_{V,1} \\ z_{V,2} \\ z_I \end{bmatrix} = \begin{bmatrix} -\frac{1}{2} & 0 & 0 \\ 0 & 0 & 1 \\ \frac{1}{2} & 1 & 1 \end{bmatrix} \begin{bmatrix} C_A \\ C_B \\ C_C \end{bmatrix}. \tag{4.31}$$

The dynamics of the reaction variants and the invariants are described by (4.29) and (4.28).

Reaction variants option for control Reaction variants fully characterize the reaction contribution, and by controlling a set of linearly independent reaction variants, the remaining dynamics of reaction invariants are asymptotically stable zero dynamics. The choice of the reaction variants is not unique, and can be instructed by compositions that need to be controlled. For example, if we want to control compositions C_B and C_C in a semi-batch reactor or CSTR of $2A \rightarrow B \rightarrow C$, the definition of variants given in (4.31) is not well-suited for the control of variants since uncontrolled species A is involved. However, if we change the first row of T into

$[0\ 1\ 1]$, we can clearly define setpoints of variants as:

$$z_V^* = \begin{bmatrix} 0 & 1 & 1 \\ 0 & 0 & 1 \end{bmatrix} \begin{bmatrix} C_A^* \\ C_B^* \\ C_C^* \end{bmatrix}, \tag{4.32}$$

where C_A^* does not need to be specified.

4.3. Asymptotic Observer (AO)

We assume that the temperature measurements for the reactor and the jacket and composition measurements for $n_r - 1$ species are available on-line. The asymptotic observer proposed in this section estimates the compositions for $n_c - n_r + 1$ species, without using the reaction kinetics. The estimated values of the reaction invariants $\hat{z}_I$ and total enthalpy $\hat{H}$ are obtained through solving the following kinetics-independent observer model:

$$\frac{d\hat{z}_I}{dt} = \frac{F_{in}}{V} z_{I,in} - \frac{F_{in}}{V} \hat{z}_I \tag{4.33a}$$

$$\frac{d\hat{H}}{dt} = H_{in} - \frac{F_{out}}{V} \hat{H} + Q_j + W_s \tag{4.33b}$$

Then, the estimates of the unmeasured compositions $\hat{C}_J \in \mathbb{R}^{n_c - n_r + 1}$ are calculated as follows:

$$\hat{C}_J = \mathbf{\Gamma}^{-1} \left(\begin{bmatrix} \hat{z}_I \\ \hat{H} \end{bmatrix} - \begin{bmatrix} \nu_I^\perp C_I \\ h_I^T C_I V_r \end{bmatrix} \right), \tag{4.34}$$

$$\text{where } \mathbf{\Gamma} = \begin{bmatrix} \nu_J^\perp \\ h_J^T \end{bmatrix} \in \mathbb{R}^{(n_c - n_r + 1) \times (n_c - n_r + 1)}. \tag{4.35}$$

$C_I \in \mathbb{R}^{n_r - 1}$ is the vector of measured compositions; $\nu_I^\perp$ and $\nu_J^\perp$ are the submatrices of the reaction invariants transformation matrix $\nu^\perp$ in (4.26), and they are constituted by the corresponding columns of measured and unmeasured species, respectively; $h \in \mathbb{R}^{n_c}$ is the molar enthalpy vector, and $h_I \in \mathbb{R}^{n_r - 1}$, $h_J \in \mathbb{R}^{n_c - n_r + 1}$ are the vectors of

the molar enthalpies of the measured and unmeasured species, respectively. The molar enthalpy of each species is temperature dependent, and can be calculated as:

$$h(T)=h_{ref} + c_P(T - T_{ref}), \tag{4.36}$$

where $h(T)$ is the molar enthalpy at the temperature T; h_{ref} is the molar enthalpy at the reference temperature T_{ref}, and $c_P \in \mathbb{R}^{n_c}$ is the heat capacity vector, assumed to be constant within the considered temperature range. The asymptotic convergence property of the observer estimates can be shown by analyzing the dynamics of the estimation errors of the unmeasured compositions as follows.

The observer estimate errors are defined as:

$$e_{z_I} = z_{r,I} - \hat{z}_{r,I} \qquad e_H = H - \hat{H}.$$

Based on (4.23), (4.28), and (4.33), the derivatives of e_{z_I} and e_H can be easily obtained as:

$$\begin{aligned} \frac{de_{z_I}}{dt} &= -\frac{F_{in}}{V} e_{z_I} \\ \frac{de_H}{dt} &= -\frac{F_{out}}{V} e_H. \end{aligned} \tag{4.37}$$

The estimation errors of the invariants exponentially converge to zero with convergence rates of $\frac{F_{in}}{V}$, and $\frac{F_{out}}{V}$, respectively. It indicates that for semi-batch reactors, where $F_{out} = 0$, the enthalpy cannot be used as an invariant for estimation, thus another composition measurement is required. As e_I and e_H converge to zero, the measured compositions converge to the true values as well.

4.3.1. Measurement Availability Condition

At least n_r independent state variables including reactor temperature need to be measured for the observer to give composition estimates for all the unmeasured species. It can be explained as the evolution of the composition states C is constrained in n_r independent directions caused by n_r independent reactions. Addi-

tionally, the matrix $\mathbf{\Gamma}$ should be full rank to obtain the unique solution for $\hat{C}_J$; this full rank condition places a restriction on the choice of measured species.

4.4. Relation Between UIO and AO

The asymptotic observer, (4.33)-(4.34), designed for CSTRs and semi-batch reactors is a special case of the open-loop UIO, (4.19), where asymptotic convergence of state estimation is guaranteed but not assignable. The existence conditions of UIO with assignable exponential convergence property and AO are summarized as follows.

Theorem 4.1. For a system given by (4.1a) - (4.1b) with uncertainty,

1. when $m > q$, the UIO observer (4.18a) - (4.18c) with assignable exponential convergence can be designed based on its invariants subsystems iff $(\tilde{A}_1, \tilde{C}_1)$ is observable;

2. when $m > q$, the UIO observer (4.18a) - (4.18c) with fixed asymptotic convergence can be designed based on its invariants subsystems iff $(\tilde{A}_1, \tilde{C}_1)$ is detectable;

3. when $m = q$, the AO (alternatively open UIO) (4.19a) - (4.19c) exists iff $\tilde{A}_1$ only has eigenvalues with negative real parts.

Theorem 4.2. (Hou & Muller, 1992) Consider system (4.1a) - (4.1b) with uncertainty, and measurement condition: $m > q$, then for its invariants model (4.16a) - (4.16b), the following statements are equivalent:

1. $(\tilde{A}_1, \tilde{C}_1)$ is detectable (observable);

2.

$$\text{rank}\begin{bmatrix} sI - \tilde{A}_1 \\ \tilde{C}_1 \end{bmatrix} = n - q, \forall s \in \mathbb{C}, Re(s) \geq 0 \ (\forall s \in \mathbb{C}); \tag{4.38}$$

3.

$$\text{rank}\begin{bmatrix} sI - A & D \\ C & 0 \end{bmatrix} = n + q, \forall s \in \mathbb{C}, Re(s) \geq 0 \ (\forall s \in \mathbb{C}). \tag{4.39}$$

Proof. The equivalence of statement 1 and 2 is given by the Popov-Belevitch-Hautus test of observability (Ghosh & Rosenthal, 1995). The proof of equivalence of statement 2 and 3 can be found in Hou & Muller (1992). □

Remark Consider a single-tank, homogeneous CSTR or semi-batch reactor, its model is (4.20). Put it into the general form, so that:

$$A = \text{diag}(-\frac{F_{in}}{V_r}) \in \mathbb{R}^{n_c \times n_c}, \quad D = v. \tag{4.40}$$

Choose output matrix $C \in \mathbb{R}^{m \times n_r}$, $m > n_r$, and $\text{rank}(CD) = n_r$. We can see that by setting $s = \frac{F_{in}}{V_r}$, $\text{rank}\begin{bmatrix} -sI - A & D \\ C & 0 \end{bmatrix} = m + n_r \leq n_c + n_r$.

It indicates that only when $m = n_c$, observability condition is satisfied. Then, actually there is no necessity to use an observer, when all the compositions are measured.

4.5. Examples

In this section, we give two numerical examples and two reaction examples. The first numerical example is eligible for using UIO with assignable estimation convergence rate; the second numerical example is qualified for being applied with open-loop UIO. The third example is a single-tank homogeneous reaction where AO is applied to estimate unmeasured compositions without using the knowledge of reaction kinetics, and the fourth example is a more complex heterogeneous reaction example, for which open-loop UIO is applied.

Example 1 from Hou & Muller (1992)

$$\dot{x} = \begin{bmatrix} -1 & 1 & 0 \\ -1 & 0 & 0 \\ 0 & -1 & -1 \end{bmatrix} x + \begin{bmatrix} -1 \\ 0 \\ 0 \end{bmatrix} \mu \tag{4.41a}$$

$$y = \begin{bmatrix} 1 & 0 & 0 \\ 0 & 0 & 1 \end{bmatrix} x \tag{4.41b}$$

Choose

$$N = \begin{bmatrix} 0 & 0 \\ 0 & 1 \\ 1 & 0 \end{bmatrix}, \quad Q = \begin{bmatrix} 1 \\ 1 \end{bmatrix}, \tag{4.42}$$

to obtain transformation matrices:

$$T = \begin{bmatrix} 0 & 0 & -1 \\ 0 & 1 & 0 \\ 1 & 0 & 0 \end{bmatrix}, \quad U = \begin{bmatrix} -1 & 1 \\ 0 & 1 \end{bmatrix}. \tag{4.43}$$

The invariants dynamics is:

$$\dot{z}_I = \underbrace{\begin{bmatrix} -1 & -1 \\ 0 & 0 \end{bmatrix}}_{\tilde{A}_1} + \underbrace{\begin{bmatrix} 0 & 0 \\ -1 & 0 \end{bmatrix}}_{E_1} y \tag{4.44}$$

$$y_I = \underbrace{\begin{bmatrix} 1 & 0 \end{bmatrix}}_{E_1} z_I \tag{4.45}$$

Since the pair $(\tilde{A}_1, \tilde{C}_1)$ is observable, we can use observer gain L to set the convergence rate, i.e. the closed-loop poles. Figure 4.1 shows the observer results with

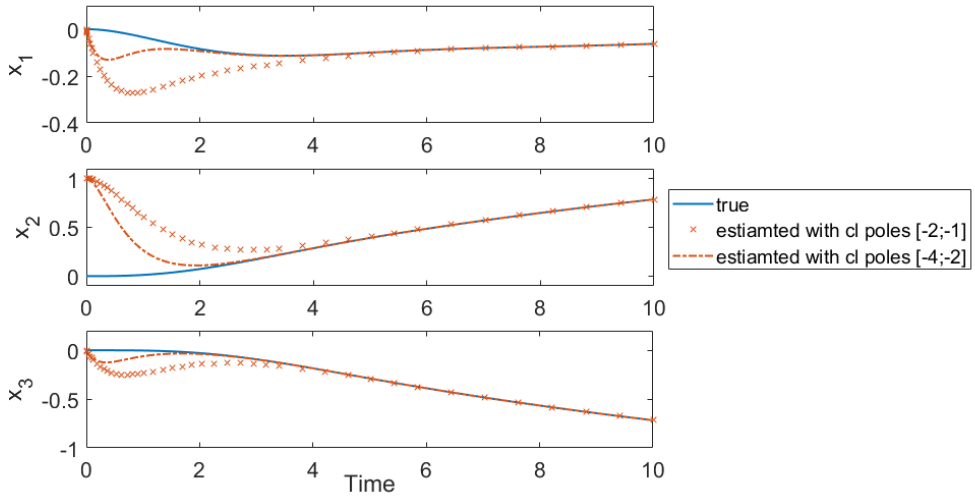

Figure 4.1: Example 1 UIO estimation results with different closed-loop poles

different gain vectors:

$$L = \begin{bmatrix} 5 \\ -9 \end{bmatrix} \text{ and } \begin{bmatrix} 2 \\ -3 \end{bmatrix}, \tag{4.46}$$

setting the closed-loop poles at $[-2,\ -1]$ and $[-4,\ -2]$, respectively. The latter one has faster convergence.

Example 2 from Hou & Muller (1992) System:

$$\dot{x} = \begin{bmatrix} -1 & -1 & 0 \\ 0 & -1 & 1 \\ 0 & 0 & -1 \end{bmatrix} x + \begin{bmatrix} 1 \\ 0 \\ 0 \end{bmatrix} \mu \tag{4.47}$$

$$y = \begin{bmatrix} 1 & 0 & 1 \\ 0 & 0 & 1 \end{bmatrix} x \tag{4.48}$$

State transformation : $z = T^{-1}x$, where

$$T^{-1} = \begin{bmatrix} 0 & 0 & 1 \\ 0 & 1 & 0 \\ 1 & 0 & 0 \end{bmatrix}, \quad z = \begin{bmatrix} z_I \\ z_V \end{bmatrix}, \quad z_I \in \mathbb{R}^2,\ z_V \in \mathbb{R}. \tag{4.49}$$

Invariants dynamics are:

$$\dot{z}_I = \tilde{A}_1 z_I, \tag{4.50}$$

$$y_I = \tilde{C}_1 \hat{z}_I \tag{4.51}$$

where

$$\tilde{A}_1 = \begin{bmatrix} -1 & 0 \\ 1 & -1 \end{bmatrix}, \quad \tilde{C}_1 = \begin{bmatrix} 1 & 0 \end{bmatrix}. \tag{4.52}$$

The UIO is:

$$\dot{\hat{z}}_I = (\tilde{A}_1 - L\tilde{C}_1)\hat{z}_I + L^* y \tag{4.53}$$

where

$$L^* = \begin{bmatrix} 0 & l_1 \\ 0 & l_2 \end{bmatrix} \tag{4.54}$$

$L = [l_1\ l_2]^T$ is the observer gain vector. The pair $(\tilde{A}_1, \tilde{C}_1)$ is only detectable, not observable. Using Theorem 4.2 (3) and setting s = -1 to test the observability of the original system, we reach the same conclusion. Therefore the convergence rate of UIO Eq. (4.53) is not entirely assignable.

Example 3: single-tank homogeneous CSTR Reaction: $\mathbf{A} + \mathbf{B} \rightarrow \mathbf{C}$. The reactor model is:

$$\begin{bmatrix} \frac{dC_A}{dt} \\ \frac{dC_B}{dt} \\ \frac{dC_C}{dt} \end{bmatrix} = \begin{bmatrix} -d & 0 & 0 \\ 0 & -d & 0 \\ 0 & 0 & -d \end{bmatrix} \begin{bmatrix} C_A \\ C_B \\ C_C \end{bmatrix} + \begin{bmatrix} F_{in} & 0 & 0 \\ 0 & F_{in} & 0 \\ 0 & 0 & F_{in} \end{bmatrix} \begin{bmatrix} C_{A,in} \\ C_{B,in} \\ C_{C,in} \end{bmatrix} + vr, \tag{4.55}$$

$$\text{where} \quad v = \begin{bmatrix} -1 \\ -1 \\ 1 \end{bmatrix}, \quad \text{and} \quad d = \frac{F_{in}}{V}. \tag{4.56}$$

We only have $n_r = 1$ reaction, therefore we only need to measure reaction temperature, for estimating $\hat{C}_A, \hat{C}_B, \hat{C}_C$. The states of the OA are the total enthalpy and two reaction invariants:

$$z_I = v^{\perp} \begin{bmatrix} C_A \\ C_B \\ C_C \end{bmatrix}, \quad \text{where } v^{\perp} = \begin{bmatrix} 1 & 0 & 1 \\ 0 & 1 & 1 \end{bmatrix}. \tag{4.57}$$

The composition estimations are shown and compared with true composition profiles in Figures 4.2 (a)-(c). The measured temperature is shown in Figure 4.2 (d). The invariants estimated and true profiles are shown in Figure 4.3 (a)-(c). The observer starts with wrong initial conditions of unmeasured compositions and converges to the true value asymptotically. The shift of steady-states are caused by the change of F_{in} and $C_{A,in}$ as shown in 4.3 (d).

Example 4: heterogeneous reaction system The asymptotic observer is applied to a simulated heterogeneous reaction system. The heterogeneous reaction example is from Bhatt et al. (2010), which is an isothermal, gas-liquid system involving the chlorination of butanoic acid. The mechanisms of mass transfer between phases and two reactions are assumed to be unknown. The sketch of the reactor is shown in Figure 4.4. In the liquid phase, one main reaction produces α-monochlorobutanoic acid (MBA) and hydrochloric acid (HCl), and one side reaction produces side product α-dichlorobutanoic acid (DBA) and HCl.

$$R_1 : BA + Cl_2 \rightarrow MBA + HCl \tag{4.58}$$

$$R_2 : BA + 2Cl_2 \rightarrow DBA + 2HCl \tag{4.59}$$

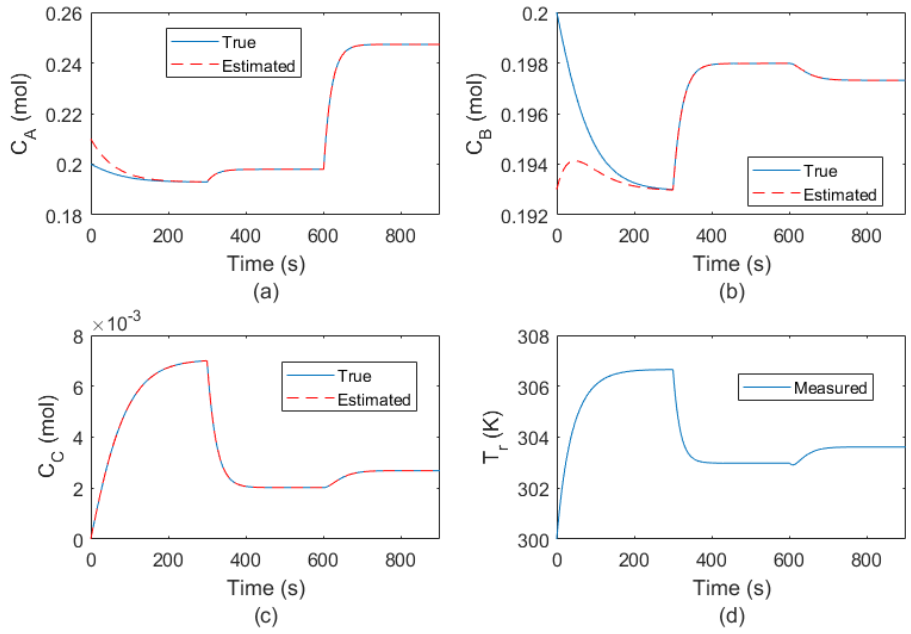

Figure 4.2: (a)-(c) Comparison plots of estimated reaction compositions with true values, and (d) plot of measured temperature

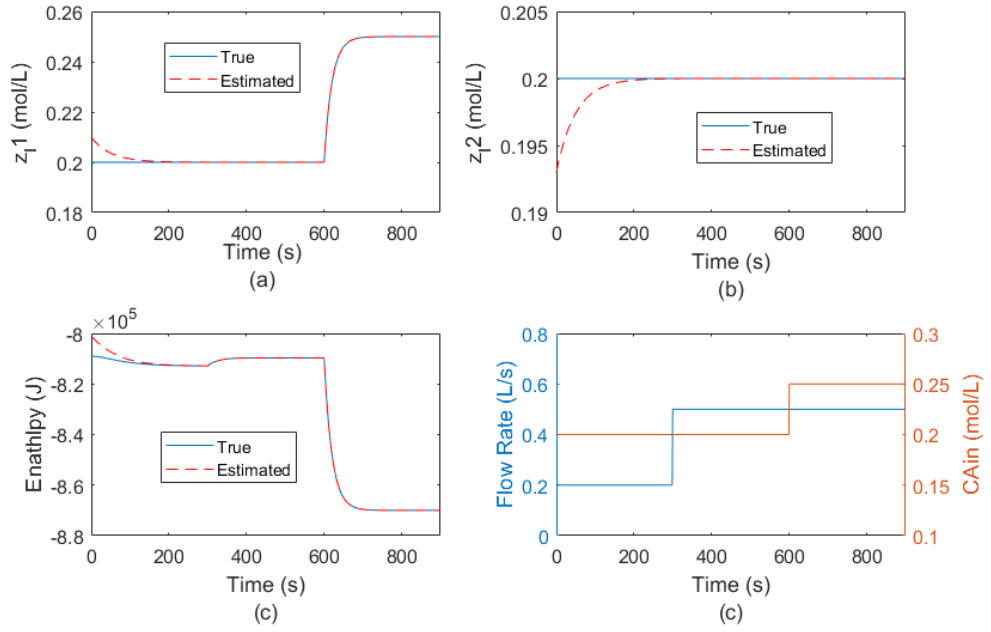

Figure 4.3: Estimated two invariants and enthalpy compared with true values, and two disturbances: F_{in} and $C_{A,in}$

Cl_2 and HCl can be found in both gas and liquid phases. The reactant Cl_2 is fed through an gas inlet, and the reactant BA is fed through the liquid phase. The reactor starts with gas phase with air and liquid phase with ethanol. Mole balances of 9 components need to be modeled to fully describe the reactor. The following equations includes 7 of them, excluding the nonreactive components: air and ethanol.

$$\begin{bmatrix} \dot{n}_{Cl_2}(g) \\ \dot{n}_{HCl}(g) \\ \dot{n}_{Cl_2}(l) \\ \dot{n}_{BA} \\ \dot{n}_{MBA} \\ \dot{n}_{HCl} \\ \dot{n}_{DBA} \end{bmatrix} = \underbrace{\begin{bmatrix} \frac{-F_{out,g}}{m_g} & & & & & & \\ & \frac{-F_{out,g}}{m_g} & & & & & \\ & & \frac{-F_{out,l}}{m_l} & & & & \\ & & & \ddots & & & \\ & & & & \ddots & & \\ & & & & & \ddots & \\ & & & & & & \frac{-F_{out,l}}{m_l} \end{bmatrix}}_{A} \begin{bmatrix} n_{Cl_2}(g) \\ n_{HCl}(g) \\ n_{Cl_2}(l) \\ n_{BA} \\ n_{MBA} \\ n_{HCl} \\ n_{DBA} \end{bmatrix}$$

$$+ \underbrace{\begin{bmatrix} \frac{1}{Mw_{Cl_2}} & 0 \\ 0 & 0 \\ 0 & 0 \\ 0 & 0 \\ 0 & \frac{1}{Mw_{BA}} \\ 0 & 0 \\ 0 & 0 \end{bmatrix}}_{B} \begin{bmatrix} F_{in,g} \\ F_{in,l} \end{bmatrix} + \underbrace{\begin{bmatrix} -1 & 0 & 0 & 0 \\ 0 & -1 & 0 & 0 \\ 1 & 0 & -1 & -2 \\ 0 & 0 & -1 & -2 \\ 0 & 0 & 1 & 0 \\ 0 & 1 & 1 & 2 \\ 0 & 0 & 0 & 1 \end{bmatrix}}_{D} \begin{bmatrix} \zeta_{Cl_2,gl} \\ \zeta_{HCl,lg} \\ r_1 V_l \\ r_2 V_l \end{bmatrix} \tag{4.60}$$

$n(g)$ represents the gas phase component's mole numbers, and $n(l)$ and n present liquid phase component's model numbers; $F_{out,g}$ is the fixed gas phase outlet mass flow rate. $F_{out,l}$ represents liquid outlet mass flow rates used to control liquid phased volume at $5.8230\ \mathrm{m}^3$. m_g and m_l are the total gas mass and liquid mass in the reactor; $F_{in,g}$, $F_{in,l}$ represent the inlet mass flow rates of Cl_2 gas into the gas phase and BA into the liquid phase, and $F_{in,g}$ is the manipulated variables to control pressure at $P = 10$ bar; $\zeta_{Cl_2,gl}$ and $\zeta_{HCl,lg}$ represent the mass transfer rates of Cl_2 and HCl; r_1 and r_2 are the reaction rates; V_l is the liquid phase volume.

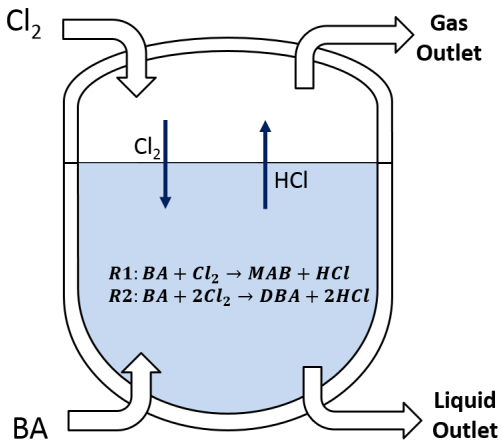

Figure 4.4: Schematic of the example heterogeneous reactor

The unknown input vector is:

$$\mu = \begin{bmatrix} \zeta_{Cl_2,gl} \\ \zeta_{HCl,lg} \\ r_1 V_l \\ r_2 V_l \end{bmatrix}. \tag{4.61}$$

Its involvement matrix D is composed of first two columns describing whether and which direction the components is transferred between two phases, and the remaining columns represent the involvement of components in the reactions. To estimate four unknown rates, we need at least four good measurements, in a sense that the evolution of the four rates can be observed from the measurements, i.e.

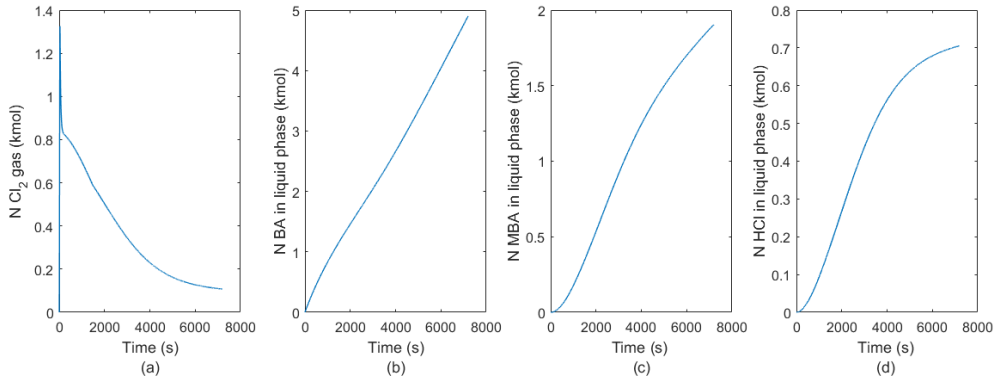

Figure 4.5: Measured compositions

$\text{rank}(D) = \text{rank}(CD) = 4$. Therefore, we choose the measurements as follows:

$$y = \underbrace{\begin{bmatrix} 1 & 0 & 0 & 0 & 0 & 0 & 0 \\ 0 & 0 & 0 & 1 & 0 & 0 & 0 \\ 0 & 0 & 0 & 0 & 1 & 0 & 0 \\ 0 & 0 & 0 & 0 & 0 & 1 & 1 \end{bmatrix}}_{C} \begin{bmatrix} n_{Cl_2}(g) \\ n_{HCl}(g) \\ n_{Cl_2}(l) \\ n_{BA} \\ n_{MBA} \\ n_{HCl} \\ n_{DBA} \end{bmatrix} \tag{4.62}$$

Figure 4.5 shows the profiles of four measured compositions that are used in the observer to estimate the unmeasured species. The observer starts with the right initial condition in this example, thus it is able to estimate the true profile perfectly. If there is an error in the initial condition, the convergence rate fixed by the dilution rates, averagely $\frac{F_{gout}}{V_g} = 0.1573s^{-1}$ and $\frac{F_l}{V_l} = 0.0167s^{-1}$, would be very slow. The control inputs were determined by a PID controller.

Dochain (2000) applied the AO to tubular reactors, and was able to improve it to an closed-loop UIO, of which the convergence rate can be arbitrarily assigned. The interconnected nature of each volume element in a tubular reactor, compared with CSTR considered as an independent single volume element, renders the system observable, and hence its states reconstructible through an exponential observer.

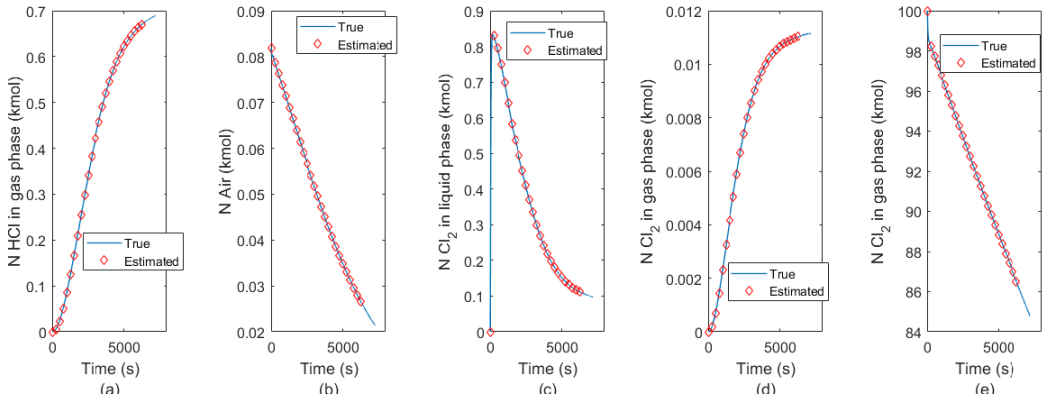

Figure 4.6: Comparison between estimated and true profiles of the unmeasured compositions

The interested readers are referred to that work.

4.6. Conclusions

In this chapter, we presented the unknown input observer in open-loop form and closed-loop form, and the asymptotic observer designed for chemical reaction systems. The connection between OA and UIO is shown. We consider the OA as an open-loop UIO, which is tailored to estimate unmeasured compositions without the knowledge of reaction kinetics. The stoichiometry in mole balances is used for constructing reaction variants and invariants, and the energy balance can be used as an extra dynamic constraint in the OA. The estimation convergence type is based on the observability of the invariants model and whether it is open-loop or closed-loop. Two numerical examples and two reaction examples are shown to illustrate the convergence issues of UIO and the application of AO.

5. Adaptive Control

In this chapter, we integrate the parameter estimation, state estimation and passivity-based control methods developed so far in the thesis, to construct the overall adaptive control framework. The adaptive control schemes presented in this chapter are constructed and adjusted with the objective of ensuring closed-loop stability.

In Section 5.1, we give the motivation of different adaptive control designs from the perspective of passivity. Passivity may not be conserved when uncertainty estimation error exists, which puts closed-loop stability under overall passivity-based adaptive control into question. To resolve this, we propose two types of adaptive controllers.

The first type of adaptive controller presented in Section 5.2 draws information from the passivity-based input estimator (PBIE) to restore the passivity of the control subsystem. The exponential stability for the closed-loop is proved.

In Section 5.3, the second type of adaptive controller does not attempt to conserve the passivity of the control subsystem, but imposes a convergence property on the uncertainty estimates. With this estimation quality assumption, we can show that overall closed-loop is asymptotically stable. In Section 5.3.3, we consider systems with partially linear structure in the internal dynamics, and show that we can use state estimates from the unknown-input observer (UIO) in the adaptive controller and achieve asymptotic stability. Section 5.3.5 gives the analysis on zero-dynamics stability of the partially linear systems with uncertainty under output feedback control.

In Section 5.4, the proposed adaptive control approach is applied to control

simulated homogeneous and heterogeneous reaction systems. We complete this chapter with conclusions in Section 5.5.

5.1. Motivation of Adaptive Controller Designs

The designs of passivity-based control scheme from Chapter 2 and estimation from Chapter 3 are centered around passivity and related stability theorems. During both developments, we obtain passive systems through transformation using derivatives and output dynamics information, and then stabilize the passive systems through proportional feedback. In this chapter, when we combine the two and form one adaptive control scheme, we wonder that if the passivity of two subsystems, one for control and one for estimation, can be maintained. We also need to investigate how the overall closed-loop stability can be shown with or without the passivity property for the control subsystem, and in the later case, the loss of passivity is caused by the uncertainty estimation error.

In Chapter 2, Theorem 2.4, we showed a general transformation to passivate the output dynamics:

$$\frac{dy}{dt} = \bar{p}(y) + D\Delta p(x) + \phi(y)u, \tag{5.1}$$

for control purpose, the mapping from transformed input u_c to output e_y, shown as follows:

$$u_c = \frac{dy^*}{dt} - L_f h(x) - L_g h(x)u, \quad e = y^* - y, \tag{5.2}$$

is passive. However, due to the existence of uncertainty Δp, the passive relationship is broken if we use an estimate $\Delta\hat{p}$ in the transformation, and $\Delta\hat{p} \neq \Delta p$. Figure 5.1 illustrates the integration of PBC and PBIE, and shows that the calculation of u in PBC uses the estimate from PBIE, and results in a non-passive control system. The consequence for lack of passivity is that we may not be able to ensure closed-loop stability through a proportional control feedback.

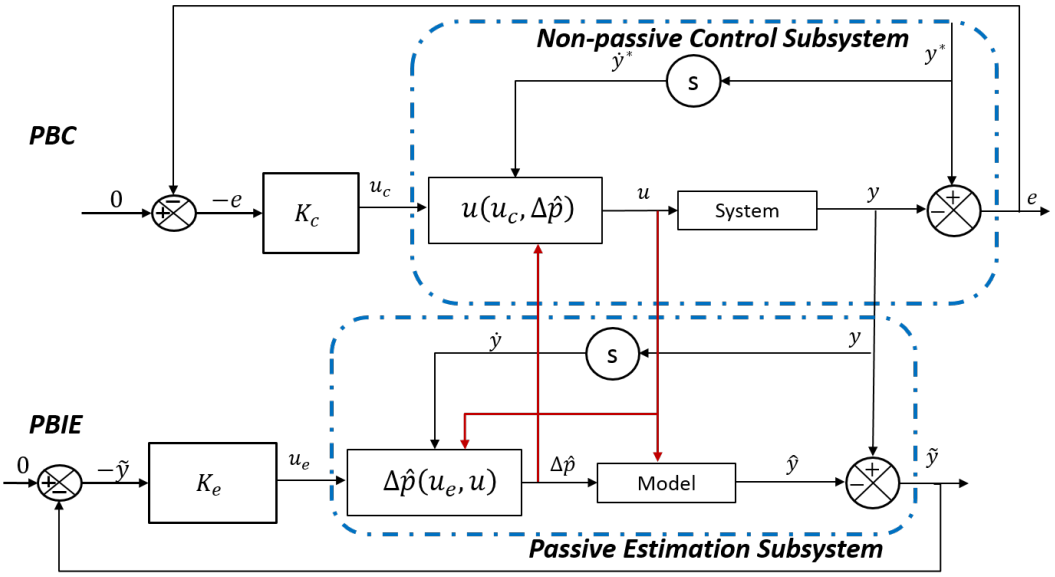

Figure 5.1: Integration of nonpassive control subsystem and passive estimation subsystem

In the rest of chapter, mainly two ways are proposed to resolve the stability issue. The first one is to compensate the estimation error and recover the passive property of the control subsystem in Figure 5.1. The second one is to impose an assumption on the uncertainty estimation quality, i.e. the estimate converges exponentially.

5.2. Design and Integration of Passive Systems

5.2.1. Adaptive Control Development

Let us revisit the nonlinear system introduced at the beginning of the thesis. The internal state space model of the system is:

$$\frac{dx}{dt} = f(x) + g(x, u) \tag{5.3a}$$

$$y = h(x) \tag{5.3b}$$

$$y_d = \dot{y} \tag{5.3c}$$

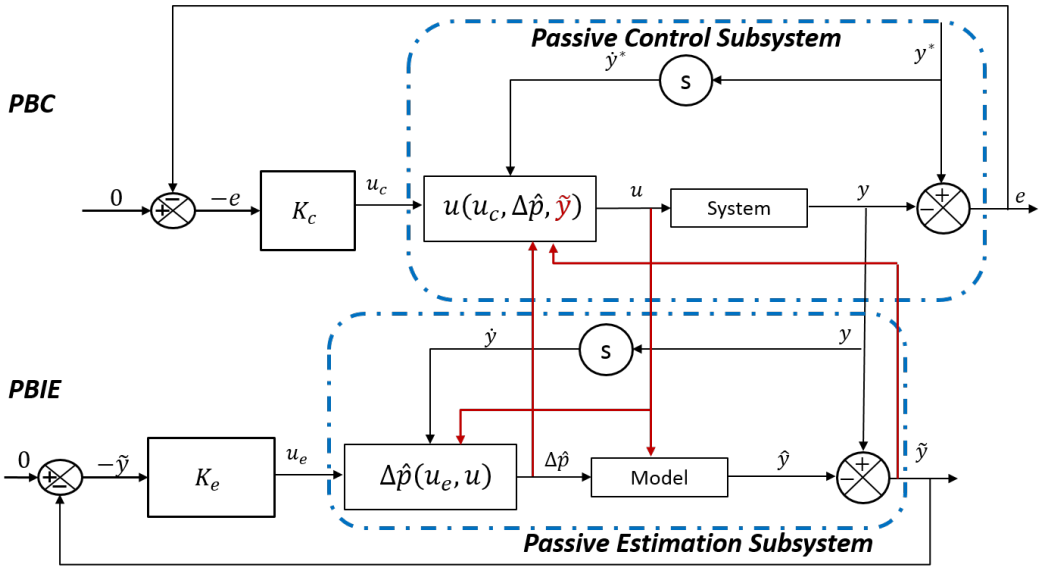

Figure 5.2: Integration of passive control subsystem and passive estimation subsystem

where $x \in \mathbf{X} \subseteq \mathbb{R}^n$, $u \in \mathbb{R}^m$, and $y \in \mathbb{R}^m$. $f,\ g,\ h$ are all sufficiently vector functions with appropriate dimensions. Assume that measurement vector y is chosen such that the derivative of y with respect to time takes the following form:

$$\frac{dy}{dt} = L_f h + L_g h = \bar{p}(y) + D\Delta p(x) + \phi(y)u, \tag{5.4}$$

where the matrix D, and $\phi(y)$ are nonsingular. $\Delta p : \mathbf{X} \to \mathbb{R}^p$ is a uncertain Lipschitz continuous function vector.

To estimate the uncertainty, PBIE is used, and the estimation error is compensated in the control passivation transformation for preserving the passivity. As shown in Figure 5.2, the block calculating the true control input u now is adjusted to takes compensation term into account, represented by $\Delta\tilde{p}$. Further details of adaptive control laws and derivations are shown in the following theorem and proof.

Theorem 5.1. Consider system (5.3) and its output dynamics (5.4) with Lipschitz continuous uncertainty $\Delta p(x)$. The closed-loop dynamics under the following

adaptive controller , for y at setpoint y^*, is globally exponentially stable.

$$\frac{d\hat{y}}{dt} = \bar{p}(\hat{y}) + D\Delta\hat{p} + \phi(\hat{y})u, \tag{5.5a}$$

$$\Delta\hat{p} = D^{-1}\left(\dot{y} + K_e\tilde{y} - \bar{p}(\hat{y}) - \phi(\hat{y})u\right), \tag{5.5b}$$

$$u^* = \phi(\hat{y})^{-1}(\dot{y}^* + K_c e_y + K_e\tilde{y} - \bar{p}(\hat{y}) - D\Delta\hat{p}), \tag{5.5c}$$

$$\bar{u} = B_f^{-1}(\dot{u}^* + K_{cf}e_u + \phi(\hat{y})^T e_y - A_f u), \tag{5.5d}$$

$$\frac{du}{dt} = A_f u + B_f\bar{u}, \tag{5.5e}$$

where eig(A_f)> 0, and A_f and B_f are nonsingular; the gain matrices K_e, K_c and K_{cf} are diagonal positive definite matrices. The error vectors are:

$$\tilde{y} = y - \hat{y}, \quad e_u = u^* - u, \quad e_y = y^* - y. \tag{5.6}$$

The exponential stability is defined in a sense that $\hat{y} \to y$, and $y \to y^*$ exponentially.

Proof. We prove the theorem using control Lyapunov function: $V = \frac{1}{2}e_y^T e_y + \frac{1}{2}e_u^T e_u + \frac{1}{2}\tilde{y}^T\tilde{y}$. Its time derivative is:

$$\dot{V} = e_y^T\dot{e}_y + e_u^T\dot{e}_u + \tilde{y}^T\dot{\tilde{y}}. \tag{5.7}$$

The last quadratic term is the Lyapunov function of PBIE, and through update law (5.5b) for estimate $\Delta\hat{p}$, we have:

$$\dot{V} = e_y^T\dot{e}_y + e_u^T\dot{e}_u - K_e\tilde{y}^T\tilde{y}, \tag{5.8}$$

The next step is to show that control equations (5.5c) and (5.5d) will render

$$\dot{V} \le -\alpha||e||^2, \quad \text{where, } \alpha > 0, e = \begin{bmatrix} e_y \\ e_u \\ \tilde{y} \end{bmatrix} \tag{5.9}$$

For convenience, we will use the following simplified notations:

$\bar{p} = \bar{p}(y),\ \hat{\bar{p}} = \bar{p}(\hat{y}),\ \tilde{\bar{p}} = \bar{p} - \hat{\bar{p}}$

$\phi = \phi(y),\ \hat{\phi} = \phi(\hat{y}),\ \tilde{\phi} = \phi - \hat{\phi}$

and for the uncertainty to be estimated: $\Delta p = \Delta\hat{p} + \Delta\tilde{p}$.

We first rewrite down the time derivative of control error of output:

$$\dot{e}_y = \dot{y}^* - \bar{p} - D\Delta p - \phi u \tag{5.10}$$

$$= \dot{y}^* - \bar{p} - D\left(\Delta\hat{p} + \Delta\tilde{p}\right) - \phi u. \tag{5.11}$$

According to (3.34), the estimation error $\Delta\tilde{p}$ through PBIE is:

$$\Delta\tilde{p} = D^{-1}(-\tilde{\bar{p}} - \tilde{\phi}u - K_e\tilde{y}). \tag{5.12}$$

Therefore,

$$\dot{e}_y = \dot{y}^* - \bar{p} - D\Delta\hat{p} + \tilde{\bar{p}} + \tilde{\phi}u + K_e\tilde{y} - \phi u = \dot{y}^* - \hat{\bar{p}} - D\Delta\hat{p} - \hat{\phi}u + K_e\tilde{y} \tag{5.13}$$

To make the first term in (5.8) negative definite, we set $\dot{e}_y = -K_c e_y$, and we could solve for u. While this value is actually used as a setpoint for u, i.e. u^*, as we augmented the original system with (5.5e), and u does not reach the computed value instantaneously. Therefore, $u^* = u - e_u$, where e_u is the error between u^* and u.

$$u^* = \hat{\phi}^{-1}(\dot{y}^* + K_c e_y + K_e\tilde{y} - \hat{\bar{p}} - D\Delta\hat{p}), \tag{5.14}$$

with which $\dot{e}_y = -K_c e_y + \hat{\phi}e_u$. Then, the time derivative of V is:

$$\dot{V} = -K_c e_y^T e_y + e_u^T(\hat{\phi}^T e_y + \dot{e}_u) - K_e\tilde{y}^T\tilde{y} \tag{5.15}$$

Set

$$\hat{\phi}^T e_y + \dot{e}_u = -K_{cf} e_u \tag{5.16}$$

and plug in

$$\dot{e}_u = \dot{u}^* - A_f u - B_f \bar{u}, \tag{5.17}$$

then solve for $\bar{u}$ to get:

$$\bar{u} = B_f^{-1}(\dot{u}^* + K_{cf} e_u + \hat{\phi}^T e_y - A_f u) \tag{5.18}$$

Above all with the control equations, the time derivative of the Lyapunov function is:

$$\dot{V} = -K_c e_y^T e_y - K_{cf} e_u^T e_u - K_e \tilde{y}^T \tilde{y} \tag{5.19}$$

$$= -\|K^{\frac{1}{2}} e\|^2 \leq -K_{\min}\|e\|^2, \tag{5.20}$$

where $K_{\min}$ is the smallest gain parameter of controller and estimator. It shows the errors will exponentially decay to zero. □

The adaptive controller includes a pseudo first order dynamics for u, (5.5e). This augmented dynamics is to ensure the solution existence of $\Delta\hat{p}$ and u. Since we derive the control and estimation both in dynamics-inversion fashion, then without the augmentation, the system of equations:

$$D\Delta\hat{p} + \phi(\hat{y})u = \dot{y} + K_e\tilde{y} - \bar{p}(\hat{y}) \tag{5.21}$$

$$D\Delta\hat{p} + \phi(\hat{y})u = \dot{y}^* + K_c e_y + K_e\tilde{y} - \bar{p}(\hat{y}), \tag{5.22}$$

were to be solved for $\Delta\hat{p}$ and u. The solution either does not exist or is not unique. The right hand sides of the above equations are in general feedback and feedfoward terms for estimation and control, respectively.

While, after the augmentation, we actually solve (5.22) for a pseudo setpoint u^*. Then the true u is calculated through integrating (5.5e), with input $\bar{u}$ determined by (5.5d), which allows u to converge to u^*.

To address this type of cascaded tracking problem, we use backstepping. This

technique is useful when the output and input cannot be related through first order differential equations. As in this case, the input $\bar{u}$ and the output y are related through second order differential equations. The backstepping control will be the topic of Chapter 6, where a passivity-based design is proposed and examined. A fuller derivation and detailed explanation of backstepping controller is deferred till then.

For the partially linear case, we can apply Theorem 5.1 straightforwardly. Consider the following scalar system:

$$\frac{dx}{dt} = ax(t) + bu(t) + d\mu(x,t), \quad b \neq 0, \tag{5.23a}$$

$$y = x, \tag{5.23b}$$

$$y_d = \dot{x}, \tag{5.23c}$$

where the state x and its time derivative $\dot{x}$ are measured; a, b, and d are constants. We want to control x at a constant or time-varying set point x^*, by manipulating $u(t)$ under the existence of uncertainty $\mu(x,t)$, which is Lipschitz continuous.

Theorem 5.2. Consider the scalar system (5.23) with Lipschitz continuous unknown time-varying input $\mu(t)$, measured state $x(t)$, and measured time derivative $\dot{x}(t)$. The adaptive controller:

$$\frac{d\hat{x}}{dt} = a\hat{x}(t) + bu(t) + d\hat{\mu}(t), \tag{5.24a}$$

$$\hat{\mu}(t) = \frac{1}{d}\left(\dot{x} + k_e\tilde{x} - a\hat{x} - bu\right) \tag{5.24b}$$

$$\frac{du}{dt} = a_f u + b_f \bar{u}, \quad a_f < 0,\ b_f \neq 0, \tag{5.24c}$$

$$u^* = \frac{1}{b}\left(\dot{x}^* + k_{c,1}e_x - ax - d\hat{\mu} + (a + k_e)\tilde{x}\right), \tag{5.24d}$$

$$\bar{u} = \frac{1}{b_f}\left(\dot{u}^* + k_{c,2}e_u + be_x - a_f u\right), \tag{5.24e}$$

where $\tilde{x} = x - \hat{x}$, $e_u = u^* - u$, $e_x = x^* - x$, can exponentially stabilize x at the desired

setpoint x^*, if the following conditions of gains are satisfied:

$$k_e > 0, k_{c,1} > 0, k_{c,2} > 0. \tag{5.25}$$

Proof. The exponential stability can be shown by the composite Lyapunov function is $V = \frac{1}{2}e_y^2 + \frac{1}{2}e_u^2 + \frac{1}{2}\tilde{x}^2$. With the adaptive controller, the time derivative of the Lyapunov function is $\frac{dV}{dt} = -k_{c,1}e_1^2 - k_{c,2}e_2^2 - k_e\tilde{x}^2$. The derivation of the controller and proof is the same as the nonlinear case after replacing the nonlinear dynamics to the linear ones. □

5.2.2. *Numerical Example*

In this section, we test the designed adaptive controller (5.5) with a nonlinear control example adapted from Wang & Ydstie (2007). The example is a scalar system:

$$\frac{dx}{dt} = -x + 2x^2 + (x^2 + 1)u + \Delta p, \quad \text{where } \Delta p = \sin(5t), \quad x(t_0) = 0.5, \tag{5.26}$$

$$y = x, \tag{5.27}$$

$$y_d = \dot{x}. \tag{5.28}$$

We want to control state x to track a sinusoidal setpoint profile: $x^* = \sin(0.5t)$ without knowing Δp. The adaptive controller parameters are: $K_e = 10,\ K_c = 1, K_{cf} = 5$. The augmented filter for u is:

$$\frac{du}{dt} = -u + \bar{u}. \tag{5.29}$$

We simulated the system with the specified controller in Matlab. In terms of the estimator performance, the PBIE starts with a wrong initial condition $\hat{x}(t_0) = 0.7$, but converges quickly to the true profile shown in Figure 5.3 (a), so does the estimated uncertainty in Figure 5.3 (b). Figure 5.3 (a) also shows that the true state under control tracks the time-varying setpoint profile after initial convergence. The control Lyapunov function exponentially decays towards zero during the simulation as shown in Figure 5.4.

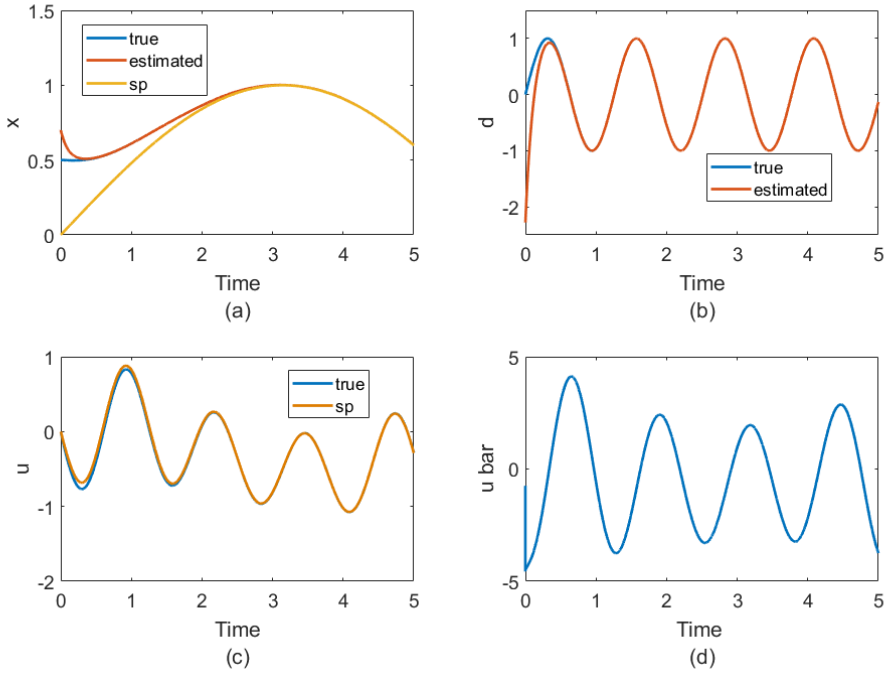

Figure 5.3: Control and estimation results of nonlinear example.

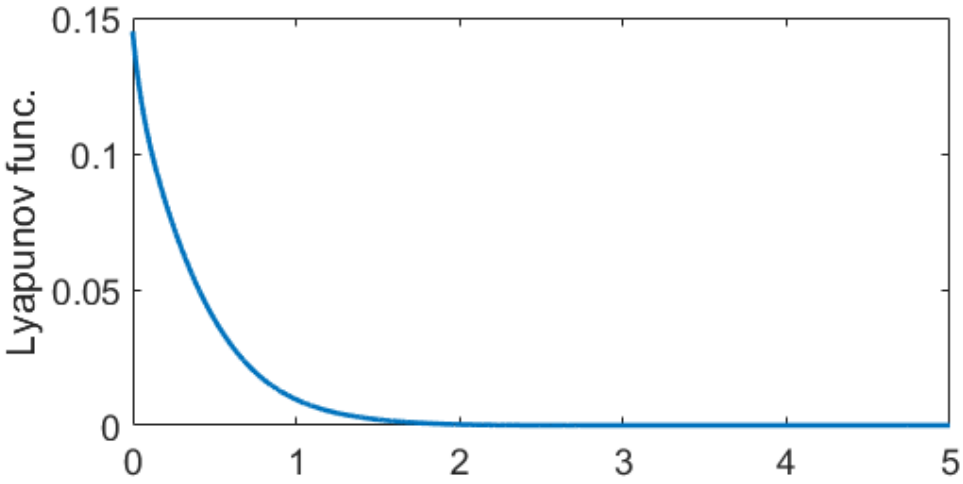

Figure 5.4: Control Lyapunov function profile.

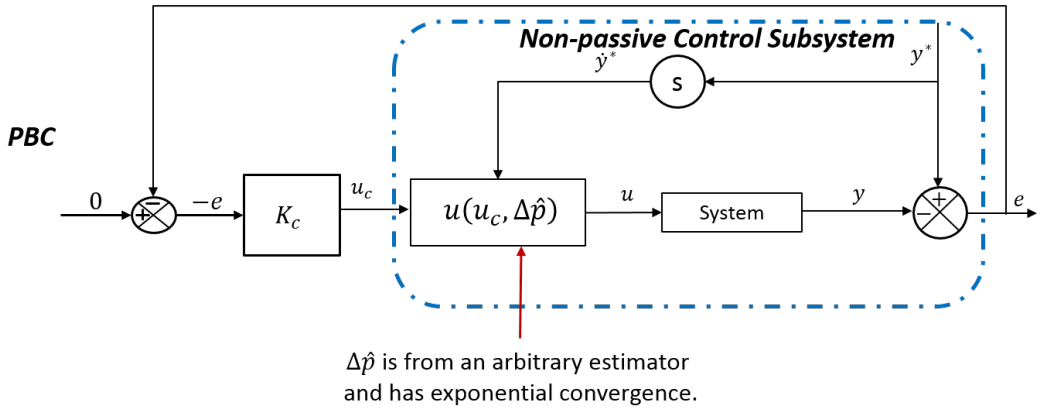

Figure 5.5: Integration of non-passive control subsystem and an exponential converging estimator

5.3. Adaptive Control via Estimators

5.3.1. Adaptive Control Development

In this section, we examine the output tracking problem again for nonlinear system (5.3) with uncertain output dynamics (5.4). We use an estimate of the uncertainty, $\Delta\hat{p}$, in the control calculation, and don't compensate for the lack of passivity resulted from estimation error.

The estimate can be from an arbitrary estimator, but we assume it to exponentially converge to the true value. With this assumption, we are able to show the closed-loop dynamics being asymptotically stable, and imply that the passivity-based controller can be used together with other qualified estimators. We give this result in the following theorem, and the schematic is shown in Figure 5.5.

Theorem 5.3. Consider single-input-single-output nonlinear system (5.3) with uncertain output dynamics (5.4). $\Delta\hat{p} \in \mathbb{R}$ is the estimate given by an estimation scheme, and the error $\Delta\tilde{p} = \Delta p - \Delta\hat{p}$ satisfies:

$$\Delta\tilde{p}(t) = \lambda\Delta\tilde{p}(t_0)e^{-k_e(t-t_0)}, \quad \text{where } k_e > 0. \tag{5.30}$$

The adaptive controller for y at y^* is designed as:

$$u^* = \frac{1}{\phi(y)}(\dot{y}^* + k_{c,1}e_y - \bar{p}(y) - D\Delta\hat{p}), \tag{5.31a}$$

$$\bar{u} = \frac{1}{b_f}\left(\dot{u}^* + k_{c,2}e_u + \phi(y)e_y - a_f u\right), \tag{5.31b}$$

$$\frac{du}{dt} = a_f u + b_f \bar{u}, \tag{5.31c}$$

where $a_f < 0$ and $b_f \neq 0$; the error vectors are:

$$e_u = u^* - u, \quad e_y = y^* - y. \tag{5.32}$$

The closed-loop dynamics is asymptotically stable if the following conditions of gains are satisfied:

$$k_1 > 0, k_2 > 0 \quad \text{and } k_e \neq \min\{k_{c,1}, k_{c,2}\}. \tag{5.33}$$

Proposition 5.4. Choice of estimator gain k_e and controller gains $k_{c,1}, k_{c,2}$ can be advised by the following inequality relation:

$$\frac{k_{c,max}^{\frac{1}{2}}(d\lambda)^2}{2k_{c,min}^{\frac{5}{2}} - 2k_e k_{c,min}^{\frac{3}{2}}} < 1. \tag{5.34}$$

This inequality ensures the attenuation of the upset from initial state estimation error $\tilde{y}(t_0)$.

Compare control laws, (5.5c), (5.31a), the former exactly accounts for the estimation error through the terms based on $\tilde{y}$, which comes from using PBIE. In the following we show the proof of Theorem 5.3 and Proposition 5.4, where the estimation mismatch is not compensated in the control laws but assumed to be exponentially convergent .

Proof. Plug in the assumed estimation error:

$$\Delta\tilde{p}(t) = \lambda\Delta\tilde{p}(t_0)e^{-k_e(t-t_0)}, \quad \text{where } k_e > 0. \tag{5.35}$$

and the control laws (5.31a), (5.31b) into (5.4), (5.31c) to obtain the closed-loop control control error dynamics as:

$$\dot{e}_y = -k_{c,1}e_y - d\Delta\hat{p} + \phi(y)e_2 \tag{5.36}$$

$$= -k_{c,1}e_y + \phi(y)e_u - (d\lambda)\Delta\tilde{p}(t_0)e^{-k_e t} \tag{5.37}$$

$$\dot{e}_u = -k_{c,2}e_u - \phi(y)e_y. \tag{5.38}$$

d is the scalar version of D. We define the following new notation for the later use in the proof, K_c is the positive control gain matrix:

$$K_c = \begin{bmatrix} k_{c,1} & 0 \\ 0 & k_{c,2} \end{bmatrix}, \quad k_{c,min} = \min\{k_{c,1}, k_{c,2}\}, \quad k_{c,max} = \max\{k_{c,1}, k_{c,2}\}. \tag{5.39}$$

The control-Lyapunov function is $V_c = \frac{1}{2}e_y^2 + \frac{1}{2}e_u^2$, and its time derivative is:

$$\begin{aligned}
\dot{V}_c &= e_y\dot{e}_y + e_u\dot{e}_u \\
&= -k_{c,1}e_y^2 - k_{c,2}e_u^2 - (d\lambda)\Delta\tilde{p}(t_0)e^{-k_e t}e_y \\
&= -\|K_c^{\frac{1}{2}}e\|^2 - (d\lambda)\Delta\tilde{p}(t_0)e^{-k_e t}e_y \\
&\leq -\|K_c^{\frac{1}{2}}e\|^2 + |d\lambda|\|\Delta\tilde{p}(t_0)|e^{-k_e t} \times \|K_c^{-\frac{1}{2}}\| \times \|K_c^{\frac{1}{2}}e\| \\
&= -\|K_c^{\frac{1}{2}}e\|\left(\|K_c^{\frac{1}{2}}e\| - |d\lambda|e^{-k_e t}|\Delta\tilde{p}(t_0)| \times \|K_c^{-\frac{1}{2}}\|\right) \\
&\leq -\|K_c^{\frac{1}{2}}e\|\left(\sqrt{k_{c,min}}\|e\| - |d\lambda|e^{-k_e t}|\Delta\tilde{p}(t_0)| \times \|K_c^{-\frac{1}{2}}\|\right)
\end{aligned}$$

Therefore, when

$$\|e(t)\| > \frac{|d\lambda|}{\sqrt{k_{c,min}}}e^{-k_e t}|\Delta\tilde{p}(t_0)| \times \|K_c^{-\frac{1}{2}}\| = \alpha(t), \tag{5.40}$$

we have

$$\dot{V}_c < 0, \quad \text{when } e = \begin{bmatrix} e_y \\ e_u \end{bmatrix} \neq 0. \tag{5.41}$$

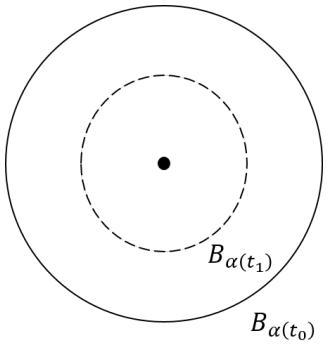

Figure 5.6: Representation of $B_{\alpha(t_0)}$ and $B_{\alpha(t_1)}$

.

It indicates that if we choose K_c large enough so that the error trajectory starts outside the ball $B_{\alpha(t_0)}$, i.e. (5.40) holds at $t = t_0$, $||e||$ will decrease until

$$||e(t)|| = \alpha(t), \quad t = t_1. \tag{5.42}$$

Next step is to examine what happens if the error trajectory enters the ball $B_{\alpha(t_1)}$.

First, we show that $B_{\alpha(t_1)}$ is a positive invariant set, indicated by $\alpha(t_1) > \alpha(t_2)$, if $t_2 > t_1$, since $\alpha(t)$ is an exponentially decreasing function of t. It ensures that at the boundary of $B_{\alpha(t_1)}$, $\frac{\partial V_c(||e(t_1)||,t)}{\partial t} < 0, \forall t > t_1$. So, once the trajectory enters the ball of $B_{\alpha(t_1)}$, it will not exit in any future time.

Then, we examine that if the error trajectory moves towards the origin after entering the ball $B_{\alpha(t_1)}$. $\exists\ t > t_1$, s.t. $||e(t)|| \leq \alpha(t)$, then $\dot{V}_c$ becomes:

$$\dot{V}_c \leq -2k_{c,min}V_c + ||K_c^{\frac{1}{2}}e|| \times |d\lambda|e^{-k_e t}|\Delta\tilde{p}(t_0)| \times ||K_c^{-\frac{1}{2}}|| \tag{5.43}$$

$$\leq -2k_{c,min}V_c + ||K_c^{\frac{1}{2}}|| \times ||e|| \times |d\lambda|e^{-k_e t}|\Delta\tilde{p}(t_0)| \times ||K_c^{-\frac{1}{2}}|| \tag{5.44}$$

$$\leq -2k_{c,min}V_c + ||K_c^{\frac{1}{2}}|| \times \frac{|d\lambda|^2}{\sqrt{k_{c,min}}}e^{-2k_e t}|\Delta\tilde{p}(t_0)|^2 \times ||K_c^{-\frac{1}{2}}||^2 \tag{5.45}$$

Integrate both sides of (5.45) and obtain:

$$V_c \leq V_c(t_0)e^{-2k_{c,min}(t-t_0)} + ||K_c^{\frac{1}{2}}|| \times \frac{|d\lambda|^2}{\sqrt{k_{c,min}}}|\Delta\tilde{p}(t_0)|^2 \times ||K_c^{-\frac{1}{2}}||^2 \int_{t_0}^{t} e^{-2k_{c,min}(t-\tau)}e^{-2k_e\tau}d\tau \tag{5.46}$$

By setting constant $\gamma = ||K_c^{\frac{1}{2}}|| \times \frac{|d\lambda|^2}{\sqrt{k_{c,min}}} \times ||K_c^{-\frac{1}{2}}||^2$, we arrive at:

$$V_c \leq V_c(t_0)e^{-2k_{c,min}(t-t_0)} + \gamma|\Delta\tilde{p}(t_0)|^2 \int_{t_0}^{t} e^{-2k_{c,min}(t-\tau)}e^{-2k_e\tau}d\tau \tag{5.47}$$

$$\leq V_c(t_0)e^{-2k_{c,min}(t-t_0)} + \frac{\gamma}{2k_{c,min}-2k_e}|\Delta\tilde{p}(t_0)|^2\left(e^{-2k_et} - e^{-2k_{c,min}(t-t_0)-2k_et_0}\right) \tag{5.48}$$

Substitute $V_c(t) = \frac{1}{2}||e(t)||^2$ into the above inequality, and solve for $||e(t)||$:

$$||e(t)||^2 \leq ||e(t_0)||^2e^{-2k_{c,min}(t-t_0)} + \frac{\gamma}{k_{c,min}-k_e}|\Delta\tilde{p}(t_0)|^2\left(e^{-2k_et} - e^{-2k_{c,min}(t-t_0)-2k_et_0}\right) \tag{5.49}$$

If $k_{c,min} > k_e$, we have

$$||e(t)||^2 \leq ||e(t_0)||^2e^{-2k_{c,min}(t-t_0)} + \frac{\gamma}{k_{c,min}-k_e}|\Delta\tilde{p}(t_0)|^2e^{-2k_et} \tag{5.50}$$

If $k_{c,min} < k_e$, we have

$$||e(t)||^2 \leq ||e(t_0)||^2e^{-2k_{c,min}(t-t_0)} + \frac{\gamma}{k_e-k_{c,min}}|\Delta\tilde{p}(t_0)|^2e^{-2k_{c,min}t+2(k_{c,min}-k_e)t_0} \tag{5.51}$$

In both cases, $||e(t)||^2$, and therefore $||e(t)||$, is exponentially stable.

Furthermore, we can analyze the impact of $k_{c,min}$ on the control error convergence rate to origin. From first terms in both (5.50) and (5.51), we can see that the convergence of the initial control error is faster with larger gain $k_{c,min}$. To analyze the influence of $k_{c,min}$ on the estimation error, we first reorganize term $\frac{\gamma}{k_{c,min}-k_e}$ by plugging in the expression of γ, and using $||K_c^{-\frac{1}{2}}||^2 = \frac{1}{k_{c,min}}$, $||K_c^{\frac{1}{2}}|| = \sqrt{k_{c,max}}$. Then,

we have

$$\frac{\gamma}{k_{c,min} - k_e}\Delta\tilde{p}(t_0)^2 = \frac{k_{c,max}^{\frac{1}{2}}(d\lambda)^2}{2k_{c,min}^{\frac{5}{2}} - 2k_e k_{c,min}^{\frac{3}{2}}}\Delta\tilde{p}(t_0)^2. \tag{5.52}$$

When choosing estimator and controller gains, the inequality relation

$$\frac{k_{c,max}^{\frac{1}{2}}(d\lambda)^2}{2k_{c,min}^{\frac{5}{2}} - 2k_e k_{c,min}^{\frac{3}{2}}} < 1, \tag{5.53}$$

should be kept in order to reduce the upset from the estimation error. But it is not necessary to ensure the closed-loop stability. □

5.3.2. *Numerical Example*

Numerical simulation of the proposed adaptive control on an example scalar system is performed in Matlab. The actual system is:

$$\frac{dx}{dt} = 10x + u + 5\sin(10t)\sin(t), \quad x(t_0) = 0, \tag{5.54}$$

where the last term is the uncertain parameter to be estimated. Here we still use PBIE as an example of exponential converging estimator. The adaptive control (5.31c), (5.31a), (5.31b) is used to control the system sequentially at constant setpoints $x^* = 5$, and $x^* = 2$. We choose the estimator gain as $k_e = 5$, and control gains as $k_{c,1} = 10$ and $k_{c,2} = 20$, respectively. The estimator starts with a wrong initial condition of $\hat{x}(t_0) = 1$. To deal with the noncontinuous step change of the setpoint, we use a first order filter:

$$x_f^* = \frac{1}{\tau s + 1}x^*, \quad \tau = 0.1, \quad x_f^*(t = 0) = 5, \quad x^* = \begin{cases} 5, & \text{for } t \in [0, 2) \\ 2, & \text{for } t \in [2, 5). \end{cases} \tag{5.55}$$

Figure 5.7 shows the results of state tracking and estimations of parameter. The estimate of μ exponentially converges to its true value, and tracks the dynamics of

the parameter. There is a slight control overshoot before the state is stabilized at the first setpoint, since the estimated parameter has relatively large difference from the true value as shown in Figure 5.8. The overshoot is not observed when the state settles at the second setpoint, since the difference at this point of time is very small. The profiles of MV and pseudo-MV $\bar{u}$ are also shown in Figure 5.7. To further investigate the effect of the estimator gain on the control performance, another simulation is performed with a larger estimator gain $k_e = 8$ and the same set of controller gains. Control results are compared in terms of control errors and Lyapunov function V_c evolution in Figure 5.8. We achieve faster parameter convergence through higher estimator gain, and reduced overshoot as shown in Figure 5.8 (a). Figure 5.9 shows the convergence of the $\|e\|$, the bump around $t = 0.5$ corresponds to the bump of the Lyapunov profile. The first intersection point of $\|e(t_1)\|$ and $\alpha(t_1)$ determines the positive invariant set, ball $B_{\alpha(t_1)}$, after which $\|e(t)\| < \alpha(t)$ before the second intersection. But, once $\|e(t)\| > \alpha(t)$, $\|e(t)\|$ starts to decrease again. The upper bound profile is only active when $UB < \alpha(t)$ and $\|e(t)\| < \alpha(t)$.

5.3.3. *Adaptive Control for Partially Linear Systems with State Estimation*

Consider the partially linear state space model:

$$\frac{dx}{dt} = Ax(t) + Bu(t) + D\mu(x,t), \tag{5.56a}$$

$$y = Cx, \tag{5.56b}$$

$$y_d = \dot{y}, \tag{5.56c}$$

where $x \in \mathbb{R}^n$, $u \in \mathbb{R}^p$, $\mu \in \mathbb{R}^q$, and $y \in \mathbb{R}^m$. $\mu(t)$ is a vector of unknown continuous functions. The output vector y can be partitioned as:

$$y = \begin{bmatrix} y_c \\ y_o \end{bmatrix}, \quad \dim(y_c) = p, \dim(y_o) = m - p. \tag{5.57}$$

y_c represents the control output, and y_o represents the remaining measured outputs. The control problem is to achieve output tracking for y_c. Recall from the

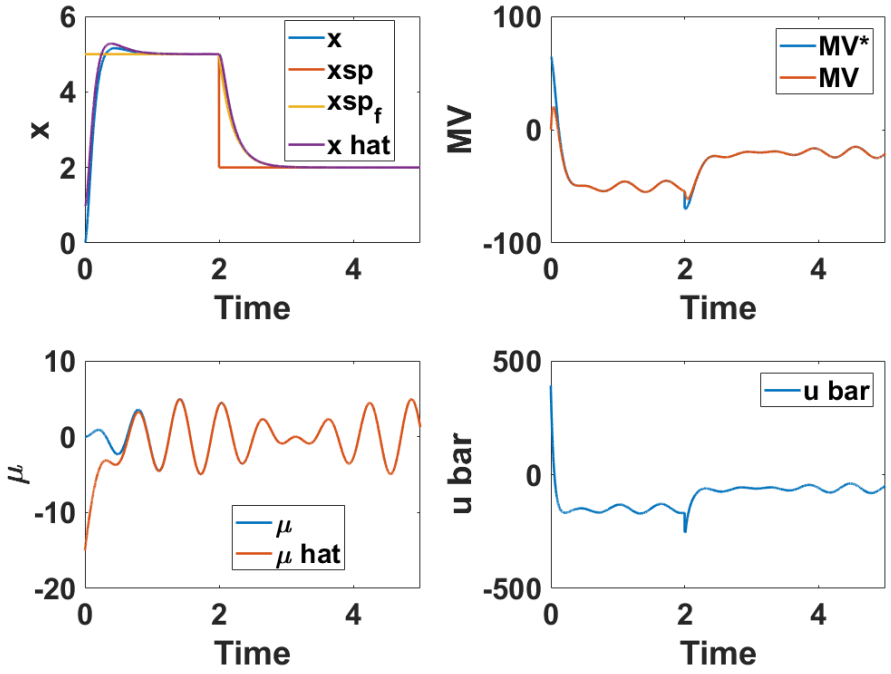

Figure 5.7: Adaptive control result for scalar system.

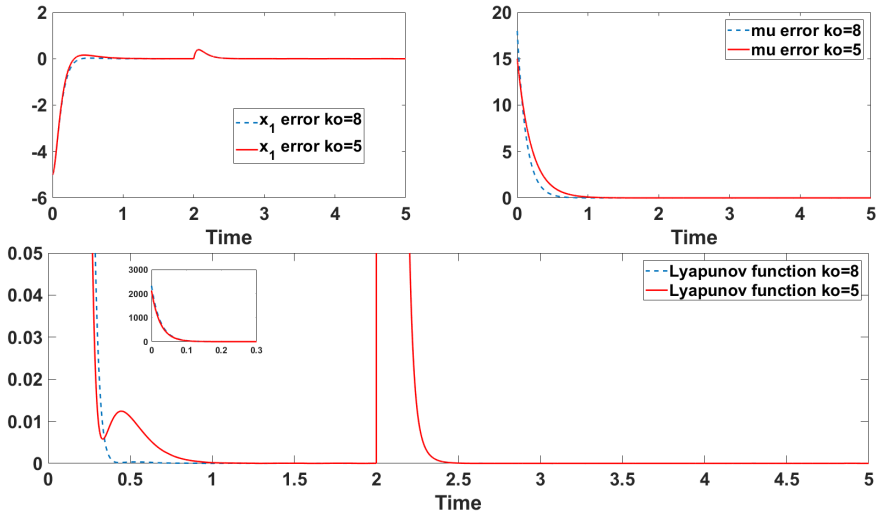

Figure 5.8: Adaptive control comparison with different estimator gains.

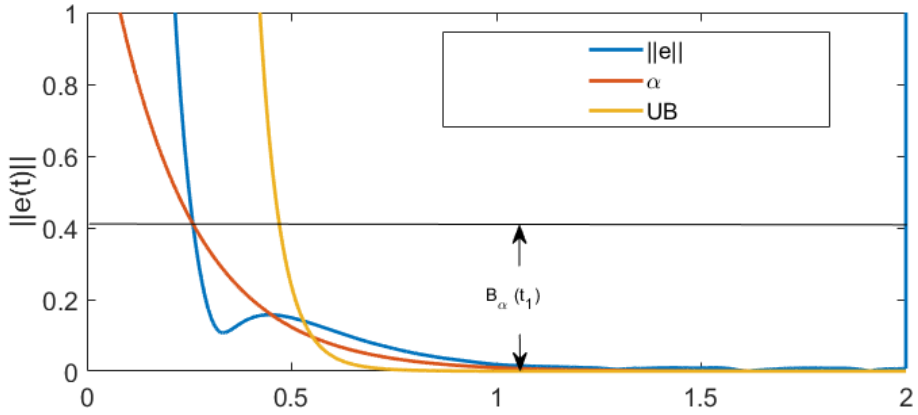

Figure 5.9: Control error norm profile and comparison with other relevant bounds.

beginning of the thesis where we proposed to write the time derivative of y_c as :

$$\frac{dy_c}{dt} = \underbrace{C_c A x + C_c D \mu}_{\Delta p(x)} + \underbrace{C_c B}_{\phi} u, \tag{5.58}$$

where C_c is the corresponding submatrix of C. We can treat the sum of first two terms as one uncertainty vector to be estimated, and used in adaptive control for y_c. The solution following that line of thinking is very similar to the one shown in Theorem 5.3

Sometimes, it is of interest to know the unknown inputs μ and unmeasured states x separately. The UIO and PBIE can be used for those two purposes, respectively. Again, the following measurement conditions need to be met for state and parameter estimation.

1. $\text{rank}(CD) = q$, which indicates that at least more than the number of unknown inputs of measurements are available, and the rank condition makes sure that the uncertainties can be observed by the outputs;

2. the existence conditions of the asymptotically stable UIO need to be met, and they are defined in Theorems 4.1 and 4.2.

Theorem 5.5. Consider system (5.56), (5.57), satisfying above measurements conditions. The adaptive controller for controlling y_c to y_c^* is composed of three parts:

a UIO, a PBIE and a cascaded PBC:

$$\text{UIO}\begin{cases} \frac{d\hat{z}_I}{dt} &= (\tilde{A}_1 - L\tilde{C}_1)\hat{z}_I + \bar{B}_1 u + (LU_2 + E_1)y, \\ \hat{z}_{V,1} &= U_1 y - U_1 C N \hat{z}_I \\ \hat{x} &= T\begin{pmatrix} \hat{z}_I \\ \\ \hat{z}_{V,1} \end{pmatrix} \end{cases} \tag{5.59}$$

$$\text{PBIE}\begin{cases} \frac{d\hat{z}_{V,2}}{dt} &= \bar{A}_{21}\hat{z}_I + \bar{A}_{22}\hat{z}_{V,2} + \bar{B}_2 u + \hat{\mu} \\ \hat{\mu} &= \dot{\hat{z}}_{V,1} + K_e(\hat{z}_{V,1} - \hat{z}_{V,2}) - \bar{A}_{21}\hat{z}_I - \bar{A}_{22}\hat{z}_{V,2} - \bar{B}_2 u \end{cases} \tag{5.60}$$

$$\text{PBC}\begin{cases} u^* &= (C_c B)^{-1}(\dot{y}_c^* + K_c(y_c^* - y_c) - C_c A\hat{x} - C_c D\hat{\mu}) \\ \frac{du}{dt} &= A_f u + B_f \bar{u} \\ \bar{u} &= B_f^{-1}(\dot{u}^* + K_{cf}(u^* - u) + C_c B(y_c^* - y_c) - A_f u), \end{cases} \tag{5.61}$$

where $\text{eig}(A_f) < 0$, and both A_f and B_f are nonsingular. $\hat{z}_{V,1}$ represents the estimated variants from the UIO, and $\hat{z}_{V,2}$ represent the estimated variants from PBIE. The difference between these two estimates are used for feedback in the PBIE. The partially linear system under the above controller is exponentially stable.

Proof. The proof is straightforward using Theorem 5.3, since the estimates of states from UIO and μ from PBIE converge exponentially. □

5.3.4. *Numerical Example*

In this section, we apply the adaptive controller to an SISO example:

$$\dot{x} = \begin{bmatrix} -1 & 1 & 0 \\ -1 & 0 & 0 \\ 0 & -1 & -1 \end{bmatrix} x + \begin{bmatrix} 1 \\ -0.5 \\ 2 \end{bmatrix} u + \begin{bmatrix} -1 \\ 0 \\ 0 \end{bmatrix} \mu \tag{5.62}$$

$$y = \begin{bmatrix} y_o \\ y_c \end{bmatrix} = \begin{bmatrix} 1 & 0 & 0 \\ 0 & 0 & 1 \end{bmatrix} x. \tag{5.63}$$

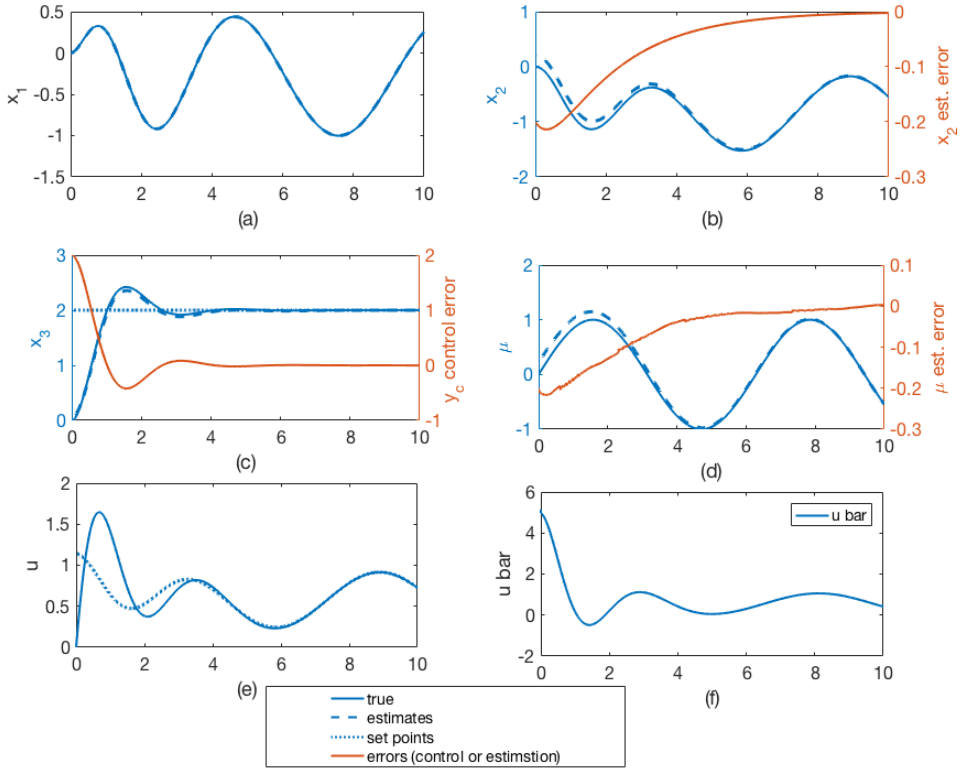

Figure 5.10: Control and estimation result

Measurement conditions are met for the existence of UIO and PBIE. With the extra measured output y_o, we can design closed-loop UIO with assignable convergence rate. The relevant design parameters chosen are: $K_e = 1$ for the PBIE, $L = [1.5000, -1.0000]$ for the UIO, and $K_c = 1$, $K_{cf} = 1$ for the PBC. The proposed adaptive controller with above specifications stabilizes y_c at the set point $y_c^* = 2$ as shown in Figure 5.10 (c). The estimation errors of $\hat{x}_2$ and $\hat{\mu}$ monotonically decrease as shown in Figures 5.10 (b) and (d). Before the estimates converge, the control output slowly oscillates around the set point.

5.3.5. Stability of Zero Dynamics

In this section, we present our stability analysis of zero dynamics obtained using passivity-based control. In Chapter 2, we conducted the analysis for a time-invariant deterministic SISO linear system. Now we are interested in exploring the

same issue when a time-varying parameter $\mu \in \mathbb{R}$ is involved. In this case, there are two input-output relationships that are relevant to the stability of zero dynamics. One is from the output y to the control input u, represented by the transfer function G_u, and the other one is from the output y to μ, represented by the transfer function G_μ. Through simulation analysis, we make the observation that the locations of zeros of G_u and the boundedness of μ determines the stability of zero dynamics.

- If G_u has nonnegative zero, the zero dynamics is unstable.
- If G_u only has negative zero, the zero dynamics is bounded-input bounded-output stable with respect of μ.

We use the following example to illustrate the above conclusions.

$$\dot{x} = \underbrace{\begin{bmatrix} -1 & 1 & 0 \\ -1 & 0 & 0 \\ 0 & -1 & -1 \end{bmatrix}}_{A} x + \underbrace{\begin{bmatrix} 1 \\ -0.5 \\ 2 \end{bmatrix}}_{B} u + \underbrace{\begin{bmatrix} -1 \\ 0 \\ 0 \end{bmatrix}}_{D} \mu, \quad \mu = \sin(t) \tag{5.64}$$

$$y = Cx. \tag{5.65}$$

The C matrix is varied, so that zeros of G_u and G_μ have different types of locations. The time-varying parameter is a bounded signal: $\mu = \sin(t)$. The control objective is to regulate y at $y^* = 2$. The passivity-based control law is:

$$u = (CB)^{-1}[\dot{y}^* + k(y^* - y) - CAx - CD\mu], \quad k = 1. \tag{5.66}$$

- Case 1: $C = [1, 1, 1]$. G_μ has zeros: $[0, 0]$, and G_u has zeros: $[-0.2 - 0.75i,\ -0.2 + 0.75i]$. The control input has cyclic profile to compensate for the sinusoidal parameter in control law (5.66). The states profiles also have trends similar to μ as shown in Figure 5.11, but it does not go unbounded.
- Case 2: $C = [1.1, 0.8]$. G_μ has zeros: $[0.447 - 0.447]$, one of which is not stable. G_u has stable zeros: $[-0.119 - 0.65i \ \ -0.119 + 0.65i]$. The internal states are BIBO as shown in Figure 5.12.

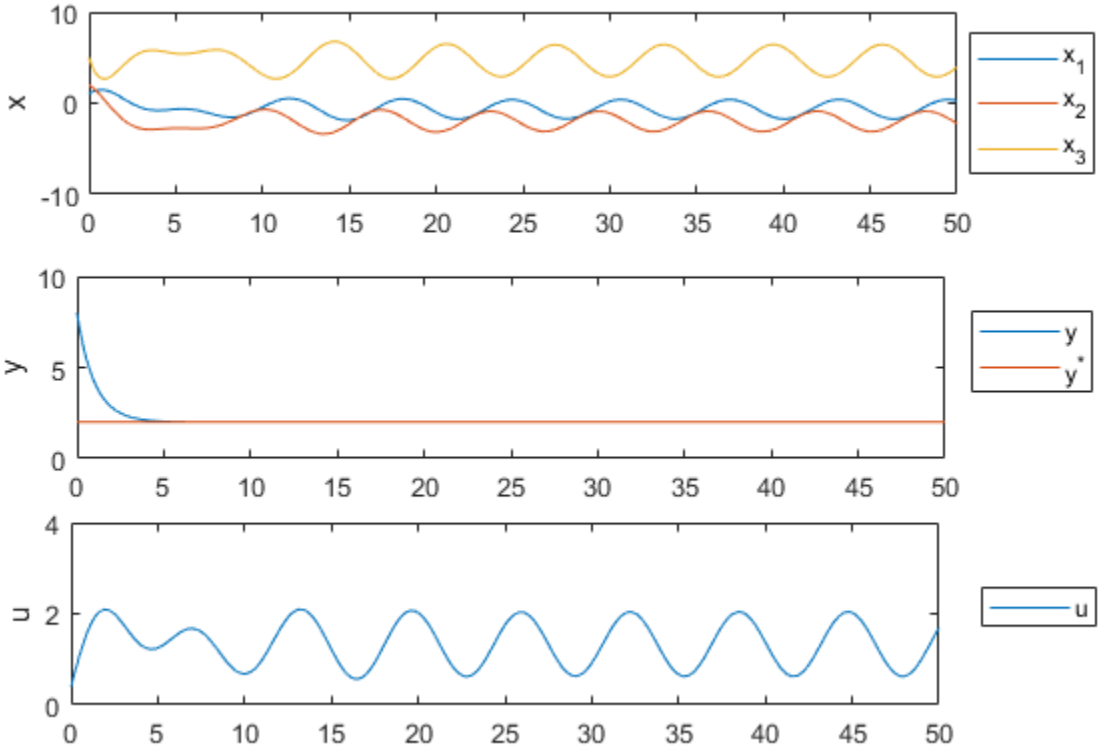

Figure 5.11: Case 1, $C = [1, 1, 1]$. G_μ has zeros: $[0\ 0]$, and G_u has zeros: $[-0.2 - 0.75i\ \ -0.2 + 0.75i]$

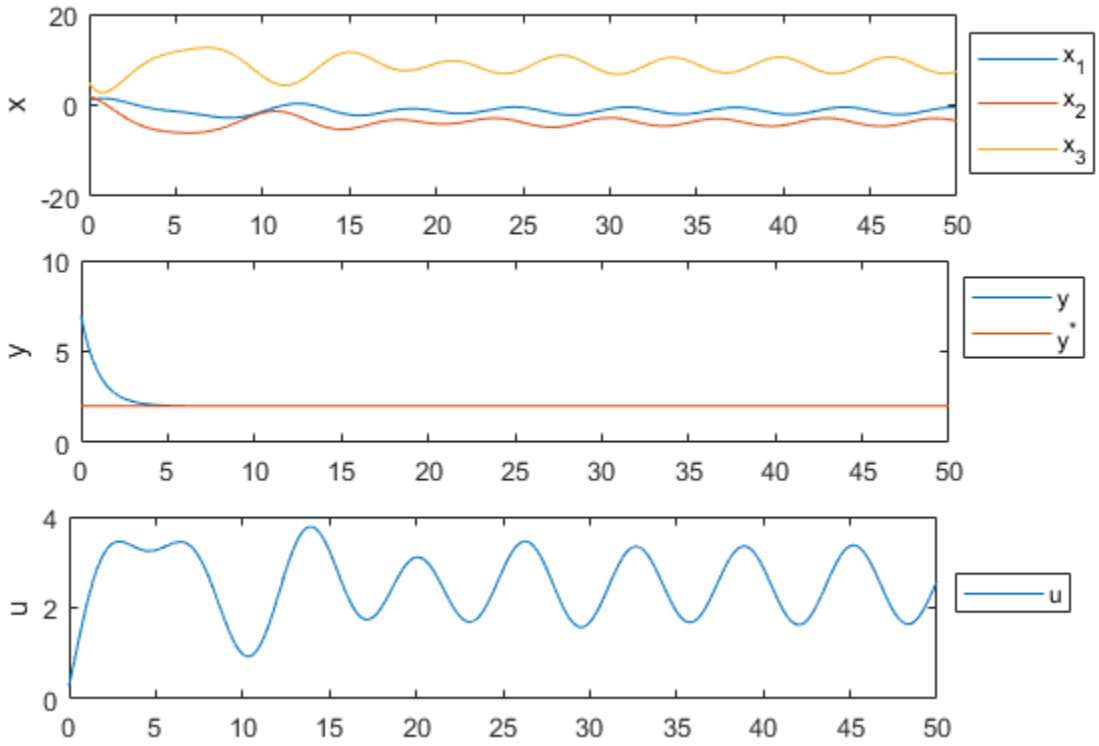

Figure 5.12: Case 2, G_μ has zeros: $[0.447 - 0.447]$, and G_u has zeros: $[-0.119 - 0.65i \; -0.119 + 0.65i]$

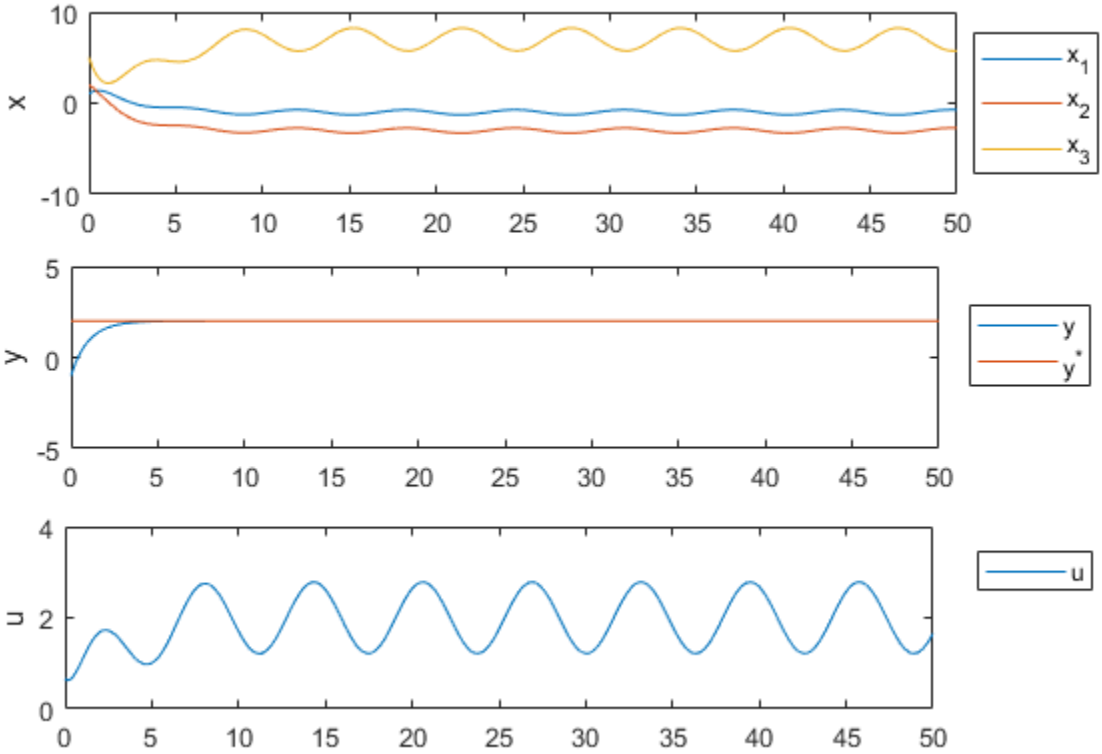

Figure 5.13: Case 3, G_μ has zeros: $[-1\ -1]$, and G_u has zeros: $[-1\ -0.6667]$

- Case 3: $C = [1, -1, 0]$. G_μ has stable zeros: $[-1\ -1]$, and G_u has stable zeros $[-1\ -0.6667]$. The internal states are BIBO as shown in Figure 5.13
- Case 4: $C = [1, 0, 0]$. G_μ has zeros: $[0\ -1]$, and G_u has one stable and one unstable zeros: $[-1,\ 0.5]$. The zero dynamics are no longer stable as shown in Figure 5.14.

5.4. Adaptive Control of Reaction Systems

In this section, we applied the proposed control method to one homogeneous and one heterogeneous reaction example. We show that, the relevant unknown inputs, i.e. the reaction rates and transfer rates. Asymptotic control convergence are obtained in both examples.

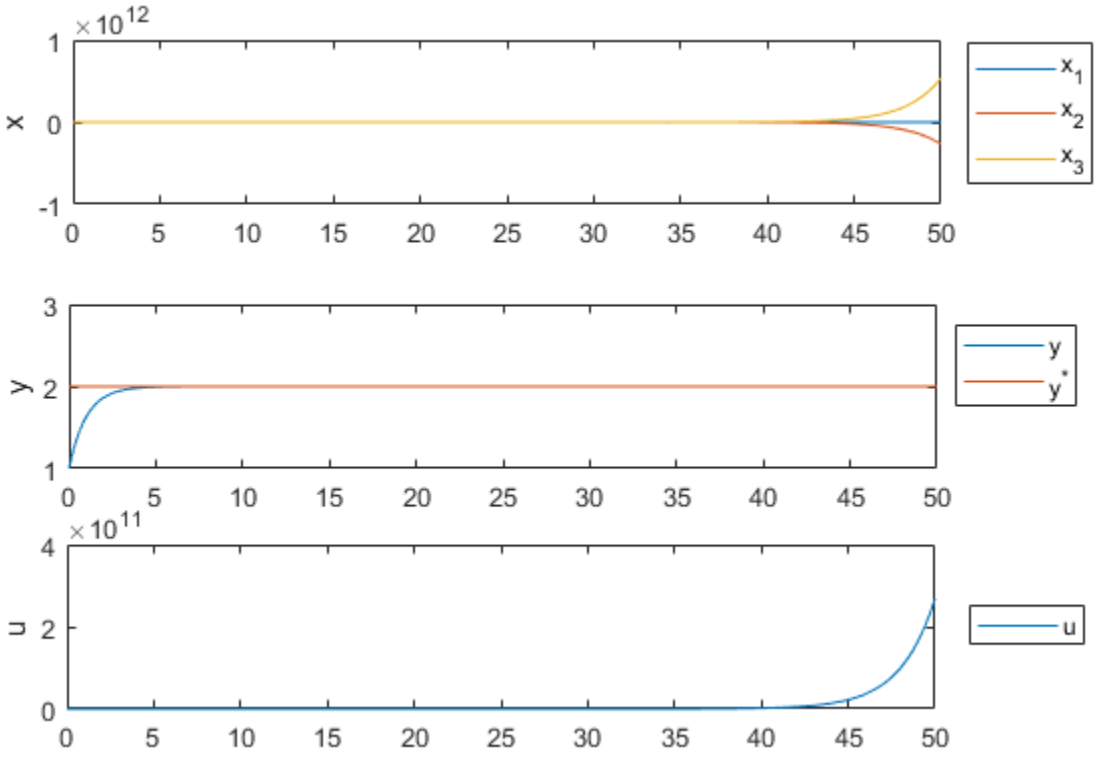

Figure 5.14: Case 4, G_μ has zeros: $[0 \ -1]$, and G_u has zeros: $[-1 \ 0.5]$

5.4.1. Homogeneous Reaction Example

We illustrate the performance of the proposed control using the reaction example: $2A \rightarrow B \rightarrow C$. The reaction rates in the simulation follow the mass-action principle:

$$r_1 = k_1 \left(\frac{N_A}{V}\right)^2 \tag{5.67}$$

$$r_2 = k_2 \frac{N_B}{V}, \tag{5.68}$$

with the Arrhenius law:

$$k_1 = k_{0,1} e^{-\frac{E_{a,1}}{RT}} \tag{5.69}$$

$$k_2 = k_{0,2} e^{-\frac{E_{a,2}}{RT}}. \tag{5.70}$$

Concentrations of A and B are measured, and need to be controlled through the respective inlet concentrations.

$$y = \begin{bmatrix} C_A \\ C_B \end{bmatrix}, \quad u = \begin{bmatrix} C_{A,in} \\ C_{B,in} \end{bmatrix} \tag{5.71}$$

The chosen output dynamics is:

$$\frac{dy}{dt} = -\frac{F}{V} y + \frac{F}{V} u + \begin{bmatrix} -2 & 1 & 0 \\ 0 & -1 & 1 \end{bmatrix} r, \quad \text{where,} \quad r = \begin{bmatrix} r_1 \\ r_2 \end{bmatrix} \tag{5.72}$$

We can find a construction of reaction variants that only involves these two species' concentrations:

$$z_V = \begin{bmatrix} -0.5 & 0 \\ -0.5 & -1 \end{bmatrix} \times \begin{bmatrix} C_A \\ C_B \end{bmatrix}, \quad z_V^* = \begin{bmatrix} -0.5 & 0 \\ -0.5 & -1 \end{bmatrix} \times \begin{bmatrix} C_A^* \\ C_B^* \end{bmatrix}. \tag{5.73}$$

We can equally control C_A and C_B through controlling z_V at z_V^*, through the synthetic MV, i.e. $z_{V,in}$. Then $z_{V,in}$ is recovered to the true MVs by inversing the trans-

formation:

$$u = \begin{bmatrix} -0.5 & 0 \\ -0.5 & -1 \end{bmatrix}^{-1} \times z_{V,in}. \tag{5.74}$$

The adaptive controller for reaction variants is:

$$\frac{d\hat{z}_V}{dt} = -\frac{F}{V}(z_{V,in} - \hat{z}_V) + \hat{r} \tag{5.75a}$$

$$\hat{r} = \frac{dz_V}{dt} + K_e(z_V - \hat{z}_V) - \frac{F}{V}(z_{V,in} - \hat{z}_V) \tag{5.75b}$$

$$z^*_{V,in} = \left(\dot{z}^*_V + K_c(z^*_V - z_V) - \hat{r} + \frac{F}{V}z_V\right)\frac{V}{F} \tag{5.75c}$$

$$\frac{dz_{V,in}}{dt} = A_f z_{V,in} + B_f \bar{u} \tag{5.75d}$$

$$\bar{u} = B_f^{-1}[\dot{z}^*_{V,in} + K_{cf}(z^*_{V,in} - z_{V,in}) + \frac{F}{V}(z^*_V - z_V) - A_f z_{V,in}] \tag{5.75e}$$

The passivity-based input estimator gain matrix is $K_e = \begin{bmatrix} 1 & 0 \\ 0 & 1 \end{bmatrix}$, and the cascade controller gains are: $K_c = \begin{bmatrix} 1 & 0 \\ 0 & 1 \end{bmatrix}$, and $K_{cf} = \begin{bmatrix} 1 & 0 \\ 0 & 1 \end{bmatrix}$. The augmented second order filter has linear dynamics with matrices: $A_f = \begin{bmatrix} -1 & 0 \\ 0 & -1 \end{bmatrix}$, and $B_f = \begin{bmatrix} 1 & 0 \\ 0 & 1 \end{bmatrix}$. The control result is shown in Figures and 5.15 and 5.16.

In this reaction control example, the variants and their setpoints can be constructed fully from measured species, so the state estimation step can be avoided. By controlling two reaction variants, therefore two reactions, we can ensure the stability of the zero dynamics. It is because of the asymptotic stability of the reaction invariants, indicating concentration C_C will be asymptotically stable as well. Above stability can be shown through the profiles of the invariant and its convergence to $z_{I,in}$ in Figure 5.17.

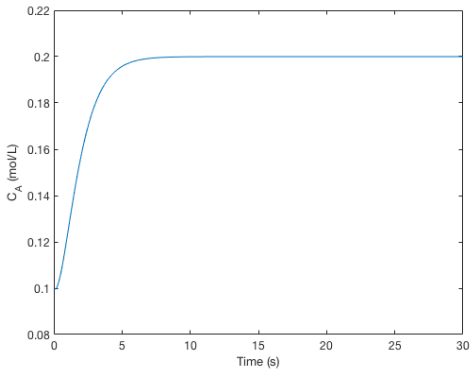

(a) C_A concentration

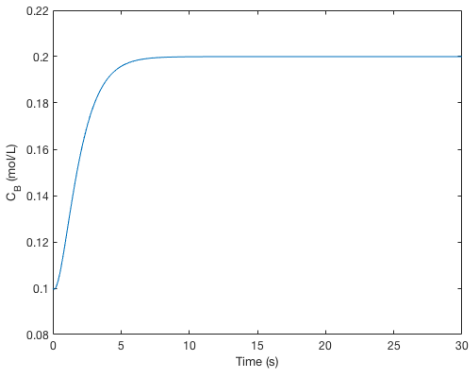

(b) C_B concentration

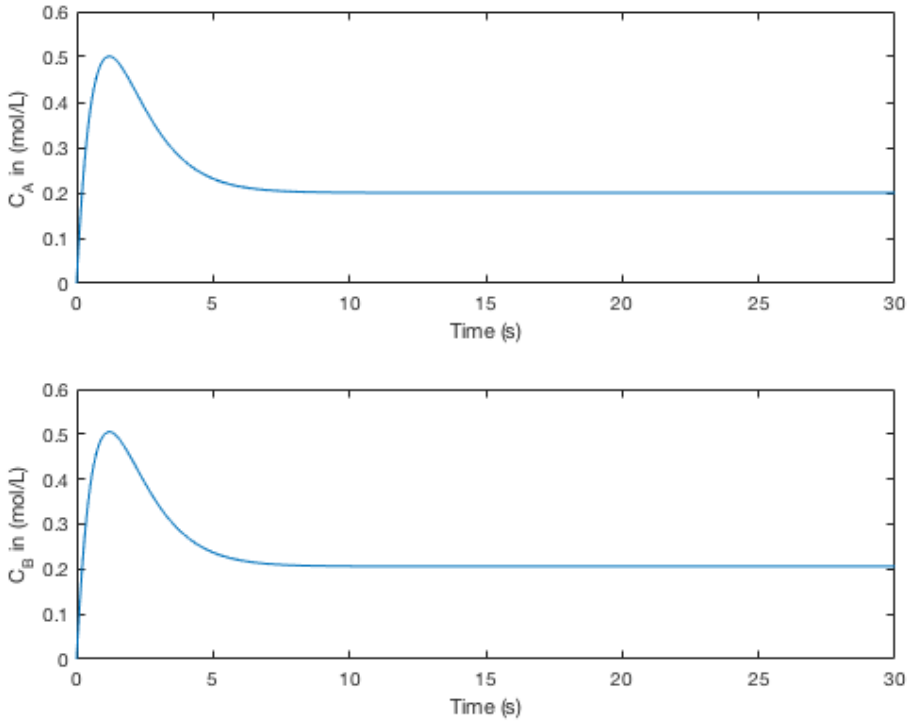

(c) MV: $C_{A,in}$ and $C_{B,in}$

Figure 5.15: Control performance of species and profiles their compositions in inlets

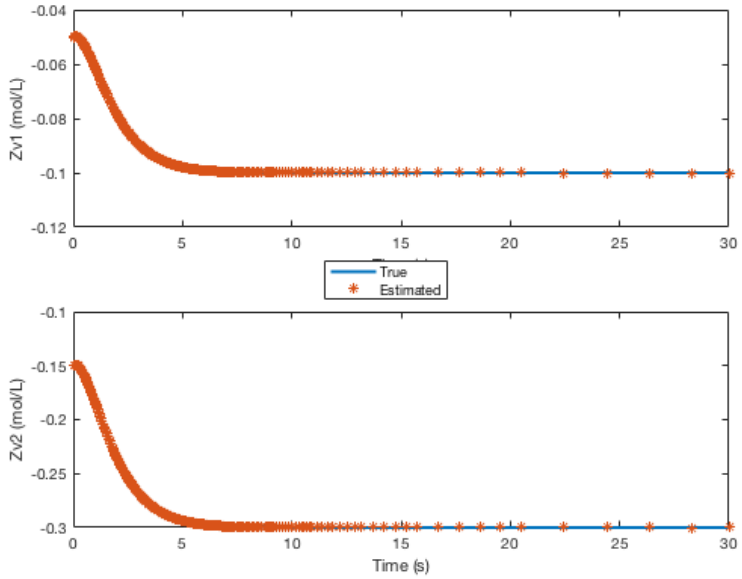

(a) z_V

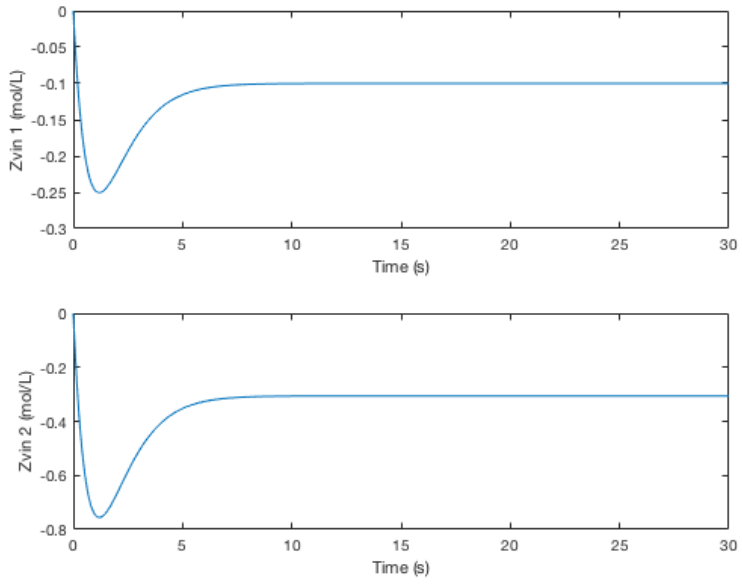

(b) $z_{V,in}$

Figure 5.16: Control performance of reaction variants z_V and profiles of the synthetic MV, $z_{V,in}$

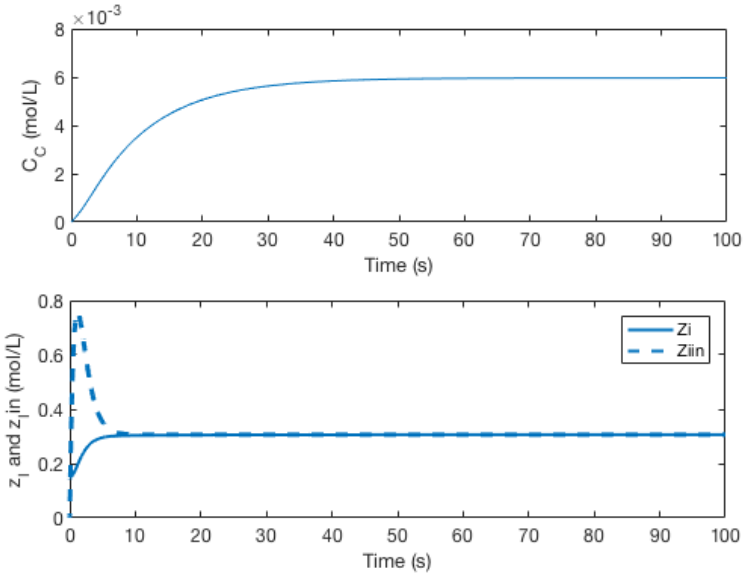

Figure 5.17: Profiles of C_C, z_I and $z_{I,in}$

5.4.2. *Heterogeneous Reaction Example*

In this section, we give a heterogeneous reaction control example, which was first introduced in Chapter 4. Based on the full state space model of the reactor (4.60), and ouptut matrix C:

$$C = \begin{bmatrix} 1 & 0 & 0 & 0 & 0 & 0 & 0 \\ 0 & 0 & 0 & 1 & 0 & 0 & 0 \\ 0 & 0 & 0 & 0 & 1 & 0 & 0 \\ 0 & 0 & 0 & 0 & 0 & 1 & 0 \end{bmatrix}, \quad C_c = \begin{bmatrix} 1 & 0 & 0 & 0 & 0 & 0 & 0 \\ 0 & 0 & 0 & 1 & 0 & 0 & 0 \end{bmatrix}, \tag{5.76}$$

we can derive the output dynamics as:

$$\begin{bmatrix} \dot{n}_{Cl_2}(g) \\ \dot{n}_{BA} \\ \dot{n}_{MBA} \\ \dot{n}_{HCl} \end{bmatrix} = \underbrace{\begin{bmatrix} \frac{-F_{out,g}}{m_g} & & & \\ & \frac{-F_{out,l}}{m_l} & & \\ & & \frac{-F_{out,l}}{m_l} & \\ & & & \frac{-F_{out,l}}{m_l} \end{bmatrix}}_{CA} \begin{bmatrix} n_{Cl_2}(g) \\ n_{BA} \\ n_{MBA} \\ n_{HCl} \end{bmatrix}$$

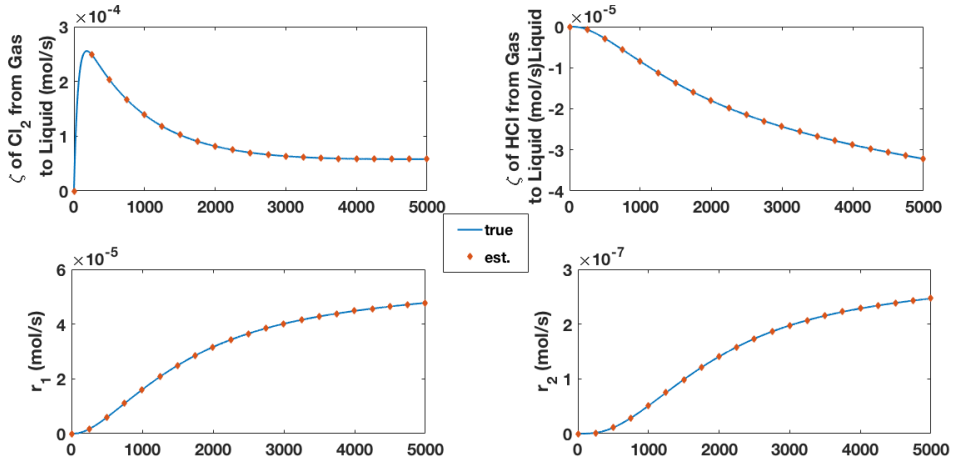

Figure 5.18: Profiles of rates in the heterogeneous reactor

$$+\underbrace{\begin{bmatrix} \frac{1}{Mw_{Cl_2}} & 0 \\ 0 & \frac{1}{Mw_{BA}} \\ 0 & 0 \\ 0 & 0 \end{bmatrix}}_{CB}\begin{bmatrix} F_{in,g} \\ F_{in,l} \end{bmatrix}+\underbrace{\begin{bmatrix} -1 & 0 & 0 & 0 \\ 0 & 0 & -1 & -2 \\ 0 & 0 & 1 & 0 \\ 0 & 1 & 1 & 2 \end{bmatrix}}_{CD}\begin{bmatrix} \zeta_{Cl_2,gl} \\ \zeta_{HCl,lg} \\ r_1 V_l \\ r_2 V_l \end{bmatrix} \tag{5.77}$$

Same as the homogeneous case, the output dynamics does not involve other unmeasured compositions, therefore estimating unmeasured compositions are not required to estimate the rates vector is not necessary. This results from matrix A being diagonal matrix in the reaction cases. Figure 5.18 shows the profiles of the rates and the estimates from PBIE, and the profiles of control inputs and outputs are shown in Figure 5.18.

5.5. Conclusions

In this chapter, we present the overall passivity-based control framework for nonlinear systems with uncertainty. The idea is based on transforming the state space model description of a process into its output dynamics including an uncertainty, and we use passivity-based techniques introduced in previous chapters to achieve

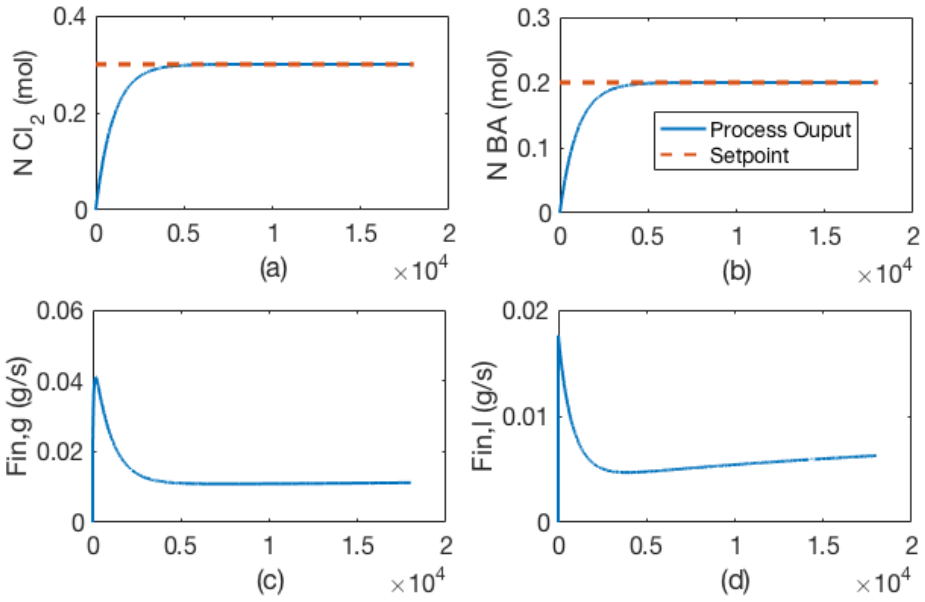

Figure 5.19: Profiles of control outputs (a, b) and control inputs (c, d)

output tracking and relevant uncertainty estimation. The transformation could be applied to reactor systems, and a range of process models derived from balance equations with appropriate measurements.

Two types of adaptive controllers are presented in this chapter from the perspective of passivity. The problem is that the passivity of a subsystem obtained through passivation transformation doesn't hold when uncertainty estimation error exists. Theorem 5.1 presents the first type of adaptive controller design that compensates for the estimation error and therefore the lack of passivity based on PBIE output feedback. The passivity of the control subsystem is restored, and the exponential stability of overall closed-loop is shown. Another type of adaptive controller presented in Theorem 5.3 shows that with exponentially converging estimates given by an arbitrary estimation method, asymptotic control convergence is obtained without extra passivity compensation. This results also implies that we are able to asymptotically control systems with special partially linear structure using state estimates from UIO, as concluded in Theorem 5.5. Also, the analysis of zero dynamics stability under output feedback control is performed, and it shows

that it is determined by the zeros of transfer functions relating the control input and control output.

From the application perspective, we apply the adaptive control with PBIE and UIO on two reaction examples, without using reaction or inter-phase transfer mechanisms.

6. Passivity-based Backstepping Control

In this chapter, we develop passivity-based control for systems with relative degree higher than one through backsteeping. Section 6.1 motivates the theory with a practical reactor temperature control problem. In Section 6.2, we present the proposed control scheme and relevant passivity and stability theorems. Application of the method on temperature control of a simulated semi-batch reactor is presented in Section 6.3. Section 6.4 shows two applications to control polymerization reactions; in the first one, passivity-based control is used to operate a simulated recipe-based polymerization reactor with several phases where each phase has different control objective and input; in the second application, we show the result of an industrial trial using the proposed control scheme. We complete the chapter with conclusions in Section 6.5.

6.1. Problem Statement

Figure 6.1 shows the schematic of a chemical reactor with a typical jacket cooling scheme for temperature regulation of three types of reactors: batch reactors, semi-batch reactors and CSTRs. The batch reactors are fed initially and emptied when reactions are complete. In semi-batch reactors, some reactants are fed while reactions proceed. In CSTRs, the reactants are added and products exit continuously so that reactions can reach a steady state. The methodology of the temperature control design developed in this chapter can be applied to all three types of reactors, while here, we use semi-batch reactor for illustration to show the strength of model-based feedback control for systems at transient state.

We model the semi-batch energy balances in the form of differential equations

of temperatures as follows:

$$\frac{dT_r}{dt} = \frac{F_{in}}{V\rho C_p}\left(\rho_{in}C_{p,in}T_{in} - \rho C_p T_r\right) - \frac{\Delta H_r r}{C_p \rho} - \frac{UA(T_r - T_j)}{V\rho C_p}, \tag{6.1a}$$

$$\frac{dT_j}{dt} = \frac{F_j}{V_j}\left(T_{j,in} - T_j\right) + \frac{UA(T_r - T_j)}{V_j \rho_w C_{p,w}}, \tag{6.1b}$$

$$\frac{dT_{j,in}}{dt} = \frac{F_{cw}}{V_{cv}}\left(T_{cw} - T_{j,in}\right) + \frac{F_{rcy}}{V_{cv}}\left(T_{rcy} - T_{j,in}\right), \tag{6.1c}$$

where T_r represents Reactor temperature; T_{cw} represents the cooling water temperature; T_{in} represents the reactor inlet temperature; T_j represents the jacket temperature; $T_{j,in}$ represents the jacket inlet temperature; T_{rcy} represents the jacket recycle stream temperature; F_{in} represents reactor inlet flow rate; F_j represents the jacket flow rate; F_{cw} represents the cooling water flow rate; F_{rcy} represents the jacket recycle flow rate; ρ represents average density of the reaction content; ρ_w represents density of the water; ρ_{in} represents the density of the reactor inlet; $C_{p,w}$ represents the heat capacity of water; C_p represents the average heat capacity of the reactor content; $C_{p,in}$ represents heat content of the reactor inlet; V represents reactor content volume; ΔH_r represents the molar reaction heat; r represents the reaction rate; U represents jacket-reactor heat transfer coefficient; V_{cv} represents the control volume.

The assumptions are: (1) the liquid phase is homogeneous and well mixed; (2) the liquid mixture is ideal, incompressible; (3) the reactor is operated at constant pressure; (4) the average density and heat capacity are constant; (5) the reaction is assumed to be exothermic ($\Delta H_r < 0$) and the reactor is equipped with only cooling capability; (6) the reaction rate is known or estimated using estimators, e.g. the PBIE.

The last differential equation models the energy balance of the mixing process of the cooling water and the jacket recycle flow. It is assumed that there is a fixed control volume, V_{cv}, after the jacket recycle stream and cold water stream meet, and that they are well mixed.

The control objective is to control the reactor temperature to a constant setpoint

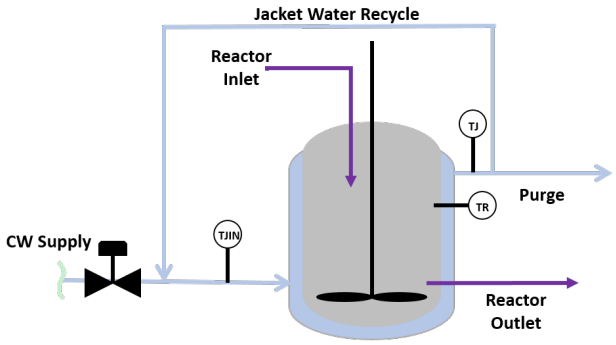

Figure 6.1: Schematic of a jacketed chemical reactor

or track a step change of the setpoint. The manipulated variable is the cooling water flow rate F_{cw}. This makes the relative degree of the system (6.1a) – (6.1c) equal to three.

6.2. Control Method Development

6.2.1. Passivity-based Backstepping Control

In Chapter 2, we introduced the passivity-based control theorems 2.4 and 2.6 to design controllers for control-affine relative-degree-one nonlinear systems. We briefly review the control development here as the foundation of the solution to high-relative degree systems.

Use following scalar system for illustration:

$$\dot{x} = f(x) + g(x)m, \quad y = x. \tag{6.2}$$

We want to control y to its setpoint y^*. The passive system is obtained by transforming the original dynamic equation of x into its control error form:

$$\dot{e} = \dot{y}^* - [f(x) + g(x)m]. \tag{6.3}$$

The synthetic input is chosen to be $u = \dot{y}^* - [f(x) + g(x)m]$ and control error e is the synthetic output. The mapping from u to e is passive. Then, the passive

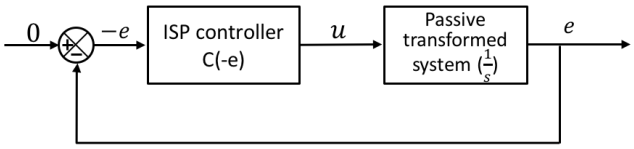

Figure 6.2: Feedback connection of a passive integrator system and an ISP controller

system is stabilized by an input strictly passive (ISP) controller. The block diagram in Figure 6.2 is an illustration of this idea.

Then, if we have the following high order system, how should we adapt the above control scheme? Here we have a third-order system with relative degree three, in the special strict-feedback form:

$$\dot{x}_1 = f_1(x_1) + g_1(x_1)x_2 \tag{6.4a}$$

$$\dot{x}_2 = f_2(x_1, x_2) + g_2(x_1, x_2)x_3 \tag{6.4b}$$

$$\dot{x}_3 = f_3(x_1, x_2, x_3) + g_3(x_1, x_2, x_3)m, \tag{6.4c}$$

$$y = x_1 \tag{6.4d}$$

Strict-feedback form means that the nonlinearities f_i and g_i in the corresponding $\dot{x}_i$ depend only on x_1,...,x_i (i = 1,2,3) (Khalil, 1996). Also, we assume that

$$g_i(x_1, ..., x_i) \neq 0, i = 1, 2, 3, \tag{6.5}$$

over the domain of interest. We can measure all the states, and want to stabilize x_1 at setpoint x_1^* through control input m. For the temperature control problem (6.1a) – (6.1c), y is the output to be controlled, and it represents T_r in our case. x_2 and x_3 are the intermediate states that directly or indirectly affect the dynamics of y. They represent T_j and $T_{j,in}$. We assume that all the three states are measured. This assumption is reasonable in industrial practice. m is the manipulated variable, and here it represents the cooling water flow rate F_{cw}. The system has a relative degree of three. The control scheme is developed in the characteristic steps of back-

stepping for the general state space model, (6.4a)–(6.4d), with relative degree three. The derivation of control is provided in Section 6.2.2.

The passivity-based backstepping control laws are:

$$x_2^* = \frac{C_1(e_1) + \dot{x}_1^* - f_1}{g_1}, \tag{6.6a}$$

$$x_3^* = \frac{C_2(e_2) + e_1 g_1 + \dot{x}_2^* - f_2}{g_2}, \tag{6.6b}$$

$$m = \frac{C_3(e_3) + e_2 g_2 + \dot{x}_3^* - f_3}{g_3}, \tag{6.6c}$$

and the closed-loop error dynamics are given by the following equations:

$$\dot{e}_1 = -C_1(e_1) + g_1 e_2, \tag{6.7a}$$

$$\dot{e}_2 = -C_2(e_2) - g_1 e_1 + g_2 e_3, \tag{6.7b}$$

$$\dot{e}_3 = -C_3(e_3) - g_2 e_2. \tag{6.7c}$$

$C_1(e_1)$, $C_2(e_2)$ and $C_3(e_3)$ are the ISP controllers used for the feedback control of x_1, x_2 and x_3, respectively. The stability and passivity properties for general systems of relative degree of n are stated in the following theorems.

Theorem 6.1. Consider the strict-feedback, cascaded system,

$$\dot{x}_1 = f_1(x_1) + g_1(x_1)x_2, \tag{6.8a}$$

$$\vdots$$

$$\dot{x}_i = f_i(x_1, ..., x_{i-1}, x_i) + g_i(x_1, ..., x_{i-1}, x_i)x_{i+1}, \tag{6.8b}$$

$$\vdots$$

$$\dot{x}_n = f_n(x_1, ..., x_{n-1}, x_n) + g_n(x_1, ..., x_{n-1}, x_n)m, \tag{6.8c}$$

$$y = x_1. \tag{6.8d}$$

$f_i : \mathbf{X} \to \mathbb{R}$, and $g_i : \mathbf{X} \to \mathbb{R}$ are sufficiently smooth functions. $g_i(x_1, ..., x_i) \neq 0, i =$

$1, .., n$. If we choose a synthetic pair of input $\mathbf{u}$ and output control error vector $\mathbf{e}$ as:

$$\mathbf{u} = \begin{bmatrix} u_1 \\ \vdots \\ u_i \\ \vdots \\ u_n \end{bmatrix} = \begin{bmatrix} \dot{e}_1 - g_1 e_2 \\ \vdots \\ \dot{e}_i - g_i e_{i+1} + g_{i-1} e_{i-1} \\ \vdots \\ \dot{e}_n + g_{n-1} e_{n-1} \end{bmatrix}, \quad \mathbf{e} = \begin{bmatrix} e_1 \\ \vdots \\ e_i \\ \vdots \\ e_n \end{bmatrix}. \tag{6.9}$$

The mapping $\mathbf{u} \to \mathbf{e}$ is passive.

Proof. The passivity between the input and output pair can be shown using the storage function $W = \frac{1}{2}\mathbf{e}^T\mathbf{e}$. Here we give the proof of the third order system case. Differentiating the storage function W,

$$\dot{W} = e_1\dot{e}_1 + e_2\dot{e}_2 + e_3\dot{e}_3, \tag{6.10}$$

and replacing the derivatives of errors with the function of defined inputs, we obtain:

$$\begin{aligned} \dot{W} =& e_1\dot{e_1} + e_2\dot{e}_2 + e_3\dot{e}_3 \\ =& e_1(u_1 + g_1 e_2) + e_2(u_2 + g_2 e_3 - g_1 e_1) + e_3(u_3 - g_2 e_2) \\ =& u_1 e_1 + u_2 e_2 + u_3 e_3 \\ =& \mathbf{u}^T\mathbf{e} \end{aligned} \tag{6.11}$$

The output $\mathbf{e}$ is passive w.r.t. the input $\mathbf{u}$. □

Theorem 6.2. Consider the system described by (6.8a)–(6.8d) and the controller described by

$$x_2^* = \frac{C_1(e_1) + \dot{x}_1 - f_1}{g_1} \tag{6.12a}$$

$$\vdots$$

$$x_i^* = \frac{C_{i-1}(e_{i-1}) + e_{i-2}g_{i-2} + \dot{x}_{i-1}^* - f_{i-1}}{g_{i-1}} \tag{6.12b}$$

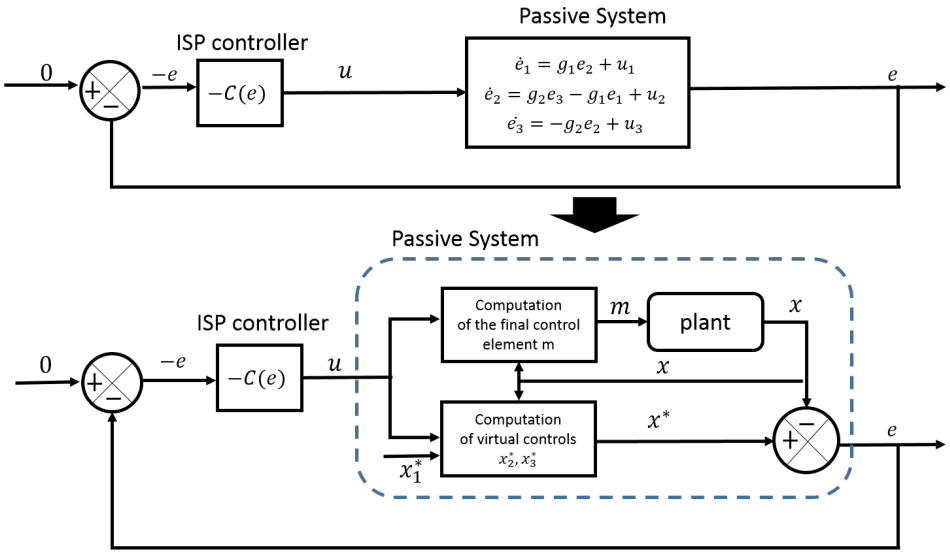

Figure 6.3: Feedback connection of a passive system of backstepping control error and an ISP controller

$$\vdots$$

$$m = \frac{C_n(e_n) + e_{n-1}g_{n-1} + \dot{x}_n^* - f_n}{g_n} \tag{6.12c}$$

If the feedback controls $C(\mathbf{e})$ are ISP controllers, then the interconnected feedback system is globally, asymptotically stable.

Proof. The proof of relative degree three case is given along with the control derivation in Section 6.2.2 by showing that the control Lyapunov function $V_3 = \frac{1}{2}e_1^2 + \frac{1}{2}e_2^2 + \frac{1}{2}e_3^2 + V_{c,1} + V_{c,2} + V_{c,3}$ is positive definite and the time derivative $\dot{V}_3$ is negative definite. It can be easily generalized for general case. □

The passive input-output mapping in Farschman et al. (1998) is actually linear, however in the case of relative degree greater than 2, the mapping is not linear anymore.

6.2.2. *Passivity-based Backstepping Control for a System with Relative Degree Three*

Here we give the derivation of the passivity-based backstepping control method with ISP controllers for a system described by (6.4a)–(6.4c).

Step 1: Define the control error states as

$$e_1 = x_1^* - x_1,\ e_2 = x_2^* - x_2, e_3 = x_3^* - x_3, \tag{6.13}$$

where x_1^* is the setpoint, and x_2^*, x_3^* are the virtual controls. The derivative of first control error can be written as:

$$\dot{e}_1 = \dot{x}_1^* - (f_1 + g_1 x_2)\,. \tag{6.14}$$

Substitute $x_2 = x_2^* - e_2$ into the above equation and rearrange it to get:

$$\dot{e}_1 = \dot{x}_1^* - (f_1 + g_1 x_2^*) + g_1 e_2. \tag{6.15}$$

The first control law for x_2^* is derived using the Lyapunov function $V_1 = \frac{1}{2}e_1^2 + V_{c,1}$, where $V_{c,1} \geq 0$ is the storage function of the first ISP controller. The derivative of $V_{c,1}$ fulfills the ISP condition:

$$\dot{V}_{c,1} \leq e_1 C_1(e_1) - \gamma_1 e_1^2, \gamma_1 > 0, \tag{6.16}$$

where γ_1 is the dissipation rate for the ISP controller.

Set

$$\dot{x}_1^* - (f_1 + g_1 x_2^*) = -C_1(e_1) \tag{6.17}$$

to obtain the following control law:

$$x_2^* = \frac{C_1(e_1) + \dot{x}_1^* - f_1}{g_1}, \tag{6.18}$$

where $C_1(e_1)$ is an ISP feedback controller. With the control law (6.18), the derivative of V_1 becomes:

$$\dot{V}_1 = -C_1(e_1)e_1 + g_1 e_1 e_2 + \dot{V}_{c,1} \leq g_1 e_1 e_2 - \gamma_1 e_1^2; \tag{6.19}$$

and the closed-loop dynamics becomes:

$$\dot{e}_1 = -C_1(e_1) + g_1 e_2. \tag{6.20}$$

Choose the l.h.s. of (6.17) as first synthetic input u_1, and combine with (6.15) to rewrite it as

$$u_1 = \dot{e}_1 - g_1 e_2. \tag{6.21}$$

Choose the first synthetic output as $y_1 = e_1$.

If this were a first order system, $e_2 = 0$, the input and output pair:

$$u_1 = \dot{e}_1, y_1 = e_1, \tag{6.22}$$

is passive. Also the closed-loop system is globally asymptotically stable, since $\dot{V}_1 \leq -\gamma_1 e_1^2$ is negative definite.

Step 2: The derivative of the second error variable is:

$$\begin{aligned} \dot{e}_2 &= \dot{x}_2^* - \dot{x}_2 \\ &= \dot{x}_2^* - (f_2 + g_2 x_3^*) + g_2 e_3 \end{aligned} \tag{6.23}$$

The augmented Lyapunov function is chosen as

$$V_2 = V_1 + \frac{1}{2} e_2^2 + V_{c,2}, \tag{6.24}$$

where $V_{c,2}$ is the storage function of the second feedback ISP controller. Taking the derivative of V_2, we have

$$\begin{aligned}\dot{V}_2 &\leq g_1 e_1 e_2 - \gamma_1 e_1^2 + e_2\left[\dot{x}_2^* - (f_2 + g_2 x_3^*) + g_2 e_3\right] \\ &\quad + e_2 C_2(e_2) - \gamma_2 e_2^2 \\ &= e_2[g_1 e_1 + \dot{x}_2^* - (f_2 + g_2 x_3^*) + g_2 e_3] + e_2 C_2(e_2) \\ &\quad - \gamma_1 e_1^2 - \gamma_2 e_2^2. \end{aligned} \tag{6.25}$$

Set

$$e_1 g_1 + \dot{x}_2^* - (f_2 + g_2 x_3^*) = -C_2(e_2) \tag{6.26}$$

to obtain the second control law for the second virtual control variable x_3^*:

$$x_3^* = \frac{C_2(e_2) + e_1 g_1 + \dot{x}_2^* - f_2}{g_2}. \tag{6.27}$$

Thus the derivative of V_2 becomes:

$$\dot{V}_2 \leq g_2 e_2 e_3 - \gamma_1 e_1^2 - \gamma_2 e_2^2. \tag{6.28}$$

The second pair of synthetic input and output are chosen similarly to the first pair. Set the l.h.s. of (6.26) as the second input u_2, and combine (6.23) to rewrite it as:

$$u_2 = \dot{e}_2 - g_2 e_3 + g_1 e_1. \tag{6.29}$$

The second output is $y_2 = e_2$.

Step 3: The derivative of the third control error is:

$$\begin{aligned}\dot{e}_3 &= \dot{x_3^*} - \dot{x}_3 \\ &= \dot{x_3^*} - (f_3 + g_3 m). \end{aligned} \tag{6.30}$$

To design the control law, choose the augmented control Lyapunov function $V_3 = V_2 + \frac{1}{2}e_3^2 + V_{c,3}$, and similar to the previous two steps, $V_{c,3}$ is the storage function of the third ISP controller. Differentiate V_3 and combine (6.28) to get:

$$\dot{V}_3 \leq g_2 e_2 e_3 - \gamma_1 e_1^2 - \gamma_2 e_2^2 + e_3 \dot{e}_3 + \dot{V}_{c,3}. \tag{6.31}$$

Replace $\dot{e}_3$ with (6.30), and apply the input strictly passive inequality condition on $\dot{V}_{c,3}$. We then obtain:

$$\begin{aligned} \dot{V}_3 &\leq g_2 e_2 e_3 - \gamma_1 e_1^2 - \gamma_2 e_2^2 + e_3[\dot{x_3^*} - (f_3 + g_3 m)] + e_3 C_3(e_3) - \gamma_3 e_3^2 \\ &= e_3[g_2 e_2 + \dot{x_3^*} - (f_3 + g_3 m)] + e_3 C_3(e_3) - \gamma_1 e_1^2 - \gamma_2 e_2^2 - \gamma_3 e_3^2. \end{aligned} \tag{6.32}$$

Set $g_2 e_2 + \dot{x_3^*} - (f_3 + g_3 m) = -C_3(e_3)$ to solve for the third control law:

$$m = \frac{C_3(e_3) + e_2 g_2 + \dot{x}_3^* - f_3}{g_3}. \tag{6.33}$$

Finally, we have $\dot{V}_3 \leq -\gamma_1 e_1^2 - \gamma_2 e_2^2 - \gamma_3 e_3^2$ being negative definite, and the origin of the following closed-loop system of control errors,

$$\dot{e}_1 = -C_1(e_1) + g_1 e_2 \tag{6.34a}$$

$$\dot{e}_2 = -C_2(e_2) - g_1 e_1 + g_2 e_3 \tag{6.34b}$$

$$\dot{e}_3 = -C_3(e_3) - g_2 e_2, \tag{6.34c}$$

is globally asymptotically stable.

6.3. Passivity-based Backstepping Control of Reactor Temperature

In this section, we demonstrate the effectiveness of the backstepping control method for temperature control in a semi-batch reactor case. First we write the

temperature differential equations in the general model form, (6.4a)–(6.4c), with

$$\begin{bmatrix} f_1(T_r) \\ f_2(T_r, T_j) \\ f_3(T_r, T_j, T_{jin}) \end{bmatrix} = \begin{bmatrix} -\frac{F_{in}}{V\rho C_p}\left(\rho_{in} C_{p,in} T_{in} - \rho C_p T_r\right) - \frac{\Delta H_r r}{C_p \rho} - \frac{UAT_r}{V\rho C_p} \\ -\frac{F_j}{V_j} T_j - \frac{UA}{V_j \rho_w C_{pw}} T_j + \frac{UA}{V_j \rho_w C_{pw}} T_r \\ \frac{F_{rcy}}{V_{cv}}\left(T_{rcy} - T_{j,in}\right) \end{bmatrix},$$

$$\begin{bmatrix} g_1(T_r) \\ g_2(T_r, T_j) \\ g_3(T_r, T_j, T_{jin}) \end{bmatrix} = \begin{bmatrix} \frac{UA}{V\rho C_p} \\ \frac{F_j}{V_j} \\ \frac{T_{cw} - T_{jin}}{V_{cv}} \end{bmatrix}.$$

Insert the corresponding terms into the control equations, (6.6a)–(6.6c), to obtain the following control laws:

$$T_j^* = T_r + [C_1(e_1) + \dot{T_r}^*]\frac{V\rho C_p}{UA} - \frac{F_{in}\rho_{in} C_{p,in}}{UA}(T_{in} - T_r) - \frac{Q_r}{UA}, \tag{6.35a}$$

$$T_{j,in}^* = [C_2(e_2) + \dot{T_j}^*]\frac{V_j}{F_j} - \frac{UA(T_r - T_j)}{\rho_w C_{p,w}}\frac{1}{F_j} + T_j + \frac{e_1 UA}{V\rho C_p}\frac{V_j}{F_j} \tag{6.35b}$$

$$F_{cw} = \frac{V_{cv}}{T_{cw} - T_j}[C_3(e_3) + \dot{T}_{jin}^*] - \frac{F_j(T_j - T_{j,in})}{T_{cw} - T_j} + \frac{F_j}{V_j}\frac{e_2}{T_{cw} - T_j}V_{cv} \tag{6.35c}$$

where Q_r is the rate of heat generated from reactions. Here, T_j^* and $T_{j,in}^*$ are the first and second virtual control variables, serving as the setpoints of T_j and $T_{j,in}$. Control laws (6.35a)–(6.35c) show that backstepping is similar to cascade with additional elements introduced to compensate for nonlinearities. The parameters used in the simulation are shown in Table 6.1. The model of the semi-batch reactor can be found in Appendix D.

In the following, we show results from two case studies. (1) Control with perfect information of parameters and proportional control. (2) Control with parameter mismatch, where the heat generation from the reaction ($Q_r = \Delta H_r r V$) is not known accurately. We compare the control performances of using proportional backstepping control and proportional-integral backstepping control in the second case.

Table 6.1: Parameters of the semi-batch simulation

Average heat capacity of the reaction content (C_p)	$0.239\ \mathrm{J/(g \cdot K)}$
Heat capacity of water ($C_{p,cw}$)	$4.184\ \mathrm{J/(g \cdot K)}$
Average density of the reaction content (ρ)	$1000\ \mathrm{g/L}$
Density of reactor inlet stream (ρ_w)	$1000\ \mathrm{g/L}$
Density of water (ρ_{in})	$1000\ \mathrm{g/L}$
Heat transfer coefficient× area (UA)	$5 \times 10^4\ \mathrm{J/s \cdot K}$
Reactor volume at t = 0	$10\ \mathrm{L}$
Reactor cooling jacket volume (V_j)	$45\ \mathrm{L}$
Control volume (V_{cv})	$40\ \mathrm{L}$
Flow rate through cooling jacket (F_j)	$300\ \mathrm{L/min}$
Temperature of cooling water (T_{cw})	$320\ \mathrm{K}$

A saturation condition is placed on the manipulated variable such that $0 \leq F_{cw} \leq 300(\mathrm{L/min})$. The upper limit is the fixed flow rate of the jacket inlet, F_j. The simulated time is 100 min, and there is an increase of the inlet flow F_{in} at t = 50 min, as shown in Figure 6.4. The increase of inlet flow rate causes the increase in the amount of the heat generated from the reaction, Q_r.

Case study without parameter uncertainty

The control performance of the first case is shown in Figure 6.5. The primary control objective T_r is well controlled at the setpoint 370 K without oscillation. Two slave control objectives T_j and $T_{j,in}$ also track the calculated setpoints very well. For $T_{j,in}$, the calculated setpoint is high when the reactor temperature is below the setpoint. An exothermic reaction is simulated and the reactor jacket is only equipped with cooling ability. Thus, when the reactor temperature is below the setpoint, the cooling water flow is saturated at zero. The proportional gains used in the simulation are: $k_{c,1}$ = 1, $k_{c,2}$ = 2, $k_{c,3}$ = 5.

Case study with parameter uncertainty

The heat generated by the reaction is the unknown parameter. It is assumed to be a constant in the controllers for the simulations in this section. Because of the parameter mismatch, we use proportional-integral (PI) feedback in the backstepping, and

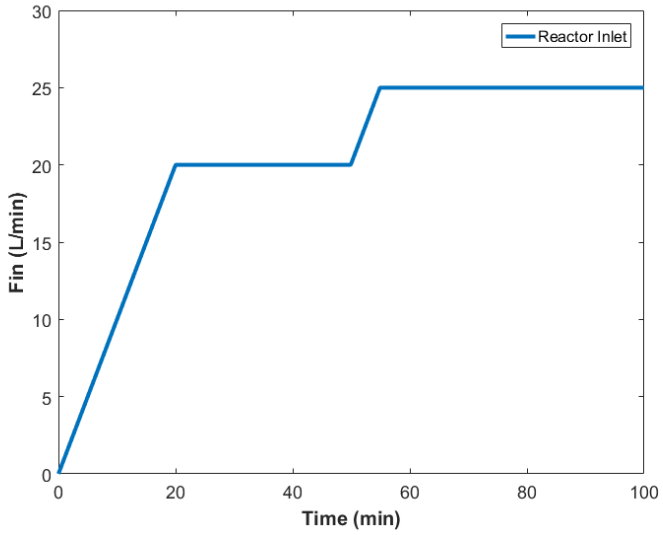

Figure 6.4: Profile of reactor inlet

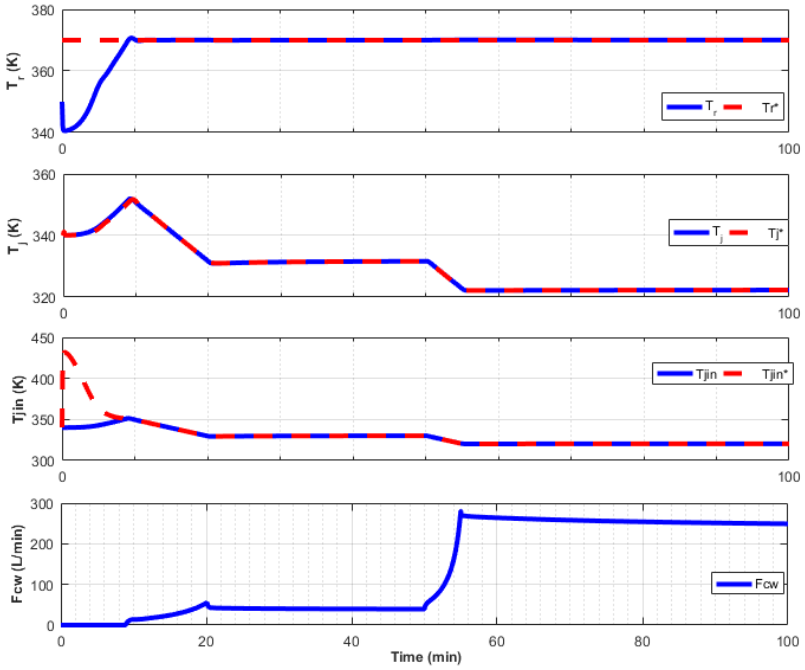

Figure 6.5: Profiles of $T_r, T_j, T_{j,in}$ and MV F_{cw} when Q_r is perfectly known

compare the result obtained using proportional-only backstepping control. The control parameters are as follows:

$$\text{P only feedback: } k_{c,1} = 1, k_{c,2} = 2, k_{c,3} = 5;$$
$$\text{PI feedback: } \quad k_{c,1} = 1, \tau_{I,1} = 1, k_{c,2} = 2, k_{c,3} = 5.$$

The integral action is only used for the control of T_r, not for the slave control objectives, $T_j, T_{j,in}$. It is because the uncertain parameter Q_r only exists in the dynamics of T_r. Figure 6.6 compares the control performances from two different feedback schemes. Comparisons of relevant metrics regarding the top level control are shown in the Table 6.2. With P feedback, the temperature is controlled with an offset due to the uncertainty mismatch, causing a very long settling time of more than 100. With PI feedback, the reactor temperature is stabilized at the setpoint without an offset, and its settling time is 34.6. PI feedback causes integral wind-up at the initial stage, which is reflected by the overshoot of T_r, with a peak value of 404.2 K, the incompetent tracking of the slave control objectives, and initial F_{cw} saturation shown in Figure 6.7.P feedback allows slave control objectives $T_j, T_{j,in}$ have better tracking w.r.t. their setpoints, but the slave setpoints are not sufficient to drive T_r to the required setpoint. Figure 6.7 also shows the true evolution of Q_r from implementing two feedback schemes and the mismatched Q_r estimation used in the control calculations.

Table 6.2: Control performance comparison when parameter uncertainty exists

Metrics	P-only passivity-based backstepping	PI passivity-based backstepping
Rise time	4.8	4.1
Settling time	> 100	34.6
Peak time	20.5	17.2
Peak	388 K	404.2 K

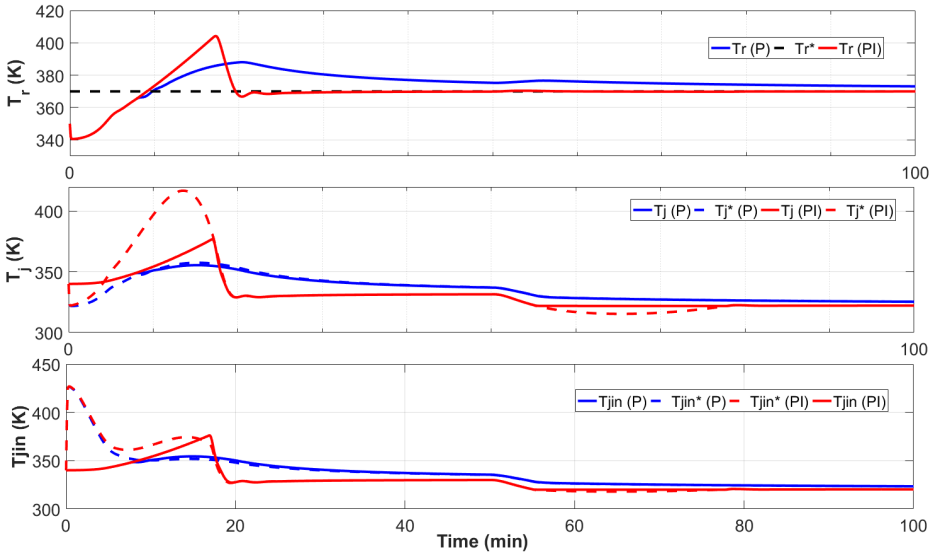

Figure 6.6: Profiles of temperatures and their setpoints with P only or PI feedback backstepping control, when Q_r is inaccurately known.

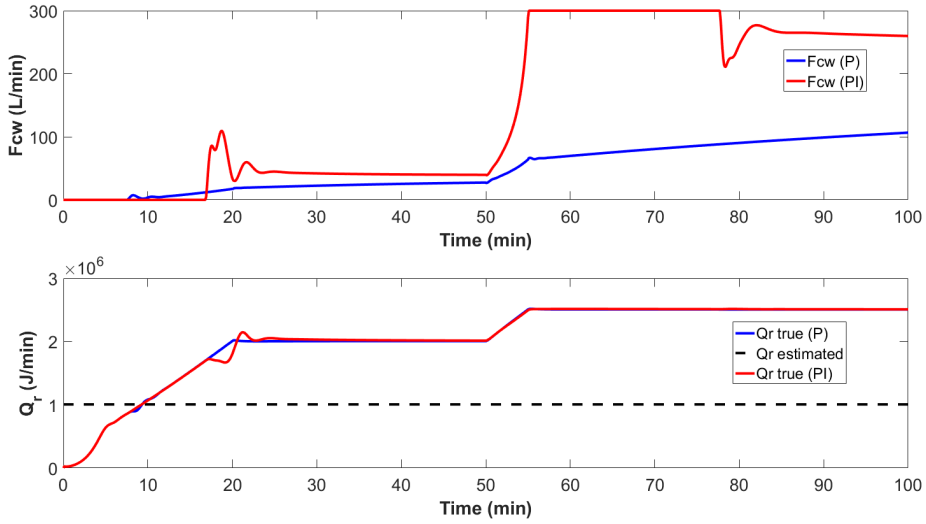

Figure 6.7: Profiles of F_{cw} and Q_r with with P only or PI feedback backstepping control, when Q_r is inaccurately known.

Table 6.3: CV and MV for 5 process phases

Phase	CV	MV
Filling	V	F_{in}
Heating up	T_r	F_{cw} and F_{hw}
Monomer feeding and reaction	T_r	F_{cw} and F_{hw}
Cooling down	T_r	F_{cw} and F_{hw}
Draining	V	F_{out}

6.4. Recipe-based Control of Semi-batch Polymerization

In this section, we illustrate the application of the proposed scheme to a semi-batch polymerization reactor. The kinetic information is not used in the control design. The polymerization process response on the MV is simulated using the reaction model developed by Crowley & Choi (1997), and detailed in Appendix D of this paper. The semi-batch polymerization process recipe is composed of five phases:

1. fill reactor with monomer solution and initiator;
2. heat the reactor up to the desired operation temperature;
3. finish feeding the rest of the monomer, and wait until polymerization completes;
4. cool the reactor;
5. drain the reactor.

For different phases, the control objectives are different. The pair of the control variable and manipulate variable is summarized in Table 6.3.

For the heating, reaction and cooling phases, the polymerization reactor temperature regulation mechanism is shown in Figure 6.8, where the jacket inlet flow becomes a tempered water flow by mixing hot and cold water streams.

6.4.1. Simulation Example and Result

The semi-batch methyl methacrylate (MMA) polymerization process proceeding with the above recipe and control is simulated. Process variables profiles are shown

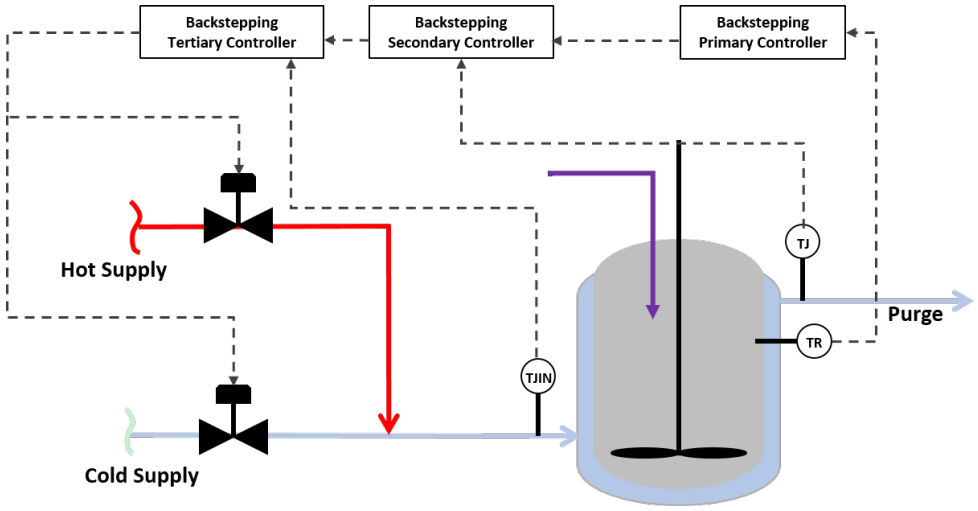

Figure 6.8: Polymerization semi-batch reactor and control setup

in Figure 6.9. Since the reaction phase takes much longer than the other phases, the profiles of the third phase are plotted with time scale in minutes, while the rest of the variables are plotted with time scale in seconds.

Figure 6.9((a)) shows the reactor holdup profile, which is the CV during the filling and draining phases. The holdup control problem has only relative degree of one, and the controller is a simple proportional feedback controller:

$$F = k(V^* - V),\ k > 0.$$

The profiles of the MV, inlet or outlet flow rates of the reactor are shown in Figure 6.9((d)), along with constant profiles for the other three phases. Figure 6.9((b)) shows the profile of reactor temperature, which is the CV of the heating, reaction and cooling phases. The temperature for those phases are well controlled, without using any modeling information of the complex polymerization in the control laws. They are coupled in one term, heat generation rate by the reaction, Q_r. Figure 6.9((c)) shows the monomer number of moles profile, and it can be observed in the reaction phase plot that after stopping the monomer solution feed, the process waits until the monomer are mostly consumed before transiting to the next cooling phase. It indicates that some on-line monitoring of residue monomer is required to

determine the timing of the transition.

6.4.2. *Industrial Application Example and Implementation Result*

Some industrial trials have been carried out to test the proposed control logic. The implemented control has two backstepping controllers cascaded at the top two levels. The primary controller equation remains the same as (6.35a). The secondary controller for $T^*_{j,in}$ is implemented with a simplified version of (6.35b):

$$T^*_{j,in} = [C_2(e_2) + \dot{T_j}^*]\frac{V_j}{F_j} - \frac{UA(T_r - T_j)}{\rho_w C_{p,w}}\frac{1}{F_j} + T_j \tag{6.36}$$

It omits term $\frac{e_1 UA}{V\rho C_p}\frac{V_j}{F_j}$, designed to compensate for the tracking error of T_j. However, with a fair assumption of the boundedness property of the process dynamics, asymptotic stability can still be maintained for the closed-loop by using high gains. The tertiary controller is a PID controller manipulating the flows of cold and hot supplies, and it is sufficient since flow control loop is much faster than previous two temperature control loops.

Figure 6.10 shows the profiles of CV, reactor temperature, MV, jacket inlet temperature, and disturbance variable (DV), monomer feed pump speed. We consider $T_{j,in}$ as MV here, since its setpoint is determined by the secondary passivity-based controller and is executed through the bottom PID controller. The setpoint of the reactor temperature is 8°C. During the period of 1500s–2200s, the process data was lost, which is represented by the flat line of temperature at the setpoint. With the available data, we can see that after the initial transition stabilizing period, the reactor temperatures is controlled quite close to the setpoint. The benefit of including the feedforward terms in the control logic can be clearly observed from the MV profile, as it responds quickly to several step changes of monomer flow rate, the disturbance here.

The values of reactor-jacket heat transfer coefficient, reaction system heat capacity and reaction heat used in control calculations are shown in Table 6.4. During the trial, C_p and U values ramp over the feed. Reaction heat is estimated by inverting

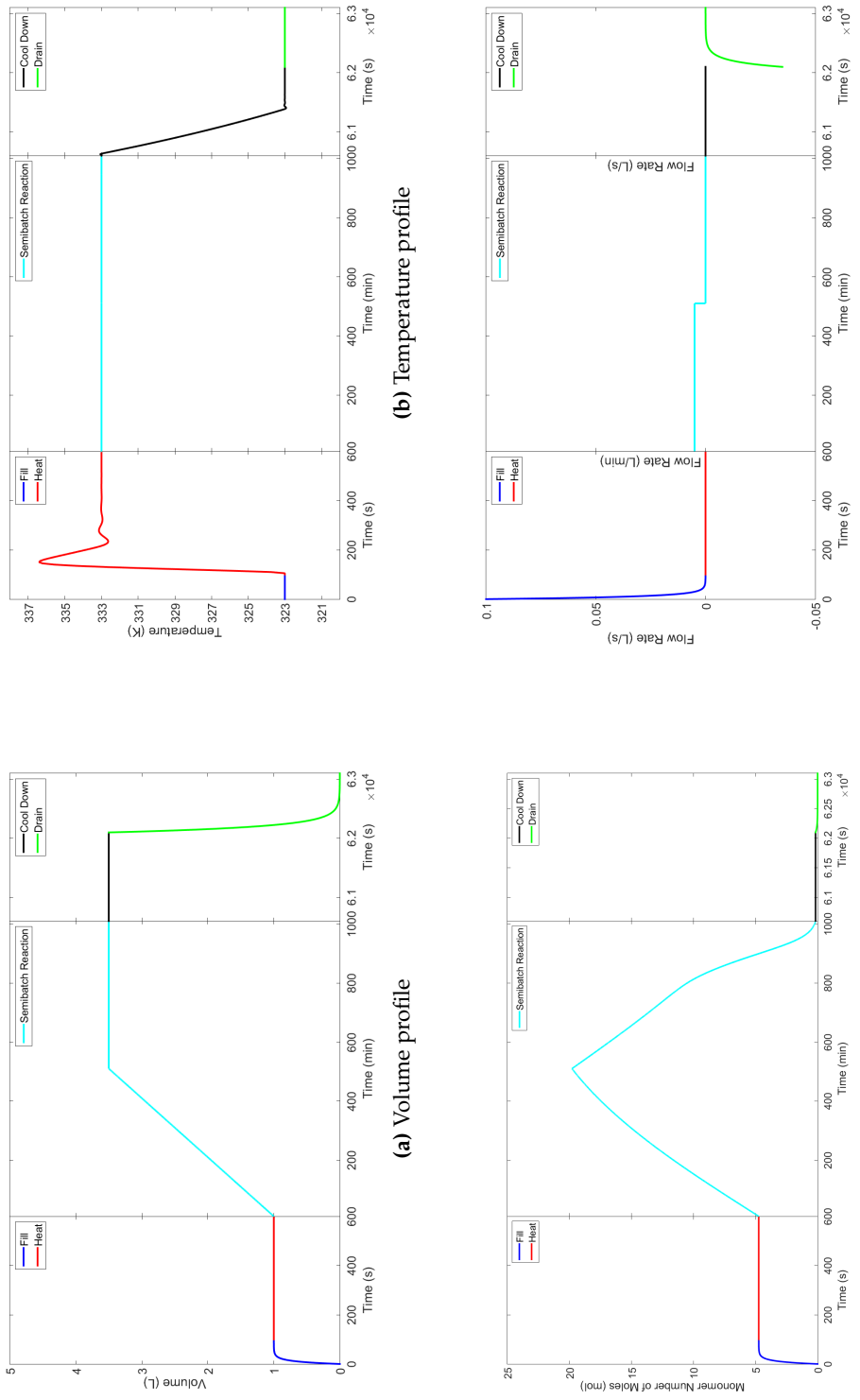

(a) Volume profile

(b) Temperature profile

(c) Monomer numbers of mole profile

(d) Reactor flow rate profile

Figure 6.9: Profiles of simulated MMA polymerization process variables

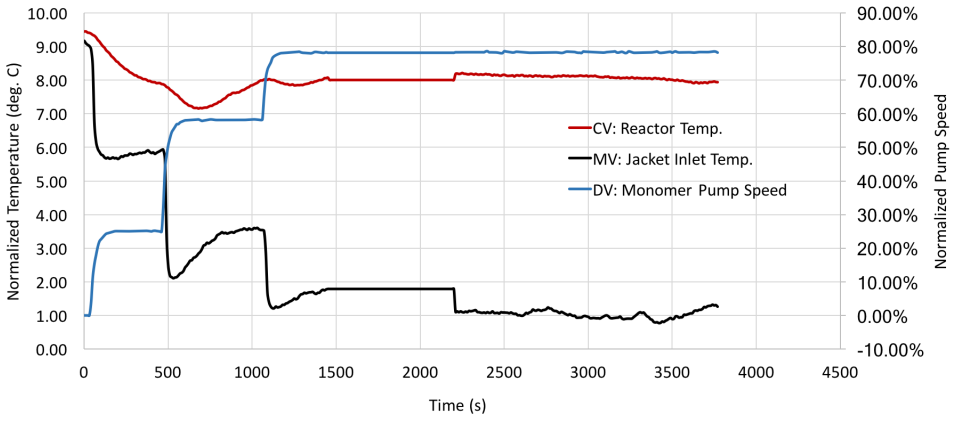

Figure 6.10: Profiles of industrial trial process variables

Parameters	Minimum	Maximum	Description
C_p (BTU/lb-degF)	0.5	1	heta capacity
M_r (lb)	5	44	mass of reaction system
U (BTU/ft^2-min-degF)	0.1	30	heat transfer coefficient
A (ft^2)	0.1	5	heat transfer area
M_j (lb)	20	20	mass of jacket content
ρ_r (lb/gal)	8.1	8.5	reaction systems density

Table 6.4: Process parameter ranges

the reactor energy balance with online temperature measurements. Related discussion of this estimation has been provided in Chapter 3. As we show in simulation results, integral action should help reducing control errors caused by estimation inaccuracy in those situations. Bounds of process parameters are listed in Table 6.4.

6.5. Conclusions

In this chapter, we proposed to use of the classic backstepping method for the semi-batch reactor energy control problem, while introducing ISP feedback controller in the control design. The passivity-based control idea, being widely used for relative degree one system, is extended to higher relative degree systems through backstepping. The stability of the closed-loop system and the passivity of the synthetic input

and output are shown. The proposed control method can be easily implemented in practice since it maintains PID as the feedback component and systematically provides explicit formula for including model-based feedfoward terms. The inclusion of PID, as the ISP component, is a practical way to ease requirement of accurate kinetic knowledge for computing reaction heat generation. The proposed control scheme also has the potential to outperform the traditional PID-only cascade control in disturbance rejection and maintaining stability. It also provides improvement for base level control by considering process models, and can be implemented in distributed control systems. Industrial trials are conducted and show satisfactory control performance.

7. Conclusions and Future Work

7.1. Conclusions

In this thesis, we developed an adaptive control framework for controlling nonlinear processes with uncertainty, and applied it to control reaction systems without the knowledge of reaction kinetics. The framework incorporates the measurements' derivative information in order to estimate the uncertainty involved in output dynamics. By using the derivative information, the control and estimation schemes do not require the modeling of the internal dynamics and states. The proposed framework allows us to control reaction systems without knowing the reaction kinetics, and estimate unmeasured compositions by utilizing the available partially linear structure of internal dynamics.

We started by defining the output dynamics involving uncertainty in the following form:

$$\frac{dy}{dt} = \bar{p}(y) + D\Delta p(x) + \phi(y)u. \tag{7.1}$$

The uncertainties, usually related to production, are all lumped into one term, $\Delta p(x)$. The structure applies to reaction systems and many other processes that can be modeled based on balance equations.

We designed the passivity-based input estimator (PBIE) that produces stable estimates of the uncertainty $\Delta p(x)$ and attenuates the noise from the derivatives of the measurements. The estimation scheme can, for example, be used to estimate the reaction rate and rates of heat transfer and generation in a reactor without using the reaction kinetics or transfer mechanism information. We show the neces-

sity of including the derivatives through stability analysis and simulation comparison between PBIE and other inversion-based estimation schemes that do not use derivative information.

We integrated the estimator with passivity-based inventory control and showed that output tracking with asymptotic stability can be achieved. The integration of the estimation scheme enables output tracking without modeling the internal dynamics, thereby saving computational and modeling cost. Moreover, we showed that if we explore the known linear structure in a reactor model, we are able to estimate the unmeasured compositions by using the asymptotic observer. We generalized this idea and developed an adaptive control approach with state estimation for nonlinear systems with a similar structure. The adaptive control scheme is tested on an example reaction system with composition control and several numerical nonlinear systems.

Another contribution from the thesis is to extend passivity-based control to high-relative degree nonlinear systems. We use backstepping to define transformations that render a high-relative degree system passive, and stabilize with input strictly passive controllers. Systems with uncertainty can be controlled by using a PI controller as the ISP component. Finally, the resulting scheme was successfully tested in an industrial example to control the temperature of a semi-batch polymerization reaction.

The thesis work has led to the following peer-reviewed publications:

1. Zhao, Z. and Ydstie, B.E. (2018). Passivity-based backstepping control of a semi-batch reactor. *Submitted for publication.*

2. Zhao, Z. and Ydtsie, B.E. (2018). Passivity-based input observer. Accepted for the *10th IFAC Symposium on Advanced Control of Chemical Processes.*

3. Zhao, Z., Capparella, T., Ferrio, J., Wassick, J. M., and Ydstie, B. E. (2017). Passivity-based back-stepping control of a semi-batch reactor. *IFAC-PapersOnLine, 50 (1), pp. 13741-13746.*

4. Zhao, Z., Wassick, J.M., Ferrio, J., and Ydstie, B.E. (2016). Reaction vari-

ants and invariants based observer and controller design for CSTRs. *IFAC-PapersOnLine, 49(7), pp.1091-1096.*

Two additional publications are under preparation:

1. *Passivity-based unknown input observer*
   This publication will present a method that integrates the UIO from Chapter 3 and the PBIE from Chapter 4 to propose an observer that estimates the states and unknown inputs simultaneously. Unlike with other input observers, we propose to use the derivative information resulted from the passivity theorem.

2. *Adaptive inventory control for nonlinear systems with uncertainty*
   The content of this publication will be mainly Chapter 5.

7.2. Future work

In practice, measurements are always corrupted with noise, which can be amplified if the numerical differentiator is not chosen carefully. Therefore, numerical derivatives are frequently avoided in parameter/input estimators. During the development of the PBIE, we showed that derivative noise was effectively attenuated. However, we also found that the attenuation is counteracted when noise is present in primary measurements. It is because the noise involved in primary measurements is amplified by the proportional feedback correction mechanism. To ensure that both noises are dampened in the estimates, integral action based on sliding mode (Levant, 1998; Wang & Ydstie, 2007) could be used. It is also possible to consider other feedback actions as long as passivity and stability are maintained. As discussed in Chapter 3, under the situation of no noise in the primary measurements, the estimation performance and also convergence analysis favor the usage of derivatives. It is also of interest to derive and compare the conditions of stabilities for methods with and without using derivatives when the assumption of absent noise is relaxed. Comparisons of implementation feasibility and estimator parameter tuning difficulty are also worthwhile.

Control and estimation with constraints is another aspect to consider for future improvement. Inclusion of physical constraints on the estimates may help to reject unmodeled disturbance and avoid aggressive estimation during the transition period. From the control perspective, control input constraint is inevitable in reality, but it may cause the breakdown of closed-loop stability. Farschman et al. (1998) give the sufficient condition of adaptive inventory control stability with control input constraints. It is of interest to look at how the proposed adaptive inventory control with PBIE fits into that result. The result could also be extended to draw conditions to ensure passivity-based backstepping control stability for high-relative degree control problems when input constraints exist. Model predictive control is also one way to deal with control constraints, and it could resolve the cumbersome cascaded structure in the case of high-relative degree problems.

One advantage of the passivity-based adaptive inventory control is its high implementability in current DCS platforms. It can be programmed in form of PID controllers for linear processes and PID with feedforward terms in the nonlinear case. It also provides insights into controller parameter tuning based on process dynamics. The feedforward term estimation scheme could also be programmed using common blocks like PID and filters. It has been proved through the successful implementation at Dow for polymerization reactor control and estimation. Therefore, we look forward to future opportunities to test the proposed control scheme in more real-world processes and use the practical insights to further improve the method.

A. Passivity-based Input Estimator Evaluation for the Case with Noises in Both Primary Measurements and Derivatives

This section presents the analysis of using PBIE on primary measurements with noise. The system is:

$$\frac{dz}{dt} = az + b\mu \tag{A.1a}$$

$$y_1 = z + \delta_1 \tag{A.1b}$$

$$y_2 = \dot{z} + \delta_2 \tag{A.1c}$$

The input observer is composed of differential equations that imitate the system using incomplete information, and the parameter update law:

$$\dot{\hat{z}} = a\hat{z} + b\hat{\mu} \tag{A.2a}$$

$$\hat{\mu} = \frac{1}{b}(y_2 + k(y_1 - \hat{z}) - a\hat{z}), k > 0 \tag{A.2b}$$

First we derive the differential equations for estimation errors, $\tilde{z}$ and $\tilde{\mu}$. Substitute $\hat{\mu}$ in (A.2a) with (A.2b) and get:

$$\dot{\hat{z}} = \dot{z} + \delta_2 + k(z - \hat{z}) + k\delta_1 \tag{A.3}$$

Subtract above equation from system state equation (A.1a) to get:

$$\dot{\tilde{z}} = -k\tilde{z} - k\delta_1 - \delta_2 \tag{A.4}$$

Follow similar steps for $\tilde{\mu}$ and obtain:

$$\dot{\tilde{\mu}} = -\frac{a+k}{b}\tilde{z} - \frac{k}{b}\dot{\delta_1} - \frac{1}{b}\dot{\delta_2} \tag{A.5}$$

The relationship between estimation erros and the measurement noises are:

$$\begin{bmatrix} \tilde{z}(s) \\ \tilde{\mu}(s) \end{bmatrix} = \begin{bmatrix} -\frac{k}{s+k} & -\frac{1}{s+k} \\ -\frac{k(s-a)}{b(s+k)} & -\frac{s-a}{b(s+k)} \end{bmatrix} \times \begin{bmatrix} \delta_1(s) \\ \delta_2(s) \end{bmatrix} \tag{A.6}$$

The amplitude ratio matrix from the frequency response of this 2 by 2, error to noise system is as follows.

$$AR = \begin{bmatrix} \frac{k}{\sqrt{k^2+\omega_1^2}} & \frac{1}{\sqrt{k^2+\omega_2^2}} \\ \frac{k}{b}\sqrt{\frac{a^2+\omega_1^2}{k^2+\omega_1^2}} & \frac{1}{b}\sqrt{\frac{a^2+\omega_2^2}{k^2+\omega_2^2}} \end{bmatrix}. \tag{A.7}$$

From the elements in the first row of AR matrix, the attenuation of both noises, δ_1 and δ_2, in state estimate is achieved if $k^2 > 1 - \omega_2^2$. However, the attention of both noises in parameter estimate cannot be achieved simutaneously. It can be shown by the exclusive ranges of k: $k^2 < a^2$ and $k^2 > a^2$, which are the solutions of attentuation conditions $AR(2,1) < |\frac{a}{b}|$ and $AR(2,2) < |\frac{1}{b}|$, respectively.

Then, we want to investigate if we can make a trade-off between attenuation two noises through choosing k. With the chosen k, the observer can overall dampen the effect of two noises in parameter estimate. Again, model the noises as sinusoidal waves:

$$\delta_1 = \overline{\delta}_1 + A_1 \sin(\omega_1 t + \phi_1),$$
$$\delta_2 = \overline{\delta}_2 + A_2 \sin(\omega_2 t + \phi_2).$$

Solve different equation (A.5) for $\tilde{\mu}$ and get:

$$\tilde{\mu} = -(\frac{k+a}{b}\overline{\delta}_1 + \frac{k+a}{bk}\overline{\delta}_2 - \alpha_{1,1,} - \alpha_{1,2})e^{-kt} + \frac{a}{b}\overline{\delta}_1 + \frac{a}{bk}\overline{\delta}_2 + \sqrt{\frac{A_1^2k^2(a^2+\omega_1^2)}{b^2(k^2+\omega_1^2)}}\sin(\omega_1 t + \theta_1)$$
$$+ \sqrt{\frac{A_2^2(a^2+\omega_2^2)}{b^2(k^2+\omega_2^2)}}\sin(\omega_2 t + \theta_2). \tag{A.8}$$

The coefficients are:

$$\alpha_{1,1} = \frac{A_1k(a+k)}{b(k^2+\omega_1)}(\omega_1\cos\phi_1 - k\sin\phi_1) \tag{A.9}$$
$$\alpha_{1,2} = \frac{A_2(a+k)}{b(k^2+\omega_2)}(\omega_2\cos\phi_2 - k\sin\phi_2) \tag{A.10}$$

The phase shifts are:

$$\tan\theta_1 = \frac{(ak-\omega_1^2)\sin\phi_1 - (a+k)\omega_1\cos\phi_1}{(a+k)\omega_1\sin\phi_1 - (\omega_1^2-ak)\cos\phi_1} \tag{A.11}$$
$$\tan\theta_2 = \frac{(ak-\omega_2^2)\sin\phi_2 - (a+k)\omega_2\cos\phi_2}{(a+k)\omega_2\sin\phi_2 - (\omega_2^2-ak)\cos\phi_2} \tag{A.12}$$

If we relate the two noises through a differentiator, i.e.:

$$\delta_1 = \overline{\delta}_1 + A_1\sin(\omega_1 t + \phi_1),$$
$$\delta_2 = \frac{d\delta_1}{dt} = \omega_1 A_1\cos(\omega_1 t + \phi_1) = \omega_1 A_1\sin(\omega_1 t + \phi_1 + \pi/2) \tag{A.13}$$

Then for δ_2, we can write:

$$\omega_2 = \omega_1 \quad A_2 = \omega_1 A_1 \quad \phi_2 = \phi_1 + \pi/2 \tag{A.14}$$

With above relations, sustained oscillatory terms in (A.8) become:

$$\tilde{\mu}_{t\to+\infty} = \sqrt{\frac{A_1^2k^2(a^2+\omega_1^2)}{b^2(k^2+\omega_1^2)}}\sin(\omega_1 t + \theta_1) + \sqrt{\frac{A_1^2\omega_1^2(a^2+\omega_1^2)}{b^2(k^2+\omega_1^2)}}\sin(\omega_1 t + \theta_2)$$
$$= \beta_1\sin(\omega_1 t + \theta_1) + \beta_2\sin(\omega_1 t + \theta_2)$$
$$= (\beta_1\cos\theta_1 + \beta_2\cos\theta_2)\sin(\omega_1 t) + (\beta_1\sin\theta_1 + \beta_2\sin\theta_2)\cos(\omega_1 t)$$

$$= \sqrt{(\beta_1^2 + \beta_2^2) + 2\beta_1\beta_2(\sin\theta_1 \sin\theta_2 + \cos\theta_1 \cos\theta_2)}\sin(\omega_1 t + \theta_3). \quad \text{(A.15)}$$

Reorganize the trigonometric functions in the second parenthesis:

$$\sin\theta_1 \sin\theta_2 + \cos\theta_1 \cos\theta_2 = \sqrt{\frac{\tan\theta_1^2 \tan\theta_2^2}{(1+\tan\theta_1^2)(1+\tan\theta_2^2)}} + \frac{1}{\sqrt{1+\tan^2\theta_1}} \times \frac{1}{\sqrt{1+\tan^2\theta_2}} \quad \text{(A.16)}$$

$$= \frac{\tan\theta_1 \tan\theta_2 + 1}{\sqrt{(1+\tan\theta_1^2)(1+\tan\theta_2^2)}} \quad \text{(A.17)}$$

The phase shifts become:

$\tan\theta_1$ remains the same as (A.11),

$$\tan\theta_2 = \frac{(ak - \omega_1^2)\cos\phi_1 + (a+k)\omega_1 \sin\phi_1}{(a+k)\omega_1 \cos\phi_1 - (\omega_1^2 - ak)\sin\phi_1}. \quad \text{(A.18)}$$

The numerator in (A.17), $\tan\theta_1 \tan\theta_2 + 1 = 0$ Thus, the sustained error in μ is:

$$\tilde{\mu}_{t\to+\infty} = \sqrt{\beta_1^2 + \beta_2^2}\sin(\omega_1 t + \theta_3) \quad \text{(A.19)}$$

$$= \sqrt{\frac{A_1^2(a+\omega_1^2)}{b^2}}\sin(\omega_1 t + \theta_3) \quad \text{(A.20)}$$

From this analysis, we found that the observer gain actually doesn't have any impact on the sustained error magnitude. It is the same as using direct inversion.

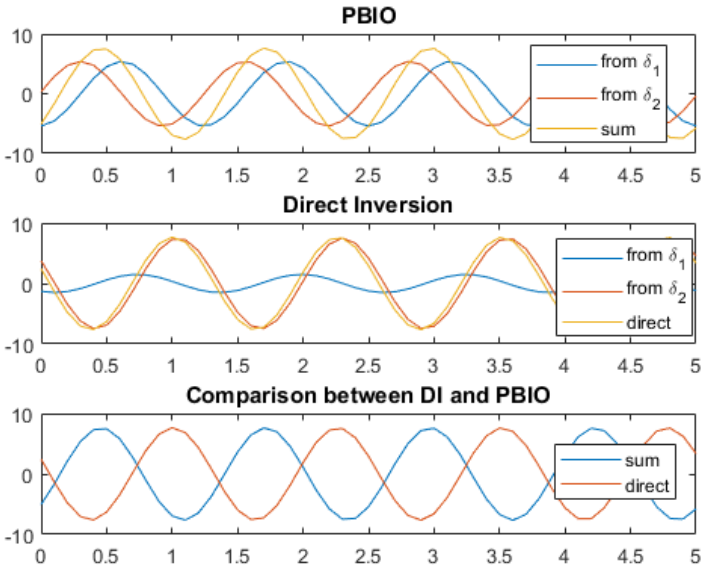

Figure A.1: $a = -1, b = 2, \omega_1 = 5, A_1 = 3, k = 5$

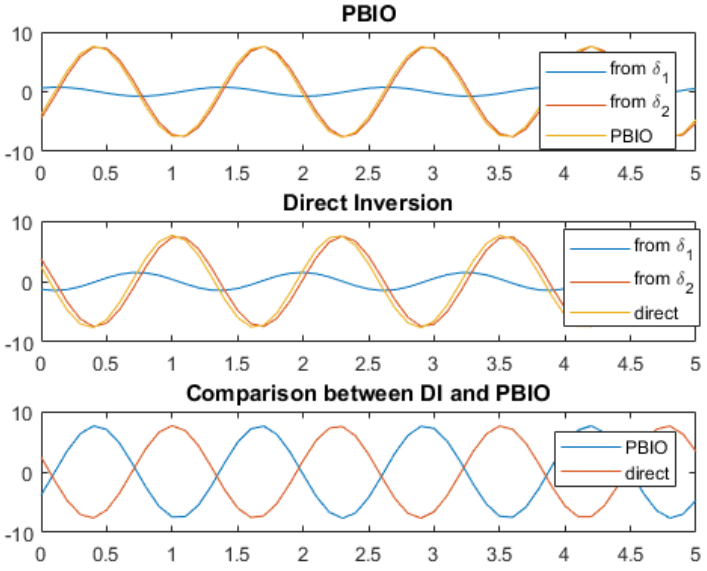

Figure A.2: $a = -1, b = 2, \omega_1 = 5, A_1 = 3, k = 0.5$

B. Derivation of PID Controller from the Perspective of Passivity-based Adaptive Control

In this section, we derive the PID formulation using measured deriavtive and dyanmics inversion. We consider the system:

$$\frac{dx}{dt} = ax + bu \tag{B.1}$$

$$y_1 = x_f \tag{B.2}$$

$$y_2 = \dot{x}_f \tag{B.3}$$

x_f is filtered measurement of x, and $\dot{x}_f$ is the filtered derivative. Set $\dot{x}^* - \dot{x} = -k(x^* - x_f)$, and substitute $\dot{x}$ with $\dot{x} \approx ax_f + bu$, to get

$$u = \frac{1}{b}(\dot{x}^* + ke_f - ax_f), \quad \text{where } e_f = x^* - x_f. \tag{B.4}$$

Substitute $ax_f = \dot{x}_f - bu_f$ into above equation to get:

$$u = \frac{1}{b}(\dot{x}^* + ke_f - \dot{x}_f + bu_f), \tag{B.5}$$

where u_f is the filtered input, and can be expressed as $u_f = \frac{1}{\tau s+1}$. Then above control law becomes further as:

$$bu - bu_f = \dot{x}^* - \dot{x}_f + ke_f \tag{B.6}$$

$$b(1 - \frac{1}{\tau s + 1})u = \dot{e}_f + k e_f \tag{B.7}$$

Solve for u and get:

$$u = \frac{1}{b}(\dot{e}_f + k e_f)(1 + \frac{1}{\tau s}) \tag{B.8}$$

$$= \frac{1}{b}\dot{e}_f + \frac{k}{b}e_f + \frac{1}{b}\frac{1}{\tau s}\dot{e}_f + \frac{k}{b}\frac{1}{\tau s}e_f \tag{B.9}$$

Organize above control law and it becomes:

$$u = (\frac{k}{b} + \frac{1}{b\tau})e_f + \frac{k}{b}\frac{1}{\tau s}e_f + \frac{1}{b}\dot{e}_f \tag{B.10}$$

The closed-loop function function from e_f to x is:

$$\frac{e_f(s)}{x(s)} = \frac{\tau s(s-a)}{s^2 + (\tau k + 1)s + 1} \tag{B.11}$$

Tuning parameters τ and k are chosen so that the closed-loop transfer function is stable, and there is no unstable zero-pole cancellation.

If the process that we are interested in controlling has uncertainty $\mu(t)$ as:

$$\frac{dx}{dt} = ax + bu + d\mu(t). \tag{B.12}$$

With the same PID controller, we have two transfer functions constituting the closed-loop dynamics:

$$\frac{e_f(s)}{x(s)} = \frac{\tau s(s-a)}{s^2 + (\tau k + 1)s + 1}, \quad \frac{e_f}{\mu(s)} = \frac{-d\tau s}{s^2 + (\tau k + 1)s + 1}. \tag{B.13}$$

The PID controller devised above is simulated to control the scalar example from Chapter 5:

$$\frac{dx}{dt} = 10x + u + d\mu, \quad \text{where } \mu = 5\sin(10t)\sin(t), \quad x(t_0) = 2. \tag{B.14}$$

Set $k = 10$, $\tau = \frac{1}{20}$, and plug in $b = 1$ in adaptive PID controller (B.10). Set the setpoint

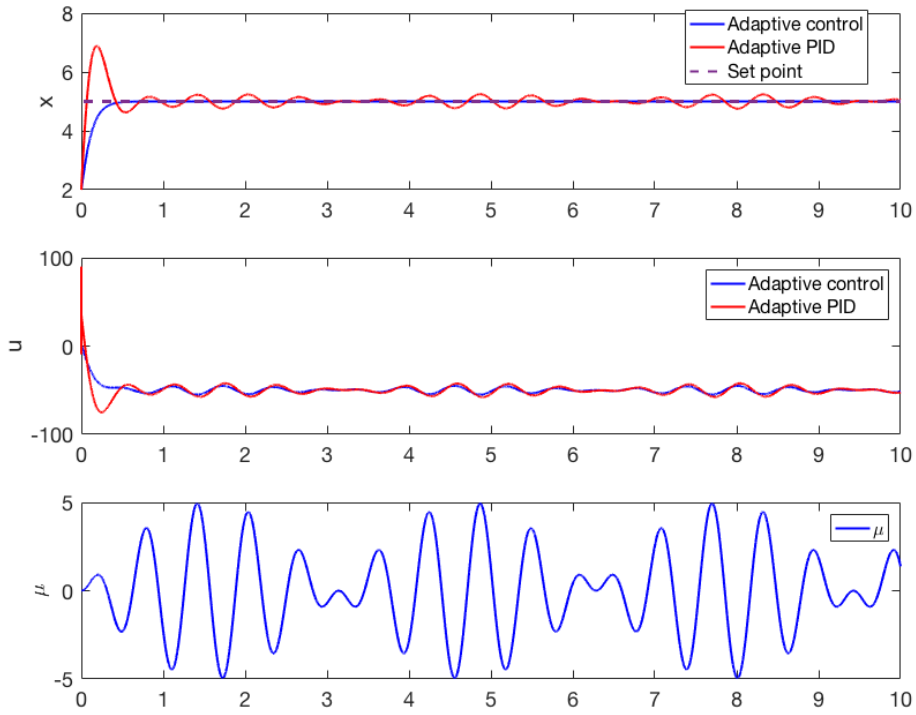

Figure B.1: Control results using adaptive control and adaptive PID

$x^* = 5$, and implement the control in Matlab simulation. Figure B.1 compares the simulated control results from the adaptive PID control and the adaptive controller designed in Section 5.3.2. The adaptive controller gives the exponentially stable control convergence. The adaptive PID is able to attenuate the influence of the cyclic unknown input μ, of which profile is shown in Figure B.1 (c).

C. Bumpless Transfer from PID Control to Passivity-based Advanced Control

C.1. Process Description and PID Control

In this section, we discuss the design of bumpless transfer for switching from basic PID control to passivity-based advanced control scheme. Numerical example and simulation result is given for illustration. The process is G(s) composed of a first order linear part with a time delay, and a nonlinear part:

$$y(t) = \frac{1}{5s+1} e^{-s} f(u) + d, \tag{C.1a}$$

where y is the measured output, u is the control input and d is the disturbance. The nonlinear term $f(u)$ is a function of constrained input u,

$$f(u) = u(t)^2, 0.01 < u(t) < 2. \tag{C.1b}$$

A constant disturbance of 1 is added on the output. The block diagram from input u to measured output y is shown in the Fig. C.1.

The PI controller is conservatively tuned assuming $u = u_{max} = 2$ using Internal Modeling Control (IMC) method. The PI controller is $PI(e(t)) = \frac{5}{12}\left(e(t) + \frac{12}{25}\int_0^t e(\tau)d\tau\right)$ to reach a closed-loop with a time constant, $\tau_c = 2$. The closed-loop block diagram is in Fig. C.2, and the control result is shown in Fig. C.3. A setpoint change is made at t = 80, and output is controlled to the new setpoint also.

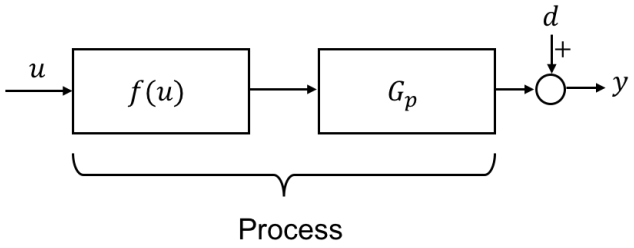

Figure C.1: Block diagram from input u to measured output y

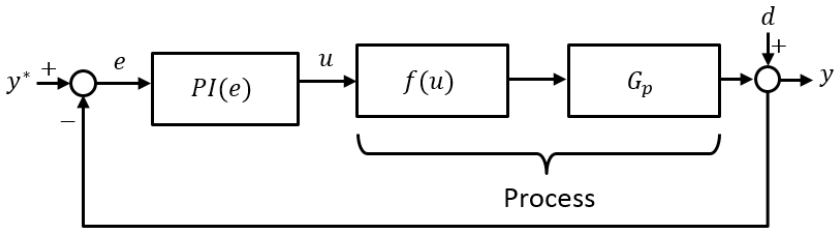

Figure C.2: Block diagram of PID control

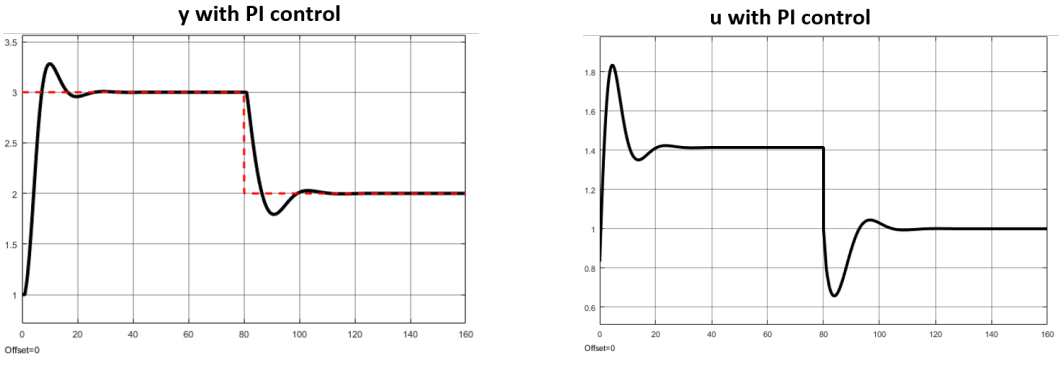

Figure C.3: Control result using PI control

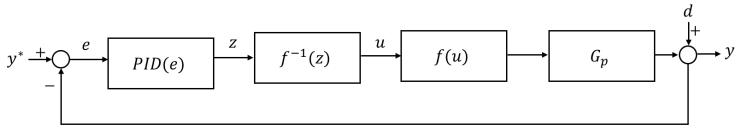

Figure C.4: Block diagram of closed-loop system with advanced control

C.2. Advanced Control and Bumpless Transfer

C.2.1. Control and Transfer Algorithms

Advanced control To form advanced control, the nonlinear part $f(\cdot)$ needs to be linearized using function $g(\cdot)$, which is defined through the condition:

$$g(\cdot) \circ f(\cdot) = 1. \tag{C.2}$$

For the example process Eqs. (C.1a, C.1b), we have:

$$g(z) = f^{-1}(z) = z^{1/2} = PID(e)^{1/2}. \tag{C.3}$$

The block diagram of the closed-loop system with advanced control is shown in Fig. C.4.

Bumpless transfer from PI control mode to advanced control mode In real implementation, transfer from PID control mode to advanced control mode may have an undesired effect on the control performance, due to sudden change of the controller output. In the following part, we show how the bumpless transfer is designed. A filter function $T(\cdot)$ is incorporated into the closed-loop for gain adjustment. The condition of the filter is that:

1. at the time of switch $t = t_0$, we still want to maintain $u(t_0) = PID(e(t_0))$, i.e. $g(T(z(t_0))) = z(t_0)$; together with Eq. (C.2), we have the definition of function $T(\cdot)$ at the time of switch:

$$t = t_0, T(\cdot) = g^{-1}(\cdot) = f(\cdot) \tag{C.4}$$

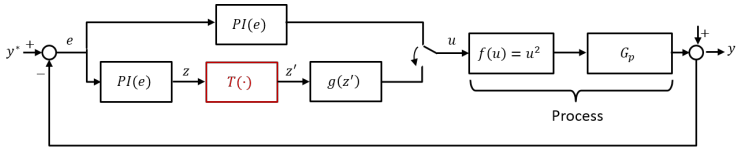

Figure C.5: Block diagram of closed-loop system with bumpless transfer from PID to advanced control

2. after the switch, the filter maintains as a constant gain adjustment:

$$t > t_0, T(\cdot) = T\left(z(t_0)\right) \tag{C.5}$$

The block diagram of the closed-loop with the bumpless transfer scheme is shown in Fig .C.5.

C.2.2. Simulation Results

The simulation is performed in Simulink as shown in Fig. C.6. During the simulation, following changes are made to show the performance of transferring between control schemes, and setpoint tracking:

1. control scheme is changed from PID control to adavanced control at time $t_0 = 40$;

2. setpoint of y is 3 when $t < 80$, and is changed to 2 when $t > 80$.

Simulations with or without bumpless transfer are performed:

1. **Without bumpless transfer**

   In this simulation the input $u(t) = z(t)^{1/2}$. At time of the switch $t_0 = 40$, the control input changes from $PID(e(t \to t_0))$ to $PID(e(t_0))^{1/2}$, as can be observed in Fig. C.7. The sudden change of the input degrades the tracking performance of the measured output, which deviates from the stabilized value at the set point $y^* = 2$. y came back around $t = 60$ with a overshot, and finally stabilize again at the set point around $t = 76$.

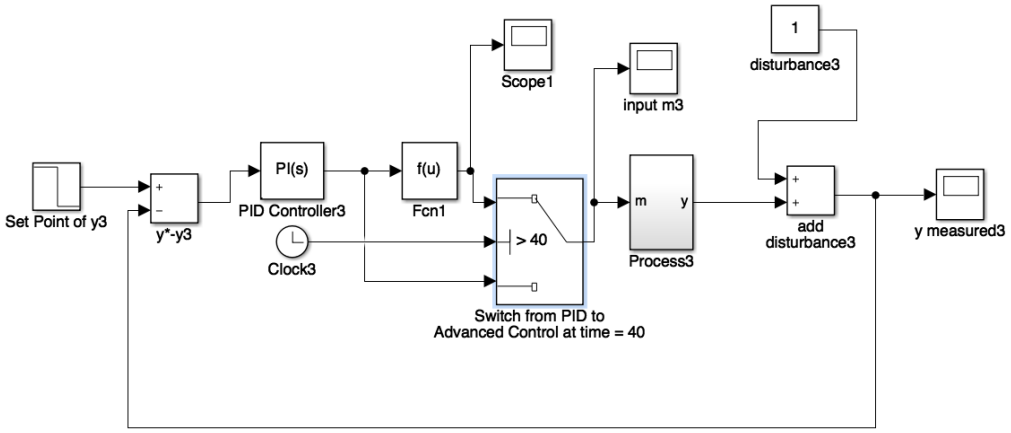

Figure C.6: Simulink Model

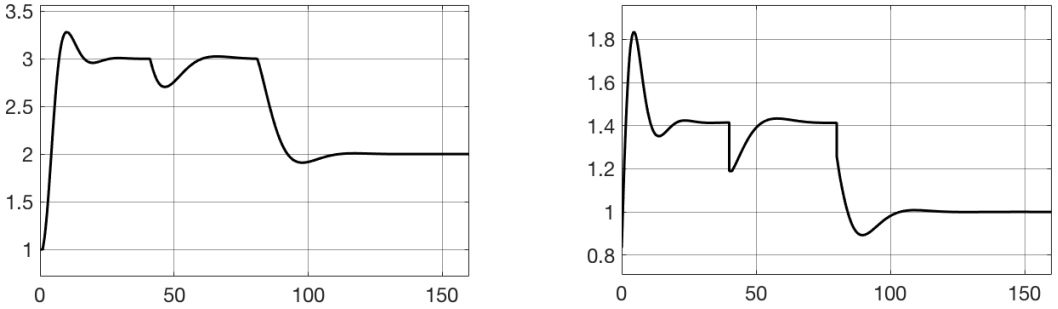

Figure C.7: Results of simulation without bumpless transfer (output profile on the left, input profile on the right)

2. **With bumpless transfer**

   In this simulation the input $u(t) = z(t_0)^{1/2} \times z(t)^{1/2}$. With the adjustment, the control input still remains $PID(e(t_0))$ when the switch happens.So it doesn't degrade control performance as shown in Fig. C.8.

C.3. Another Design of Compensation Block for Bumpless Transfer

The MV determined by advanced control is:

$$u(t) = \frac{1}{u(t)} PID(e), \tag{C.6a}$$

$$= \frac{1}{m(t)^2} PID(e) \tag{C.6b}$$

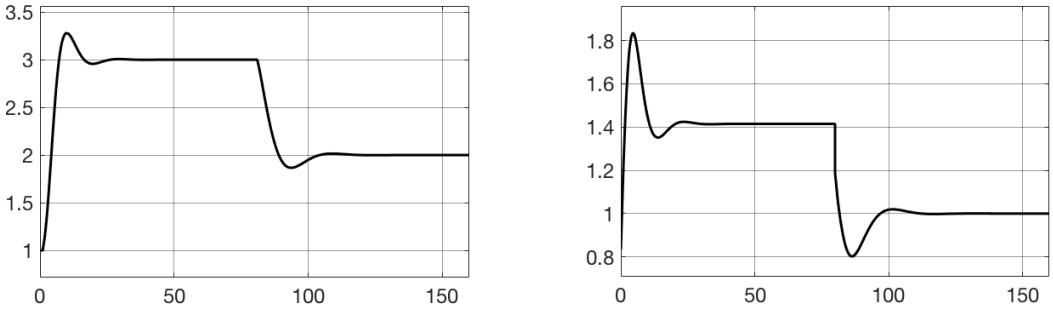

Figure C.8: Results of simulation with bumpless transfer (output profile on the left,input profile on the right)

$$= PID(e)^{1/3} \tag{C.6c}$$

where $\frac{1}{u(t)}$ in Eq. C.6a is the nonlinear gain. The simulation is performed in Simulink as shown in Fig. C.9. During the simulation, following changes are made to show the performance of transferring between control schemes, and setpoint tracking:

1. control scheme is changed from PID control to adavanced control at time $t_0 = 40$;
2. setpoint of y is 3 when $t < 80$, and is changed to 2 when $t > 80$.

Simulations with two transfer strategies are performed:

1. **Without bumpless transfer**

   In this simulation the nonlinear control gain is just $\frac{1}{u(t)}$. As shown in Fig. C.10, the stabilized output y dropped from the set point after the control switch. Eventually, the output converges back to the setpoint, and the set-point change is tracked. A similar profile of the input is shown in Fig. C.10.

2. **With bumpless transfer**

   In this simulation is nonlinear control gain is normalized w.r.t. $\frac{1}{u(t_0)}$, i.e. $\frac{1/u(t)}{1/u(t_0)}$. With the adjusted nonlinear gain, the switch doesn't degrade control performace as shown in Fig. C.11.

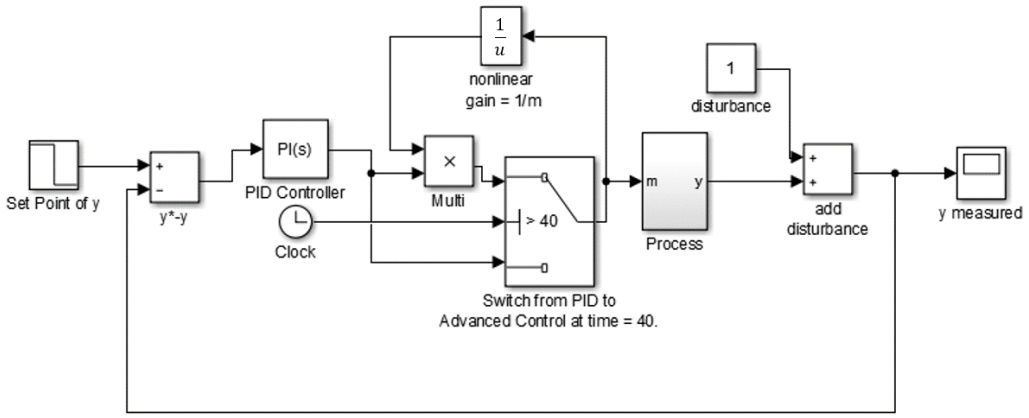

Figure C.9: Simulink Model

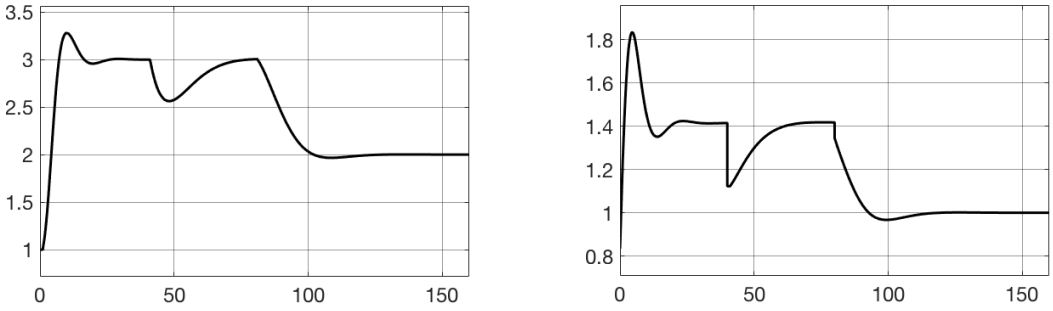

Figure C.10: Results of simulation without bumpless transfer (output profile on the left, input profile on the right)

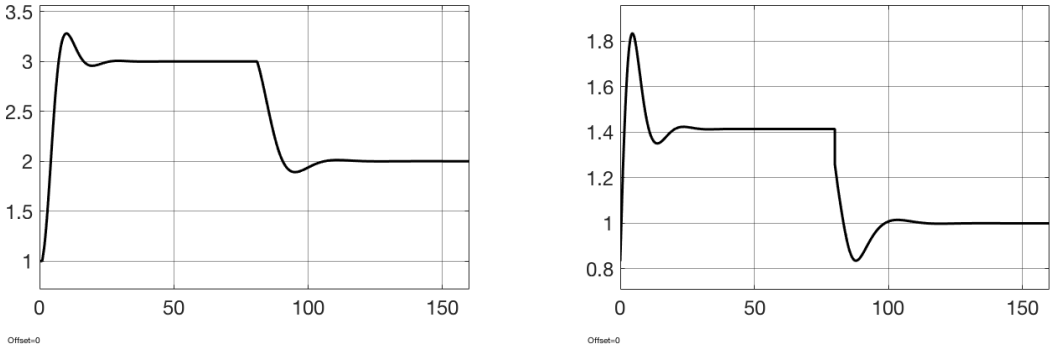

Figure C.11: Results of simulation with bumpless transfer (output profile on the left, input profile on the right)

D. Reaction Models Used for Simulations

D.1. Semi-batch Reaction Model

We simulate an $A \rightarrow B$ reaction, and model the species' concentrations and volume as follows:

$$\frac{dC_A}{dt} = F_{in}C_{A,in} - k_0 e^{\frac{-E_a}{RT_r}} C_A \tag{D.1a}$$

$$\frac{dC_B}{dt} = k_0 e^{\frac{-E_a}{RT_r}} C_A \tag{D.1b}$$

$$\frac{dV}{dt} = F_{in}, \tag{D.1c}$$

where C_A represents concentration of reactant A, C_B represents concentration of product B, k_0 pre-exponential factor, E_a represents activation energy, R gas constant.

Together with the differential equations of the temperatures, (6.1a) – (6.1c), they constitute the model of the semi-batch reactor. The reaction kinetic parameters are listed in Table D.1.

Parameters	Values
k_0 (min^{-1})	7.2×10^10
ΔH_r (J/mol)	-5×10^4
$\frac{E_a}{R}$ (K)	8750

Table D.1: Simulated reaction kinetic parameters

D.2. MMA Polymerization Model

The MMA free-radical polymerization mechanism is as follows:

Initiation:

$$I_2 \xrightarrow{k_d} 2I^*$$
$$I^* + M \xrightarrow{f} P_1^*$$

Propagation

$$P_i^* + M \xrightarrow{k_p} P_{i+1}^*$$

Chain transfer

$$P_i * + M \xrightarrow{k_{fm}} D_i + P_i^*$$
$$P_i^* + S \xrightarrow{k_{fs}} D_i + S^*$$

Termination

$$P_i^* + P_j^* \xrightarrow{k_t} D_i + D_j$$

I_2 represents initiator; I^* represents the free radical; M represents the monomer; P_i^* represents the living polymer chain with length i; D_i represents the dead polymer chain with length i.

The kinetic model is composed of balance equations of initiator, monomer, and solvent:

$$\frac{dC_{I_2}}{dt} = -k_d C_{I_2} \tag{D.2}$$
$$\frac{dC_M}{dt} = -2fk_d C_{I_2} - (k_p + k_{fm}) C_M \sum_{i=1}^{i=n_{max}} C_{P_i^*} \tag{D.3}$$

Parameters	Relation equations
Initiation rate constant (s^{-1})	$k_d = 1.90 \times 10^{17} exp(-\frac{34277}{RT})$
Propagation rate constant (s^{-1})	$k_p = 7.00 \times 10^{6} exp(-\frac{6300}{RT})$
Transfer to monomer rate constant ($\frac{L}{s \times mol}$)	$k_{fm} = 2.90 \times 10^{11} exp(-\frac{17957}{RT})$
Transfer to solvent rate constant ($\frac{L}{s \times mol}$)	$k_{fs} = 1.02 \times 10^{9} exp(-\frac{15702}{RT})$
Disproportionation rate constant (s^{-1})	$k_t = g_t \times 1.77 \times 10^{9} exp(-\frac{-2800}{RT})$

Table D.2: MMA polymerization kinetic parameter calculation equations

$$\frac{dC_S}{dt} = -k_{fs} C_S \sum_{i=1}^{i=n_{max}} C_{P_i^*} \tag{D.4}$$

The sum concentration of living monomer is modeled using relation: $\sum_{i=1}^{i=n_{max}} C_{P_i^*} = (\frac{f k_d C_{I_2}}{k_t})^2$. The reaction kinetic constants relations with reaction condition are tabulated in Table D.2. Gel effect is also considered, which is reflected in the disproportionation rate constant calculation equation. More details regarding the MMA polymerization model can be found in Crowley & Choi (1997).

E. NUMERICAL DIFFERENTIATION

This section gives a review of several numerical differentiators, that uses different approaches to estimate derivatives of signals measured with or without noise. The Savitzky-Golay filter and deadbeat differentiator assume the signal as a polynomial of time; the sliding mode differentiator assumes the measured signal as a control setpoint, and the derivatives are the control input that drives the estimated state to the setpoint. The formula of the methods are listed below.

- Savitzky-Golay filter (Baedecker, 1985) calculation of jth order time derivative is usually in a discrete convolution form. For a case, that the original signal is assumed to be a n-th degree polynomial, and we have $2m$ evenly spaced measurements, then the derivatives of a middle point indexed 0 is estimated through:

$$\hat{y}_n^{(j)}(0) = \sum_{i=-m}^{m} h_i^j y_i. \tag{E.1}$$

  h_i are convolution weightings derived from solving a least squares polynomial regression problem, and usually can be found in a lookup table.

- Assume the signal is a N-th degree polynomial function of time:

$$y(t) = \sum_{i=0}^{N} \frac{a_i}{i!} t^i \tag{E.2}$$

  Deadbeat differentiator (Reger & Jouffroy, 2009) for the jth order time deriva-

tive is:

$$\hat{y}^{(j)} = \int_0^T G_j(T,\delta) y(t-\delta) d\delta, \quad j = 0, 1, ..., N, \tag{E.3}$$

where the convolution kernel:

$$G_j(T,\delta) = \frac{(N+j+1)!}{T^{j+1} j!(N-j)!} \sum_{k=0}^{N} \frac{(-1)^k (N+k+1)!}{(j+k+1)(N-k)!(k!)^2} (\frac{\delta}{T})^k, \tag{E.4}$$

T is the length of an arbitrary constant time window.

- Sliding mode differentiator (Levant, 1998) formulation is:

$$\dot{\hat{y}} = u \tag{E.5}$$

$$u = u_1 - \gamma |\hat{y} - y|^{\frac{1}{2}} \text{sign}(\hat{y} - y) \tag{E.6}$$

$$\dot{u}_1 = -\alpha \text{sign}(\hat{y} - y), \tag{E.7}$$

where u is the estimated first order derivative, $\hat{y}$ is the estimated signal, y is the measured signal. $\alpha, \lambda > 0$ are design parameters.

BIBLIOGRAPHY

Aguilar, R., Martınez-Guerra, R., & Poznyak, A. (2002). Reaction heat estimation in continuous chemical reactors using high gain observers. *Chemical Engineering Journal*, *87*(3), 351–356.

Aguilar-López, R. (2003). Integral observers for uncertainty estimation in continuous chemical reactors: algebraic-differential approach. *Chemical Engineering Journal*, *93*(2), 113–120.

Ali, J. M., Hoang, N. H., Hussain, M. A., & Dochain, D. (2015). Review and classification of recent observers applied in chemical process systems. *Computers & Chemical Engineering*, *76*, 27–41.

Asbjørnsen, O. A. (1972). Reaction invariants in the control of continuous chemical reactors. *Chemical Engineering Science*, *27*(4), 709–717.

Asbjørnsen, O. A. & Fjeld, M. (1970). Response modes of continuous stirred tank reactors. *Chemical Engineering Science*, *25*(11), 1627–1636.

Baedecker, P. A. (1985). Comments on least-squares polynomial filters for initial point and slope estimation. *Analytical Chemistry*, *57*(7), 1477–1479.

Bao, J. & Lee, P. L. (2007). *Process Control: The Passive Systems Approach*. Springer Science & Business Media.

Bastin, G. & Dochain, D. (1990). *On-line estimation and adaptive control of bioreactors*. Elsevier.

Bhatt, N., Amrhein, M., & Bonvin, D. (2010). Extents of reaction, mass transfer and flow for gas- liquid reaction systems. *Industrial & Engineering Chemistry Research*, *49*(17), 7704–7717.

Biswas, P. & Samanta, A. N. (2013). Backstepping control of polymerization reactor. In *Control Conference (ASCC), 2013 9th Asian*, (pp. 1–5). IEEE.

Chen, J., Patton, R. J., & Zhang, H.-Y. (1996). Design of unknown input observers and robust fault detection filters. *International Journal of control*, *63*(1), 85–105.

Co, T. & Ydstie, B. (1990). System identification using modulating functions and fast fourier transforms. *Computers & chemical engineering*, *14*(10), 1051–1066.

Corless, M. & Tu, J. (1998). State and input estimation for a class of uncertain systems. *Automatica*, *34*(6), 757–764.

Crowley, T. J. & Choi, K. Y. (1997). Calculation of molecular weight distribution from molecular weight moments in free radical polymerization. *Industrial & Engineering Chemistry Research*, *36*(5), 1419–1423.

Darouach, M., Zasadzinski, M., & Xu, S. J. (1994). Full-order observers for linear systems with unknown inputs. *IEEE transactions on automatic control*, *39*(3), 606–609.

Dochain, D. (2000). State observers for tubular reactors with unknown kinetics. *Journal of process control*, *10*(2-3), 259–268.

Dochain, D., Couenne, F., & Jallut, C. (2009). Enthalpy based modelling and design of asymptotic observers for chemical reactors. *International Journal of Control*, *82*(8), 1389–1403.

Dochain, D., Perrier, M., & Ydstie, B. E. (1992). Asymptotic observers for stirred tank reactors. *Chemical Engineering Science*, *47*(15), 4167–4177.

Farschman, C. A., Viswanath, K. P., & Ydstie, B. E. (1998). Process systems and inventory control. *AIChE journal*, *44*(8), 1841–1857.

Fjeld, M., Asbjørnsen, O. A., & Astróm, K. J. (1974). Reaction invariants and their importance in the analysis of eigenvectors, state observability and controllability of the continuous stirred tank reactor. *Chemical Engineering Science*, *29*(9), 1917 – 1926.

Ghosh, B. K. & Rosenthal, J. (1995). A generalized popov-belevitch-hautus test of observability. *IEEE transactions on automatic control*, *40*(1), 176–180.

Gopaluni, R., Mizumoto, I., & Shah, S. (2003). A robust nonlinear adaptive backstepping controller for a CSTR. *Industrial & Engineering Chemistry Research*, *42*(20), 4628–4644.

Hoang, H., Couenne, F., Gorrec, Y. L., Chen, C.-L., & Ydstie, B. E. (2012). Passivity based controller and observer of exothermic chemical reactors*. *IFAC Proceedings Volumes*, *45*(15), 377 – 384. 8th IFAC Symposium on Advanced Control of Chemical Processes.

Hoang, N. H., Couenne, F., Le Gorrec, Y., Chen, C., & Ydstie, B. E. (2013). Passivity-based nonlinear control of cstr via asymptotic observers. *Annual Reviews in Control*, *37*(2), 278–288.

Hoang, N. H., Dochain, D., Ydstie, B. E., et al. (2014). Partial inventory control of the cstr via reaction-dependent generalized inventories. In *19th IFAC World Congress*.

Hou, M. & Muller, P. (1992). Design of observers for linear systems with unknown inputs. *IEEE Transactions on automatic control*, *37*(6), 871–875.

Hua, C., Liu, P. X., & Guan, X. (2009). Backstepping control for nonlinear systems with time delays and applications to chemical reactor systems. *IEEE Transactions on Industrial Electronics*, *56*(9), 3723–3732.

Khalil, H. K. (1996). Nonlinear systems. *Prentice-Hall, New Jersey*, *2*(5), 5–1.

Kokotović, P., Krstić, M., & Kanellakopoulos, I. (1992). Backstepping to passivity: recursive design of adaptive systems. In *Decision and Control, 1992., Proceedings of the 31st IEEE Conference on*, (pp. 3276–3280). IEEE.

Krstic, M., Kokotovic, P. V., & Kanellakopoulos, I. (1995). *Nonlinear and Adaptive Control Design*. New York, NY, USA: John Wiley & Sons, Inc.

Lee, H. & Tahk, M.-J. (1999). Generalized input-estimation technique for tracking maneuvering targets. *IEEE transactions on Aerospace and Electronic Systems*, *35*(4), 1388–1402.

Levant, A. (1998). Robust exact differentiation via sliding mode technique. *automatica*, *34*(3), 379–384.

Li, K., Chan, K. H., Ydstie, B. E., & Bindlish, R. (2010). Passivity-based adaptive inventory control. *Journal of Process Control*, *20*(10), 1126 – 1132.

Luenberger, D. (1971). An introduction to observers. *IEEE Transactions on Automatic Control*, *16*(6), 596–602.

Mboup, M., Join, C., & Fliess, M. (2007). A revised look at numerical differentiation with an application to nonlinear feedback control. In *Control & Automation, 2007. MED'07. Mediterranean Conference on*, (pp. 1–6). IEEE.

Mhamdi, A. & Marquardt, W. (2004). Estimation of reaction rates by nonlinear system inversion. *IFAC Proceedings Volumes*, *37*(1), 167 – 172. 7th International Symposium on Advanced Control of Chemical Processes (ADCHEM 2003), Hong-Kong, 11-14 January 2004.

Moreno, J. A. & Dochain, D. (2008). Global observability and detectability analysis of uncertain reaction systems and observer design. *International Journal of Control*, *81*(7), 1062–1070.

Park, Y. & Stein, J. L. (1988a). Closed-loop, state and input observer for systems with unknown inputs. *International Journal of Control*, *48*(3), 1121–1136.

Park, Y. & Stein, J. L. (1988b). Closed-loop, state and input observer for systems with unknown inputs. *International Journal of Control*, *48*(3), 1121–1136.

Preisig, H. & Rippin, D. (1993). Theory and application of the modulating function methodii. algebraic representation of maletinsky's spline-type modulating functions. *Computers & Chemical engineering*, *17*(1), 17–28.

Preisig, H. A. (1988). The use of differential information for batch reactor control. In *American Control Conference, 1988*, (pp. 671–676).

Reger, J. & Jouffroy, J. (2009). On algebraic time-derivative estimation and deadbeat state reconstruction. In *Decision and Control, 2009 held jointly with the 2009 28th Chinese Control Conference. CDC/CCC 2009. Proceedings of the 48th IEEE Conference on*, (pp. 1740–1745). IEEE.

Rodrigues, D., Billeter, J., & Bonvin, D. (2015). Control of reaction systems via rate estimation and feedback linearization. In *Keynote address at the 25th European Symposium on Computer Aided Process Engineering (ESCAPE) - PSE 2015*.

Rodrigues, D., Srinivasan, S., Billeter, J., & Bonvin, D. (2015). Variant and invariant states for chemical reaction systems. *Computers Chemical Engineering*, *73*, 23 – 33.

Salehi, S. & Shahrokhi, M. (2009). Adaptive fuzzy backstepping approach for temperature control of continuous stirred tank reactors. *Fuzzy Sets and Systems*, *160*(12), 1804–1818.

Schuler, H. & Schmidt, C.-U. (1992). Calorimetric-state estimators for chemical reactor diagnosis and control: review of methods and applications. *Chemical Engineering Science*, *47*(4), 899 – 913.

Seborg, D. E., Mellichamp, D. A., Edgar, T. F., & Doyle III, F. J. (2010). *Process dynamics and control*. John Wiley & Sons.

Srinivasan, B., Amrhein, M., & Bonvin, D. (1998). Reaction and flow variants/invariants in chemical reaction systems with inlet and outlet streams. *AIChE Journal*, *44*(8), 1858–1867.

Tatiraju, S. & Soroush, M. (1998). Parameter estimator design with application to a chemical reactor. *Industrial & engineering chemistry research*, *37*(2), 455–463.

Wang, J. & Ydstie, E. B. (2007). Robust inventory control system. *IEEE Transactions on Control Systems Technology*, *15*(4), 768–774.

Wang, S.-H., Wang, E., & Dorato, P. (1975). Observing the states of systems with unmeasurable disturbances. *IEEE transactions on Automatic Control*, *20*(5), 716–717.

Welch, G. & Bishop, G. (1995). An introduction to the kalman filter. Technical report, Chapel Hill, NC, USA.

Zhao, Z., Wassick, J. M., Ferrio, J., & Ydstie, B. E. (2016). Reaction variants and invariants based observer and controller design for cstrs. *IFAC-PapersOnLine*, *49*(7), 1091–1096.